Experimental investigation of the behaviour and fate of block copolymers in fouling-release coatings

Noguer, Albert Camós

Publication date:
2016

Document Version
Publisher's PDF, also known as Version of record

Experimental investigation of the behaviour and fate of block copolymers in fouling-release coatings

Albert Camós Noguer

Ph.D. Thesis

Department of Chemical and Biochemical Engineering,
Technical University of Denmark (DTU)
DK-2800 Kgs. Lyngby, Denmark
and
Department of Fouling Control Systems, Hempel A/S
DK-2800 Kgs. Lyngby, Denmark

2016

Preface

This dissertation summarizes the outcome of three years of research towards the Industrial Ph.D. degree at the Technical University of Denmark (DTU). The work presented in the thesis has been carried out at the Department of Chemical and Biochemical Engineering at the Technical University of Denmark and at the Department of Fouling Release Systems of Hempel A/S. Associate Professor Søren Kiil has been the main supervisor, and Professor Søren Hvilsted and Ph.D., Fouling Release Systems Department manager, Stefan Møller Olsen have co-supervised this project. It has been has been funded by The Danish Ministry for Science and Technology and Hempel A/S.

The completion of this project would not have been possible without the help and support from a great number of people comprising supervisors, colleagues, family and friends, among others. Some have contributed by giving advice and counselling, while others have made the everyday life more pleasant. To all of you, I would like to express my deepest gratitude. Gràcies. Tak.

Summary

Fouling-release coatings (FRC) were developed as an environmentally friendly alternative after the ban of highly toxic antifouling coatings based on tributyltin. Poly(dimethylsiloxane) (PDMS) has been the most widely used polymer for FRC, and its fouling-inhibition properties have been enhanced by addition of copolymers. Examples of these copolymers include phenyl-modified PDMS or poly(ethylene glycol) (PEG)-based copolymers (e.g. triblock PEG-b-PDMS-b-PEG). These copolymers diffuse from the bulk to the surface of the coating upon immersion and modify the physicochemical properties of the surface. FRC provide superior fuel savings to the shipping industry on the first stages of immersion compared to other current technologies, albeit its performance declines over time.

This project is mainly concerned with improving the understanding of FRC and identifying the causes that result in the worsening of the fouling-inhibition properties of these complex systems, specially focusing on the behaviour and fate of the block copolymers used as additives. The development of various methods to visualize and quantify processes involving these copolymers are presented. Chapter 1 provides an overview on marine biofouling, and the evolution and state-of-the-art in biofouling prevention. In Chapter 2, the scope, aims and hypotheses of this project are set. Chapter 3 studies the diffusion and biofouling-inhibition properties of PEG-based surfactants and copolymers added to PDMS and Chapter 4 analyses the distribution and behaviour of PEG-b-PDMS-b-PEG copolymers in PDMS coatings by fluorescence means. Chapter 5 investigates the degradation of PDMS-PEG-based copolymers in FRC immersed in seawater. Chapter 6 consists of a long-term field study regarding the release/loss of these block copolymers from fouling-release coatings.

A coating based on a PDMS binder has been employed as model system in the thesis. The effect of the addition of various PEG-based surfactants and copolymers (i.e. amphiphiles) was investigated by a novel method developed in this project, and the diffusion coefficient and biofouling-inhibition properties of the different amphiphiles were studied. The results showed that there is a moderate dependence of the diffusion coefficient on the molecular weight of the molecule. The diffusion coefficients obtained were relatively high for all the investigated compounds with molecular weights (M_w) ranging from 600 to 4000 g/mol. Moreover, the biofouling-inhibition properties are not dependant on the diffusion coefficient of the amphiphiles, but mainly depend on the chemistry of the hydrophobic block, with PDMS-PEG-based copolymers providing the best results. Hence, the anchoring capabilities and stability of the copolymer on the surface of the coating are proven to be a central aspect of the performance of these FRC.

A novel fluorescent-labelled triblock PEG-b-PDMS-b-PEG copolymer was synthesized in this project to visualize the distribution and behaviour of PDMS-PEG-based copolymers in PDMS coatings. Images obtained by confocal microscopy proved that the copolymer molecules assemble in spherical domains inside the PDMS coating. The domains are smaller close to the surface and larger in the bulk of the film (with domains as large as 7 µm in diameter). The diffusion of copolymer from the bulk to the interfaces of the PDMS film could be observed by following the fluorescence intensity at different depths over time.

The chemical stability of PDMS-PEG-based copolymers in PDMS coatings immersed for up to 30 months in seawater in Singapore was also investigated. The copolymer remaining in the coatings after exposure was extracted and isolated, and its chemical composition was analysed. An increase in the relative content of PDMS was observed, probably due to the imperfect isolation process. However, no traces of degradation products were found, and it was observed that the molecular weight of the copolymer did not change over time. Therefore, it was concluded that the copolymer molecules remaining in the coating after 30 months of immersion did not suffer significant degradation. Conversely, the studied copolymers could be degraded in the laboratory under a range of conditions and the degradation products were successfully identified, mainly consisting of esters arising from the oxidative degradation of the PEG block. Further experiments showed that degradation can also occur in the bulk of the coatings depending on the physical properties and chemical composition of some of the constituents of FRC, both for coatings immersed in seawater and others kept in the laboratory in dry conditions.

The release/loss of copolymer from FRC was also studied, and the effect of different variables such as seawater temperature and the addition of biocide were addressed. Approximately 300 experimental coatings exposed to seawater for up to 5 years were analysed and the results exhibited a large scatter in the data, mainly attributed to differences in the coatings compositions. However, some comparable formulations suggest that seawater temperature has an important effect on the loss of copolymer from PDMS-coatings, while the initial concentration of copolymer has no influence for copolymer concentrations as high as 7 wt%. In addition, the initial concentration of biocide showed diverse effects, with biocide-containing coatings leading to higher copolymer losses in the first stages of immersion and larger copolymer retention values in long-term exposure, indicating that the addition of biocide strongly influences the release profile of these copolymers from FRC.

In summary, the addition of block copolymers is a successful method to impart biofouling-inhibition properties to fouling-release coatings. The development of new methodologies has allowed the investigation of the behaviour and fate of these block copolymers in FRC. While the performance of these copolymers is not limited by its diffusion properties in the film, attention should be put on the physical properties and chemical composition of the copolymer and other coating constituents. These variables have an important influence on the anchoring, release and degradation of these copolymers, which dictate the long-term performance of fouling-release coatings.

Table of contents

1. Marine biofouling and its prevention

1.1 Marine biofouling

1.1.1 Marine biofouling and its consequences

Marine biofouling, also known as marine biological fouling, is the settlement and accumulation of different organisms such as bacteria, algae and animals on surfaces immersed in seawater [1,2]. The presence of biofouling on immersed surfaces has severe adverse effects such as reducing the heat transfer efficiency in heat exchangers [3] or inducing/enhancing corrosion in ship ballast tanks [4] and other immersed structures [5]. Moreover, it has been an obstacle for some offshore renewable technologies (e.g. offshore wind power and wave energy plants) [6]. Furthermore, biofouling causes detrimental effects on marine aquaculture. It was estimated in 2004 that the global yearly costs associated with the presence of biofouling in aquaculture farms reached between $1.5 and $3 billion [7]. Buoys, sensors and underwater pipelines are also vulnerable to biofouling.

The presence of biofouling has also been reported to be a problem in other areas outside the marine environment. For example, separation membranes, biosensors and drug-release systems have been reported to suffer from biofouling [8]. In biomedicine, the adsorption of proteins and platelets (also known as thromobcytes) in blood-contact devices has been reported to result in thrombogenic problems, as well as problems in contact lenses, prosthesis, catheters and implants have been described [9–11]. It has been demonstrated that the formation of a biofilm is an essential factor in the evolution and persistence of infections on biomedical devices and implants, and that antibiotic agents are less effective when combating bacteria in the form of biofilms [11]. It was estimated in the 2000s [11,12] that healthcare associated infections resulted in economical losses >$3 billion alone in the United States.

In the shipping industry, the negative economical and environmental effects of the settlement of biofouling on ship hulls have been previously studied [1,13–15], and can be summarized in:

- Higher frictional resistance and weight of the hull due to the presence of fouling, which leads to a decrease in speed and manoeuvrability. The additional fuel consumption required to compensate for the speed loss results in higher costs and increased release of greenhouse-effect and other gases (i.e. CO_2, SO_2 and NO_x).
- Additional maintenance costs due to the increased frequency of dry-docking and other corrective measures such as hull cleaning, with the associated increase of raw materials consumed and residues generated. Added losses due to the loss of transportation of goods while the vessel is under maintenance.
- Added fuel consumption due to settlement of biofouling on the propellers.
- Deterioration of the coatings, with the decrease of their protective (e.g. anticorrosive) and aesthetical (e.g. discoloration) properties, resulting in corrosion of the ship hull.
- Translocation of invasive species from different environments.

Figure 1.1. Biofouling settlement on the propeller of a vessel. Courtesy of Hempel A/S.

The increase in frictional resistance of ships has been the main driver for developing better coatings in terms of antifouling performance. However, determination of the precise impact of biofouling on fuel consumption is not simple. The influence of biofouling on frictional resistance depends on several factors such as the kind of vessel, its speed and the type and extent of biofouling present on the ship hull. For example, while the frictional resistance accounts for less than 40% of the total resistance for high-speed trading ships, this value can increase to 70-90% for slow trading ships (for fouling-free hulls) [16,17]. Different studies have investigated the economical impact of biofouling on fuel consumption, both on hydrodynamic laboratory studies and full-scale ships [13,18–20]. The first studies were published in the first half of the 19th century and estimated maximal penalties of more than 100% in fuel consumption for heavy fouled ships [13]. Schultz et al. [19,20] estimated in the 2000s the impact of biofouling on two conventionally-powered middle-sized ships of the US Navy. It was concluded that the presence of heavy fouling on those ships could result in an increase in the required shaft power between 76% and 86%. Moreover, the presence of fouling on the propellers of ships has a detrimental effect on the efficiency of the propellers. Some early studies reported additional fuel consumption of up to 10% for fouled propellers [13], though others have reported lower values in the range of 3-4% [14]. Nonetheless, these values are relatively high if the area of the propeller is taken into account (for example, the area of the propeller accounts for 0.5% of the submerged area for large single-screw ships [14]).

In 2012, it was reported that 300.000.000 tonnes of fuel are consumed yearly by waterborne transportation around the world [8]. Therefore, the potential benefits of adopting preventive measures to combat biofouling are widely recognized. The use of antifouling coatings was estimated in 2009 [21] to provide annual fuel savings of $60 billion and 384 million tonnes of CO_2 reduction. To further improve the performance of antifouling and fouling-release coatings, many efforts have been directed towards better understanding the processes and species involved in marine biofouling and the possible strategies to prevent or diminish its negative consequences.

1.1.2 The process of marine biofouling

Marine biofouling is a complex process in which both micro- and macroorganisms settle on immersed surfaces. More than 4000 marine organisms had been identified in fouled structures back in 2000 [1], though probably more species are yet to be identified. The process of biofouling has been traditionally divided into four main steps, which have been summarized in Table 1.1.

Table 1.1 Summary of the main steps in the settlement of biofouling

Step	Main compounds and organisms involved	Characteristics	References
Molecular fouling (few minutes after immersion)	Proteins and polysaccharides	Consists of the adsorption of organic molecules on the immersed surface. Results in changes of the physicochemical properties of the surface (e.g. wettability and electric charge).	[22,23]
Primary colonization (1h – 24h after immersion)	Bacteria and diatoms	Based on two steps: reversible physical adsorption + irreversible adhesion driven by the secretion of EPS[a]. Rapid growth of the biofilm due to cell-division reproduction mechanism.	[15,24,25]
Secondary colonization (1 week after immersion)	Spores of macroalgae and protozoa	Based on initial attachment and followed by permanent adhesion triggered by the secretion of EPS.	[22]
Tertiary colonization (few weeks after immersion)	Larvae of macrofoulers	Complex settlement mechanisms involved. Macrofoulers generate EPS[a] of diverse compositions based on carbohydrates, proteins and proteoglycans.	[26,27]

[a] Extracellular polymeric substances

The biofouling process was believed to consist of a collection of sequential steps, as described above. Therefore, it was assumed that the settlement of biofouling on an immersed surface could be suppressed by inhibiting the first stages of the colonization process [28]. In other words, if the adsorption of organic molecules and bacteria could be supressed, no macrofouling would be observed. However, it was shown that the process is not necessarily sequential, i.e. biofouling of macrofoulers can for example occur without the presence of previous colonizers on the surface [28]. Nontheless, the presence of “previous stages” of biofouling has been reported to facilitate adhesion of larger organisms [15].

1.1.3 The marine environment

Different parameters of the marine environment have been shown to have an important effect on the settlement of biofouling on ship hulls and its prevention. They have been summarized in Table 1.2.

Table 1.2 Description of the main parameters influencing the settlement of biofouling

Parameter	Variables and processes regarding biofouling settlement and prevention influenced	References
Temperature (-2°C - 35°C)	Growth of bacteria, diatoms and barnacles.	[13,29,30]
	Release of biocides and solubility/polishing rate of the binder of some antifouling coatings.	[1,31,32]
	Surface properties of thermo-responsive polymers used to prevent biofouling.	[33]
Salinity (~3.5 wt%)	Growth of biofouling species such as bacteria and molluscs.	[13,34]
	Fouling-inhibition properties of some zwitterionic polymers employed to prevent biofouling.	[35]
Chemical composition	Fe and Ca are essential for biofilm formation.	[27,36,37]
	Transition metals can catalyse the degradation of some polymers used to prevent biofouling.	[35]
	Differences in abundance and community structure of biofilms have been observed on antifouling coatings containing different biocides.	[38]
pH (~ 8.2)	Survival/mortality of marine organisms.	[39]
	Non-fouling properties of some zwitterionic polymers.	[40,41]
Dissolved gases (0.1 - 0.6 vol%)	Growth of biofouling.	[1]
	Oxidation of copper-based biocides in antifouling coatings.	[1]
Availability of nutrients	Growth rate, community structure and diversity of biofouling.	[36,42]
Geography and Season		[1]
Sunlight		[43]
Vessel speed		[13,42,44]
	Release of biocides and dissolution of the binder from some antifouling coatings.	[1,45]

1.1.4 Strategies to prevent biofouling

Coatings based on different inorganic and organic toxic agents have been widely used and have shown their effectiveness in supressing the biofouling process, but with a high environmental cost [1]. Moreover, polymers with specific physicochemical properties have been used as coatings to debilitate the bond strength between the bioadhesive and the surface, in the so-called fouling-release coatings [2,46].

Inspired by the various stages involved in the biofouling process, other approaches have been employed to minimize or delay the growth of biofouling. For example, bacteria use a communication system between cells called quorum sensing, which plays an important role in biofilm formation [28,36]. Quorum sensing allows single cells to act as a macrocommunity and cooperate to adapt to changing conditions and find the best surfaces to attach and areas with higher concentration of nutrients, among others.

Therefore, strategies to negatively affect the process of quorum sensing have been studied with the aim of hindering biofouling settlement [3,36].

In addition, strategies to alter the adhesives and cements secreted by different fouling species have also been investigated. Enzymes have been explored as a way to dissolve/degrade the adhesives secreted by these species with positive results [24]. Similarly, calcium has been shown to be an important component in the process of biofilm formation [27,37] and its shortage has demonstrated to be an effective method to block the production of bioadhesives, though this has not been successfully implemented for antifouling purposes [24].

1.2 Antifouling coatings

1.2.1 History

Concerns regarding the presence of fouling on ship hulls have been considered for more than 2000 years [13]. Phoenicians and Carthaginians were said to use pitch and copper sheathing on ship bottoms, though the use of wax, tar and asphalt in very early times has also been reported [13]. The Greeks used arsenic and sulphur mixed with oil in the 5th century B.C [13]. The first spread antifouling strategy was lead sheathing, which was adopted by Spain, France and England in the 16th century [13]. However, it was proven that lead resulted in corrosion in some iron parts of the ship (e.g. the rudder) [1]. Therefore, lead was gradually substituted by copper for the sheathing of ships. In the late 18th century, the use of iron to build ships augmented. However, it was early found that copper sheathing could not be used to protect iron ships due to copper's corrosion effect on iron [13]. Hence, other solutions were developed.

The first American shipbottom coating was produced in 1908 [13]. The idea of using antifouling coatings was not new. Different ideas based on dispersing a toxic agent in a matrix had been previously developed [1]. In 1860, "McIness" and "Italian Morevian", both antifouling coatings, were developed. These coatings were based on dispersing copper sulphate in a hot-plastic matrix, and their superior properties were rapidly recognized [13]. The development of AF coatings underwent significant changes after World War II with the development of petroleum-based synthetic polymers, which started to be employed in antifouling coatings [13]. In the 1950s, the high toxicity of tributyltin (TBT) compounds was reported by Van de Knok and coworkers, and in the 1960s the AF properties of TBT compounds were successfully commercialized in antifouling coatings [1]. The first patent on the use of TBT in antifouling coatings was granted to Milne and Hails in 1977 [47]. Thereafter, the development of different antifouling coatings significantly increased. The principal kinds of antifouling coatings and their constituents are presented in the following sections.

1.2.2 Coatings constituents

Commercial coatings are complex mixtures of compounds that are added to confer the coatings with different properties. In the case of antifouling coatings, the main properties are: antifouling performance, durability, adhesion to the substrate, smoothness, ease of application, drying-time, pot-life, safety, aesthetical properties and economical cost. To achieve a good balance of the aforementioned

properties, the following ingredients are usually mixed: binder, pigments, biocides, fillers, solvents and additives. The amount and nature of each component vary depending on the kind of coating.

1.2.2.1 Binder

The binder is the main component of a coating formulation, and dictates to a large extent its mechanical properties and durability. Most commercial coatings are based on natural or synthetic resins/polymers such as rosin, methyl methacrylate copolymers and poly(dimethylsiloxane) (PDMS) [28]. The selection of the binder is mainly determined by the working mechanism of the coatings. For example, for soluble-matrix coatings, a binder soluble in seawater such as rosin must be chosen, while for smooth non-soluble fouling-release coatings, PDMS is usually used.

The film-forming properties of the binder depend on its chemistry and interaction with the other components of the coating. Some binders form the film by a simple physical drying process. That is, the solvent evaporates and the binder forms a solid film without any chemical process taking place. Others undergo chemical reactions to form a chemically-bonded crosslinked film. The crosslinking process can be triggered by a range of sources comprising heat, UV radiation and catalysts.

1.2.2.2 Pigments

Pigments include both organic and inorganic solids, which can be toxic or non-toxic [28]. Toxic pigments are categorized as “biocides” and are addressed in the following section. Non-toxic pigments are usually added to coatings to provide colour and opacity [28], though it has been reported that some mechanical strength is also provided [46]. Some examples may be iron oxide (Fe_2O_3) or titanium dioxide (TiO_2).

1.2.2.3 Biocides

Biocides used in antifouling coatings can be divided into inorganic and organic biocides, depending on their chemistry. The two groups of biocides are briefly described below. It should be noted that the antifouling activity of most biocides differ depending on the biofouling organism studied, with some biocides being more effective against organisms like bacteria and others showing best antifouling properties against invertebrates [1,28]. However, some biocides have toxic effects over a wide range of marine organisms and are known as broad-spectrum biocides. Due to the complexity of the biofouling community in seawater, broad-spectrum biocides have traditionally provided superior antifouling properties.

Different parameters have been used to quantify the antifouling effect of biocides. Some of these parameters quantify the amount required to inhibit biofouling (e.g. MIC - minimum inhibitory concentration or EC50 – effective concentration that inhibits 50% of biofouling growth). Others focus on the required concentration to have lethal effects (e.g. LC50 - lethal concentration that kills 50% of the biofouling organisms) [28,48,49]. The so-called no-observable-effect level (NOEL) has been used for environmental purposes [50]. Release rates in the order of tens of $\mu g \cdot cm^{-2} \cdot day^{-1}$ have been reported for traditional biocides used in antifouling coatings [32,51–53].

1.2.2.3.1 Inorganic biocides

Metal-based inorganic biocides consist mainly of metallic oxides that are dissolved in seawater, providing some toxicity and thus antifouling properties to the coatings. The most important metal-based biocide is copper oxide (Cu_2O), which is added as biocidal pigment in most antifouling commercial coatings. The two main biocidal mechanisms of metallic ions are overloading and membrane partitioning [28]. The former works by increasing the concentration of the metal inside the living cell and disrupting its metabolism. The latter works by penetrating the cell membrane and interfering with some of the membrane functions. In addition to Cu_2O, copper (I) thiocyanate (CuSCN) and zinc oxide (ZnO) have been used as biocidal pigments. The solubility and toxicity of other metal-based pigments such as titanium (IV) and iron (III) oxides still remain to be fully studied [1,31].

1.2.2.3.2 Organic biocides

Organic biocides, mostly metal-free, are usually added to antifouling coatings as co-biocides to boost the toxicity and antifouling performance of Cu_2O-based coatings. The main function of these co-biocides is to provide antifouling protection against the entire spectrum of fouling organisms, since some species are tolerant to copper [54] . Some of the mostly used organic biocides are shown in Figure 1.2 including Diuron, chlorothalonil and SeaNine, though many others have been explored as potential antifouling agents.

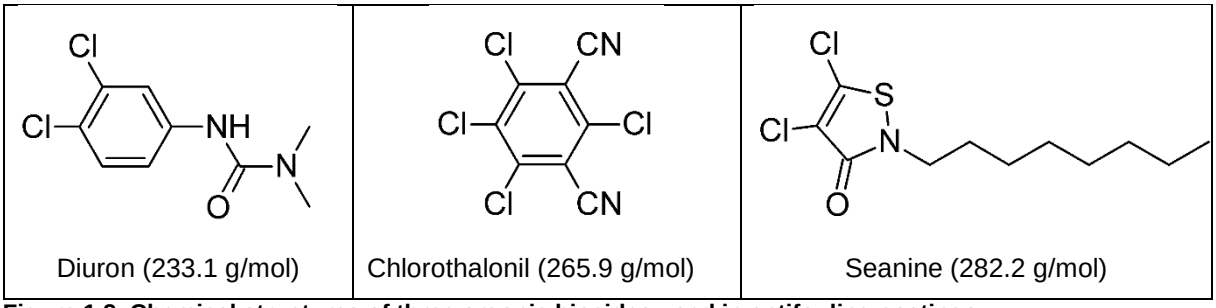

Diuron (233.1 g/mol)	Chlorothalonil (265.9 g/mol)	Seanine (282.2 g/mol)

Figure 1.2. Chemical structures of three organic biocides used in antifouling coatings.

1.2.2.4 Fillers

Fillers are solid inorganic particles finely dispersed in the binder matrix that are used for different purposes. Silica (SiO_2) is for example added to PDMS-based coatings to improve their mechanical properties, while silicates, sulphates and carbonates have been employed in traditional antifouling formulations. Fillers are also used to improve the thixotropic properties of coatings or to decrease the price of the coatings due to their low cost (i.e. “extenders”) [28].

1.2.2.5 Solvents

Solvents are usually added to the formulation to solubilize the binder and procure a homogeneous mixture of the components that can be easily applied on a ship hull. Mixtures of solvents are usually used, to achieve an optimal combination of evaporation rate and solubilizing effect of the different components [28]. Some examples of solvents include xylene and butanol. Concerns with the amount of volatile organic carbon (VOC) have pushed the development of coatings on two different ways. On one side, solvents have been substituted with water when possible [28]. Otherwise, lower amounts of solvents have been used to decrease VOC levels [55].

1.2.2.6 Additives

Finally, different additives have been added to provide a range of properties to coatings. They are typically added in low amounts (a few weight percent). Examples of such additives include antifoaming agents, plasticizers, UV absorbers and levelling agents [28].

1.2.3 Types of antifouling coatings

Different antifouling coatings have been developed up to date to combat biofouling. Depending on their working mechanism, these can be classified into insoluble-matrix, soluble-matrix and self-polishing coatings. A brief description for each type of coating is provided in Table 1.3. An example is shown in Figure 1.3, where release of tributyltin (TBT) from self-polishing copolymer (SPC) coatings is illustrated.

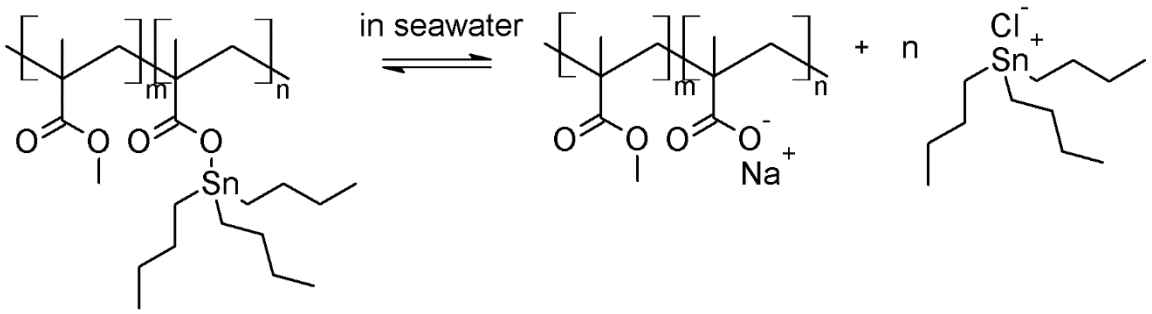

Figure 1.3. Reaction mechanism involved in the release of tributyltin (TBT) from self-polishing coatings (SPC-TBT) coatings.

1.2.4 Drawbacks

In spite of the promising antifouling properties of TBT, the negatively environmental consequences of its toxicity were soon detected. In 1974, the first signs of abnormal shell growth in oysters were reported in the coast of England [56]. The most extensive studies were undertaken in France in the 1980s. His and Robert [57,58] studied the effects of TBT in *Cassiopea grass* oysters and proved that concentrations as low as 50 ng/l had negative effects on growth of oysters larvae [59]. At the same time, Alzieu and coworkers [60,61] studied the effect of TBT-based biocides released from antifouling coatings on the growth of oysters in the French coast. Due to environmental concerns, the use of TBT was gradually banned. France was the first country to legislate on the use of TBT-based AF coatings in 1982, and imposed a ban for ships smaller than 25 m [56,62]. Similar legislations followed in UK (1985), US (1988) and Japan (1990). Finally, the International Maritime Organization (IMO) approved in 1998 a complete ban of TBT starting in 2008 [56]. The early effects of the legislative measures had a clear effect on the amounts of TBT and malformation growth rates of oysters. Alzieu et al. [62,63] reported a significant drop in the malformation indices of oysters grown in the French Atlantic coast after 1982. However, the results were limited in the Mediterranean [50].

Table 1.3. Main properties of the different types of antifouling coatings

	Insoluble-matrix coatings	Soluble-matrix coatings	Self-polishing copolymer (SPC) coatings
Binder	Insoluble in seawater. For example, epoxy or chlorinated rubber.	Physical-drying and soluble in seawater. For example, rosin.	Hydrolytically unstable in seawater. For example, acrylic-based copolymers.
Biocides	Metallic pigments (e.g. Cu_2O).	Metallic pigments (e.g. Cu_2O).	Toxic molecules covalently bonded to the polymeric matrix, usually as esters in an acrylic backbone (e.g. tributyltin (TBT)). Addition of Cu_2O is typical.
Working principle	The biocidal pigments are physically dispersed in the binder. The biocides are dissolved by contact leaching, leaving behind a leached layer that becomes thicker over time.	The biocidal pigments are physically dispersed in the binder. The biocides and the binder are dissolved in seawater, leaving behind a leached layer.	The unstable ester bond is hydrolysed and the biocide is released, leaving behind a leached-layer. The increasing amount of carboxylate groups result in eventual erosion of the coating.
Strengths	The mechanical properties of the coatings do not dramatically deteriorate over time due to the insolubility of the binder.	The leached-layer is thin due to the dissolution of the binder. Lower amounts of biocides are necessary compared to insoluble-matrix coatings. Can be improved by addition of synthetic organic resins (known as controlled depletion coatings (CDP)).	High control of the release-rate of biocide and binder polishing. The polishing rate can be tuned to provide optimal properties for low and high speed vessels. Extended dry-docking intervals of up to 5 years. Yearly savings of $3 billion in fuel consumption and $2.7 billion in extended dry-docking time (for TBT-SPC in the 1990s).
Limitations	The release rate of biocide significantly decreases due to the increasing leached layer. High loadings of biocides are used to compensate for the decrease in release rate, with economical and environmental penalties. The surface roughness significantly increased due to leaching of high amounts of biocides, which further facilitates biofouling settlement.	Poor mechanical properties due to dissolution of the binder. The dissolution rate of the binder is dependent on the speed of the vessel, being insufficient in idle conditions and excessive while sailing at high speeds.	Only biocides which can be linked to the backbone of the binder can be employed. High toxicity of some biocides (e.g. TBT).
References	[1,13,64]	[1,13,64]	[1,2,28,64,65]

1.3 Alternatives to antifouling coatings

There have been significant efforts in the last decades to develop non-toxic coatings to defy the settlement of biofouling on ship hulls. This process has been mainly driven by the concerns and regulations regarding the use of biocides in antifouling coatings, with the reduction or complete ban of effective toxic coatings (e.g. SPC-TBT antifouling coatings) [66].

All the alternatives (mostly non-toxic) to antifouling coatings have relied on two different mechanisms: detachment and prevention of biofouling. These two mechanisms pursue to withstand fouling at different stages of the biofouling process earlier described. Briefly, when biofoulants settles on the hull of a ship, they are first reversibly adsorbed on the surface, and then adhesives are secreted, which results in the irreversible loss of motility of the biofouling species [46]. These adhesives secreted by biofoulants adhere to the substrate in a manner that depends on both the properties of the bioadhesive and the substrate.

Based on the previous explanation, the two mechanisms can be described. In the “prevention of biofouling” approach, the surface is chemically modified to avoid the initial steps of settlement of the biofouling species, mainly the reversible adsorption of organic molecules, bacteria and diatoms. By keeping the biofouling species away from the surface, biofouling settlement is inhibited. These coatings are usually known as non-stick coatings. In the “detachment of biofouling” approach, the main idea is to allow the settlement of biofoulants, but decrease the strength of the bond between the adhesive and the substrate. If the adhesion strength is sufficiently low, the bond can be fractured by the action of hydrodynamic forces generated by the sailing of the vessel or the weight of the biofilm [46]. These coatings are usually known as fouling-release coatings.

1.3.1 Fouling-release coatings (FRC)

Fouling-release coatings (FRC) rely mainly on the “detachment of biofoulants” mechanism, where the adhesion strength between the bioadhesives and the surface of the coating is minimized. These coatings were initially developed at the same time as SPC coatings, but the effectiveness provided by SPC coatings hindered their development [2]. In addition to reducing the release of biocides to the marine environment, FRC also have the advantage of being formulated with lower amounts of solvents, which diminishes the release of VOC to the atmosphere. A total conversion from antifouling to fouling-release coatings was estimated on 2011 to prevent the annual consumption of 20 million litres of solvents [55].

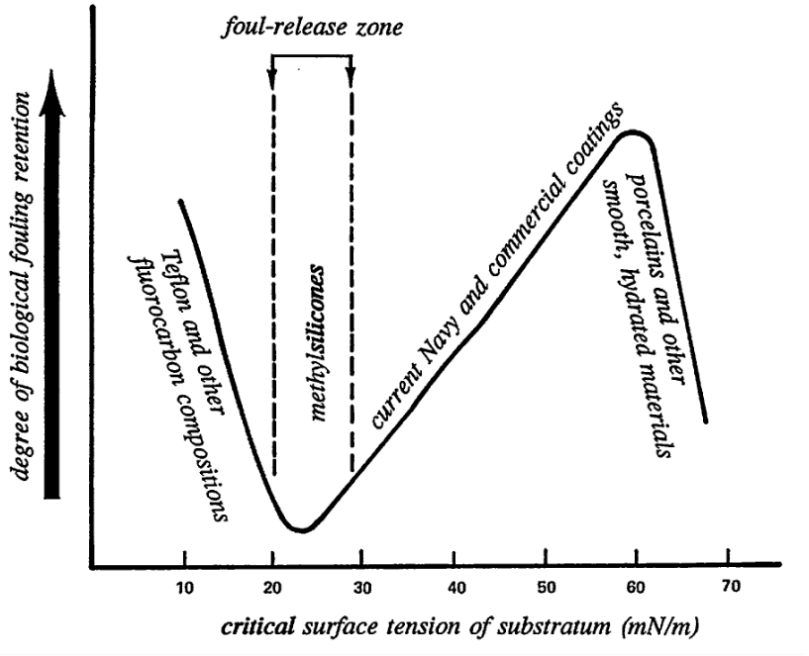

Figure 1.4. "Baier curve" showing the empirical relationship between the critical surface tension of the substrate and the retention degree of biological fouling. Reprinted with permission from [67].

The first studies dealing with the ease of release of biofoulants appeared in the 1970s. R. E. Baier [68,69] studied the degree of biofouling retention on different polymeric substrates with different wettability. A correlation between the critical surface energy (γ_c) of the substrates and biofouling retention was observed as illustrated in Figure 1.4. There is a minimum in the biofouling retention degree between 22 and 24 mN/m and a maximum at approximately 60 mN/m [67]. The minimum in biofouling retention around 23 mN/m is provided by materials based on methylsilicone polymers and different theories have been suggested to explain this minimum [46,70]. Dexter et al. [71] obtained similar results after investigating the settlement of bacteria on substrates with different critical surface tension. Becka and Loeb [72] investigated the adhesion strength of barnacles on different polymeric surfaces and the required stress of removal. It was shown that depending on the polymer chosen, the adhesion strength of the barnacles could increase by a factor of up to 10. Moreover, they showed that the stress required to detach barnacles from different polymeric substrates could be correlated to the surface energy of the polymer (not critical). In this case, no maximum or minimum could be found, i.e. the release-stress required was lower as the surface energy decreased for all the polymers investigated. However, it should be noted that polysiloxanes were not included in the analysis.

S.C. Dexter [73] also attempted to find a relationship between the critical surface energy of different materials and the adhesion strength of biofoulants, following Baier's findings. Dexter found that both the energy of the surface and the adherent should be taken into account, and that the relative adhesion strength could be correlated to both variables. Therefore, the adhesion strength could be minimized by matching the critical surface tensions of the polymer and the bioadhesive and by decreasing their interactions [74], in agreement with other previous studies [75,76].

Brady and Singer [77] studied the adhesion of biofoulants from the perspective of fracture mechanics and found that, in addition to the properties of the surface, the mechanical bulk properties of the polymers investigated also had an effect on adhesion strength. The elastic modulus (E, also known as Young's modulus) of the material was demonstrated to have a strong effect on the relative adhesion of biofoulants. It was shown that the Baier curve in Figure 1.4 could be represented as a straight line, when both E and γ_c were taken into account, following a law where the relative adhesion is proportional to the square-root product of E and γ_c [77], as shown in Figure 1.5.

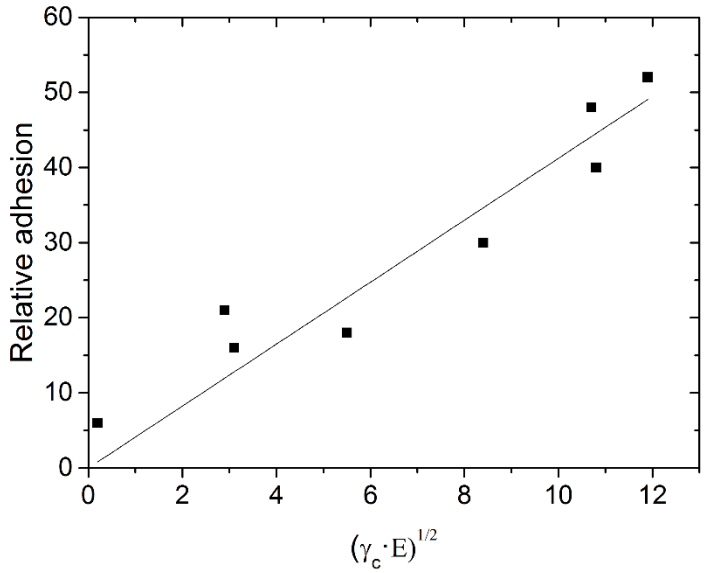

Figure 1.5. Relationship between the relative adhesion of biofouling as function of the square-root of the product of critical surface tension (γ_c) and elastic modulus (E) of the substrate, adapted from [77].

Moreover, the influence of the coating thickness on the relative adhesion has been studied both with epoxies (which simulate barnacle adhesives [78]) and with real barnacle adhesives [66]. It was found that the pull-off force required to detach biofoulants from methylsilicone-based polymers decreased as the film thickness increased. Others have additionally found evidence of the effect of interfacial slippage on the adhesion and removal of biofouling from some polymeric surfaces such as poly(dimethylsiloxane) (PDMS) [51].

Brady and Singer [77] studied the mechanisms involved in the adhesion of biofoulants, describing the following four main principles: (1) chemical bonding (2) electrostatic interactions, (3) mechanical interlocking and surface roughness and (4) diffusion of adhesives into the substrate film. Both the chemical bonding and the electrostatic interactions can be minimized by employing non-polar hydrophobic surfaces according to Brady and Singer [77].

Amongst all the studied polymers, fluorine-based polymers and silicones (i.e. polysiloxanes) present the best properties as fouling-release coatings due to their low values of E and γ_c and are presented below.

1.3.1.1 Fluorine-based FRC

Fluorine-based polymers have been explored as fouling-release coatings mainly due to their very low critical surface tension and surface energy, with values as low as γ_c = 8 mN/m when CF_3 groups are

available at the surface of the coating [79]. The use of fluoropolymers for fouling-release coatings was first patented in 1973 by T. Berque, who described the application of poly(tetrafluoroethylene) (PTFE) and fluorinated ethylene-propylene copolymers for protection of ship hulls [2]. In 1990, R.F. Brady [80] reported a vessel coated in the 1970s with a fluorinated-urethane fouling-release coating that had been operative for 12 years. Though the ship suffered from biofouling, this could be easily removed with water pressure.

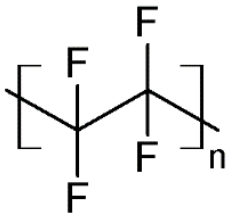

Figure 1.6. Chemical structure of the repeating unit of poly(tetrafluoroethylene) (PTFE).

Fluoropolymers are characterized for exhibiting high physical and chemical resistance and having hydrophobic and low-energy surfaces. Among the main advantages of the use of fluorine-based polymers in FRC, their very low (critical) surface energy has been the main driver. Moreover, the closely-packed CF_3 groups on the surface do not permit molecular diffusion [46], which impedes the penetration of bioadhesives in the coating film. Furthermore, the chemical stability of fluoropolymers towards UV, salinity, pH and organic solvents has made of this family of polymers a good candidate for FRC [2]. Fluorine-modified acrylates, epoxies and urethanes have been developed for fouling-release purposes, as described elsewhere [2,81].

Nonetheless, some major drawbacks have been an obstacle to their wide use. For example, the low solubility of fluoropolymers in most organic solvents has been a challenge regarding its application on ship hulls. In addition, fluoropolymers possess elastic modulus of approximately 0.5 GPa [74], and therefore significant stresses are required to detach biofoulants which already fouled the ship hull. The modulus of polysiloxanes is, for comparison, approximately 100 times lower [74]. Moreover, it has been reported that the surfaces of fluoropolymers present high degree of irregularities and roughness, which allow for accumulation of biofouling and mechanical interlocking between bioadhesives and the coating [2,46]. Furthermore, the highly polar C-F bond has been suggested to contribute to the accumulation of biofouling over time on PTFE surfaces, in spite of its non-polar nature [2].

1.3.1.2 Silicone-based FRC

Silicone-based polymers, particularly poly(dimethylsiloxane) (PDMS) elastomers, have been long recognized as a potential alternative to biocide-based antifouling coatings due to their low critical surface tension and elastic modulus. They were developed at the same period as SPC coatings, but were not commercialized until the 1980s. The first patent regarding the use of crosslinked silicones for ship hulls in the marine environment was granted to Robbart in 1961 [82]. It has been shown that barnacle's adhesive strength can be decreased below 0.1 MPa on silicone-based FR coatings [66,83]. Bond strengths of 0.1 MPa permit the detachment of the biofoulants at moderate vessel speeds. It has been shown that barnacles start to detach from silicones at speeds between 15 and 20 knots [84].

PDMS is characterized for being a hydrophobic polymer with very low glass transition temperature (T_g), about -145°C. Low T_g has been suggested to minimize mechanical interlocking between biofoulants and the PDMS surface [85,86]. The properties exhibited by PDMS result from the particular chemistry of the Si atom and the PDMS backbone (see Figure 1.7). PDMS possesses Si-O-Si bonds with very large angles (~145°) and low surface energy side groups (-CH_3) [86]. Moreover, PDMS is characterized by a very low elastic modulus (E) and surface roughness, two main factors determining the adhesion strength of biofouling [46]. This unique combination of properties confers PDMS high flexibility and mobility of the backbone with hydrophobic mobile pendant CH_3 groups on the surface. Coupled with its very favourable bulk properties, PDMS has been recognized as a great material for fouling-release purposes. On the other side, PDMS presents different disadvantages, mainly arising from its poor adhesion and mechanical properties. PDMS might suffer from peeling or damaging under service conditions, which limits its use as long-term solution against biofouling [46].

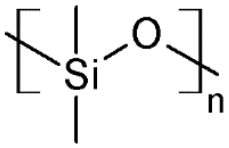

Figure 1.7. Chemical structure of the repeating unit of poly(dimethylsiloxane) (PDMS).

The biofouling protection of PDMS-based coatings has been improved by addition of “silicone oils” [2,46]. Milne [87] first in 1977 added a phenylmethylpolysiloxane oil to a PDMS coating to improve its fouling-release properties, and many other “oils” have been employed since then [2]. These “oils” are mostly oligomers and copolymers with different chemical compositions and structures and will be covered in a later section. It has been reported that these “oils” diffuse to the surface of the coating upon immersion [88,89]. Other studies [90,91] have shown that silicone-based coatings might present non-crosslinked PDMS chains on the surface, mostly originating from the incomplete curing of the binder. Berglin and Gatenholm [91] analysed detached barnacles from silicone coatings and detected presence of PDMS on the adhesives surface, which supports the idea of the barnacles settling on top of the “silicone oils” or non-crosslinked PDMS chains, which favours its release when hydrodynamic forces occur. In addition, it has been shown that cement produced by barnacles on PDMS-based fouling-release coatings have different structure and morphology when compared to other polymeric surfaces, which also favours its detachment [27].

Two main routes have been used to improve the mechanical properties of PDMS elastomers. On one side, inorganic fillers such as silica (SiO_2) and carbon nanotubes have been added to PDMS [2,46,92]. These fillers improve the mechanical properties by reinforcing the elastomeric structure [46,93,94]. However, these fillers can have some side effects, such as changing the hydrophobicity of the PDMS surface [46] or influencing the diffusivity of certain compounds through the elastomeric matrix [93,95]. This might affect the diffusion and fouling-release properties of the aforementioned “silicone oils”. Additionally, incorporation of polyurethane (PU) segments has also been investigated as a solution to the poor adhesion and durability properties of PDMS [2]. One of the first attempts to use silicone-PU systems for fouling-release purposes was in 1991, when R. R. Brooks patented the use of a siloxane-PU binder for biofouling inhibition [96]. Afterwards, PDMS-PU coatings have been explored by Webster

and coworkers [97,98]. The incompatibility of the PDMS and the PU moieties and their differences in surface free energy result in the so-called “self-stratification” of the coating, with a PDMS layer segregated on the surface that provides the low surface energy, and the polyurethane below, which provides tougher mechanical properties and better adhesion to the primer. Although the use of PDMS-PU coatings for fouling-release purposes has been patented by different groups [96,98,99], there is to our knowledge no commercial PDMS-PU coating for fouling-release purposes. Similarly, PDMS elastomers have been functionalized with epoxy and urea segments to improve their mechanical properties [2]. Recently, Marceaux et al. [100] copolymerized PDMS with poly(organosilazanes) and used it as binder for fouling-release coatings with superior mechanical properties. Finally, adhesion promoters (also known as coupling agents) have been added to PDMS-based coatings to enhance adhesion by covalent bonding with the substrate [2].

1.3.1.2.1 Crosslinking of PDMS elastomers

PDMS elastomeric coatings are mostly based on a crosslinked PDMS polymer. The crosslinking process of the coating film requires three components: a reactive PDMS binder, a crosslinker and a catalyst. Although many more routes can be used to crosslink PDMS elastomers, the two main routes in the FRC industry are the hydrosilylation and the condensation mechanisms [2]. The two processes are depicted in Figure 1.8.

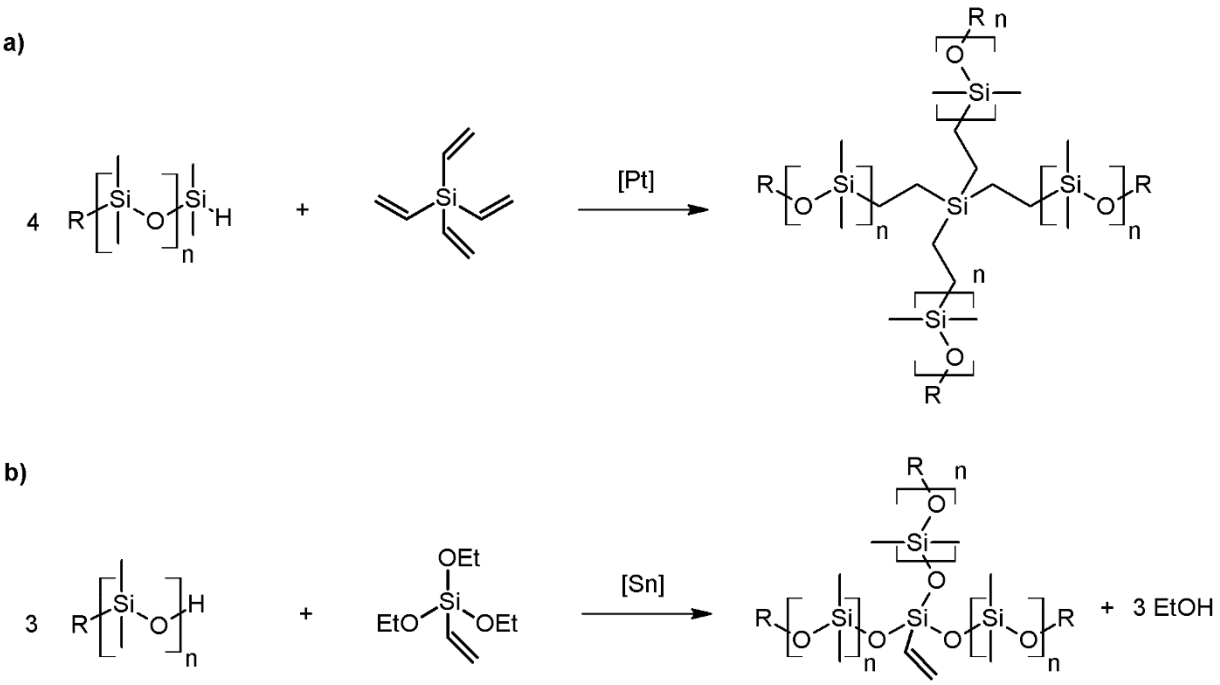

Figure 1.8. Crosslinking mechanisms used for PDMS binders: hydrosilylation (a) and condensation (b).

In the hydrosilylation cure route, a hydride-terminated PDMS is mixed with a crosslinker containing a number of vinyl groups in the presence of a platinum catalyst. Under mild conditions, the addition reaction of the Si-H across the double bond of the crosslinker takes place [101]. This route has the drawback of the potential toxicity of the platinum catalyst and the inhibition character of some oleophilic compounds that might be present [2], though no by-products are generated. In the condensation cure route, a silanol-terminated PDMS is mixed with a crosslinker containing a number of alkoxy groups in

the presence of a tin/titannate catalyst and moisture, that acts as cocatalyst [101]. Low molecular weight alcohols are generated as by products, though this mechanism is less sensitive to contaminants and therefore more robust. Nonetheless, some side reactions including the linear condensation of silanol groups have been reported [102]. A more detailed explanation of the curing mechanisms for silicones can be found elsewhere [101].

1.3.1.3 Fluorine-modified silicone-based FRC

It has been attempted to merge the key advantages of siloxanes and fluorine-based polymers to obtain coatings with very low values of elastic modulus, surface roughness and (critical) surface tension. Martinelli et al. [103] added acrylic polymers containing fluorinated and siloxane pendant groups as non-reactive additive (i.e. oil) to a PDMS-based coating. The settlement of cyprids was largely prevented by the addition of the polymer compared to the unmodified PDMS coating. Grunlan et al. [104] cured some PDMS-based coatings with a fluoro-modified crosslinker to decrease the settlement and favour the release of algae and barnacles. Thanawala and Chaudhury [79] prepared a perfluoroether additive, which was added to a PDMS coating. In this case, the perfluoroether-additive had a reactive end-group that allowed crosslinking with the PDMS matrix. Marabotti et al. [105] synthesized a copolymer containing both PDMS, PTFE and poly(ethylene glycol) (PEG) segments, and added it as ”oil” to a PDMS coating with successful results. With the incorporation of hydrophilic moieties such as polyethers, the fouling-release coatings were imparted some biofouling-inhibition properties. The use of non-stick strategies in fouling-release coatings will be discussed in a later section.

1.3.1.4 Drawbacks of FRC

In spite of the many advantages provided by fouling-release coatings and the amount of research and improvements within this technology, there are a series of challenges that still need to be overcome.

Traditional fouling-release coatings have relied on hydrophobic low-surface energy polymers to reduce the adhesion strength between the biofouling species and the coating. However, it has been reported that some organisms such as diatoms adhere more strongly on hydrophobic than hydrophilic surfaces [106]. These cannot be released by hydrodynamic forces as high as 30 knots [2] and have a significant impact on the frictional resistance of the ship [19,20]. In addition, the hydrophobic character of the surface of PDMS and fluorine-based coatings has been reported to change over time under immersion. This has been attributed to the thermodynamically driven rearrangement of polymer chains on the surface of the polymers [2,107]. The surfaces become thereby more hydrophilic, resulting in diminished fouling-release properties. Furthermore, fouling-release coatings rely mostly on hydrodynamic forces to keep ship hulls fouling-free. Hence, idle periods of the vessel result in rapid growth of biofouling on the coatings [108]. Finally, PDMS-based coatings still suffer from poor adhesion and mechanical properties.

From an environmental point of view, it has been suggested that the release of certain compounds from PDMS-based FRC might have harmful effects. For example, non-crosslinked PDMS chains, “silicone oils” and Pt- and Sn-based catalysts have been suggested as possible toxicity sources [2]. Nonetheless, several toxicological analysis have determined that the exudates from silicone coatings are not toxic to algae and crustaceans [109,110].

Finally, the long-term stability of silicone fouling-release coatings has been an issue in some areas. It has been reported that PDMS can undergo depolymerisation [2,101], oxidative degradation [8,101], hydrolysis [111], biotic degradation [101] and UV degradation [101], and significant amounts of mass loss (up to 2% per week) have been reported for underwater PDMS films [112]. Due to all these disadvantages, alternative strategies to withstand biofouling have been explored.

1.3.2 Non-stick coatings

Non-stick coatings rely on the "prevention of biofoulants" mechanism, where the biofoulant species are kept away from the surface of the coating, so that adsorption and irreversible settlement of biofoulants are supressed. This has been achieved by different means, mainly by modifying the physicochemical properties of the outermost layer of the immersed surface in different ways. Introduction of different chemistries [35,113], topographies [114] or toxic agents [42] are some of the methodologies employed to that purpose. These have intended to exploit mechanisms such as electrostatic repulsion, steric hindrance or water hydration to prevent the settlement of biofouling on different substrates [10,115–117]. In contrast to FR coatings, it has been shown that surface energy is not a key factor regarding non-stick surfaces [113]. These coatings are also known as "non-fouling", "biopassive", "inert", "antiadhesive" and "repellent" [118].

1.3.2.1 Functionalization of surfaces

Different approaches have been use to functionalize immersed surfaces with different molecules that provide fouling-inhibition properties, mainly comprising polymers and other organic moieties. These methods can be divided between physical- and chemical-based methods.

In physical-based methods, the functionalization of the surface does not involve chemical reactions and can be usually achieved in milder conditions [119]. Methods within this group include:

- Application of a thin layer (i.e. coating) of the polymer/copolymer on top of the surface [106,120].
- Adsorption of the polymer on the surface [121,122].
- Adsorption of a block copolymer. One of the blocks has attraction for the surface (i.e. acts as "anchor"), while the other block is the polymer that provides non-fouling properties. Methods such as Langmuir-Blodgett [123,124] and adsorption of block copolymers from micellar dispersions [119] are examples of this approach.
- Diffusion of surface-active "oils" from a polymer matrix (presented in a later section).
- Micro/nanoporous substrates with infused liquids. This approach relies on the fabrication of porous substrates, and the later infusion of a liquid on the pores of the substrate. The infused liquid (usually a polymer or copolymer) is capable of providing non-fouling properties while being stable due to interactions with the micro/nanoporous substrate [125]. This strategy is known as slippery liquid-infused porous surfaces (SLIPS).
- Other strategies have been employed, including application of a coating consisting of silica particles with covalently attached molecules on the surface [126] or PDMS coatings containing carboxyl-modified carbon nanotubes fillers [92].

On the other side, chemical-based methods take advantage of chemical reactions to functionalize surfaces with different polymeric moieties. This functionalization is assumed to provide better long-term stability due to the covalent bond between the surface and the non-fouling chemical molecule/chain. However, it is more expensive and not feasible in some big-scale applications. Some of the methods within this group include:

- Grafting polymers from a surface. In this approach, the surface to be functionalized is provided with a chemical initiator, and monomers and catalysts are usually found in a solution in contact with the surface. Upon contact with the initiators, polymerization takes place and polymer chains start growing from the surface as illustrated in Figure 1.9 [127–130].
- Grafting polymers to a surface. In this method, a polymer containing a reactive end-group is covalently bonded to a surface that contains a "chemical anchor". Therefore, there is higher control over the properties of the polymer chains, since these are previously polymerized in well-controlled conditions and then attached to the surface. However, lower grafting densities are obtained by this method due to steric hindrance [35,113,129,130].
- Addition of reactive polymers and copolymers (i.e. "reactive oils", described in a later section).

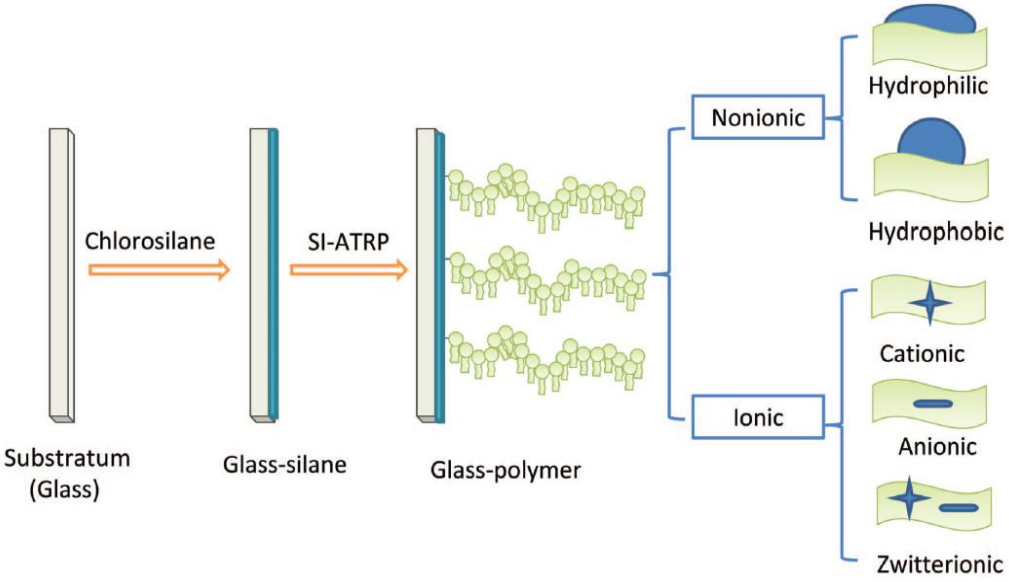

Figure 1.9. Schematic illustration of the grafting of different polymers from a glass surface. Reprinted with permission from [127].

The functionalization of surfaces with polymer chains results in a structure known as polymer brush as shown in Figure 1.10. Two main parameters characterize the properties of the brush, namely the length of the chains (i.e. molecular weight of the polymer) and the grafting density (i.e. spacing between neighbouring chains). These two parameters, together with the solvent-polymer compatibility determine whether the polymeric brush displays a "mushroom-like regime" or a "high-density brush regime", as described elsewhere and illustrated in Figure 1.10 [124].

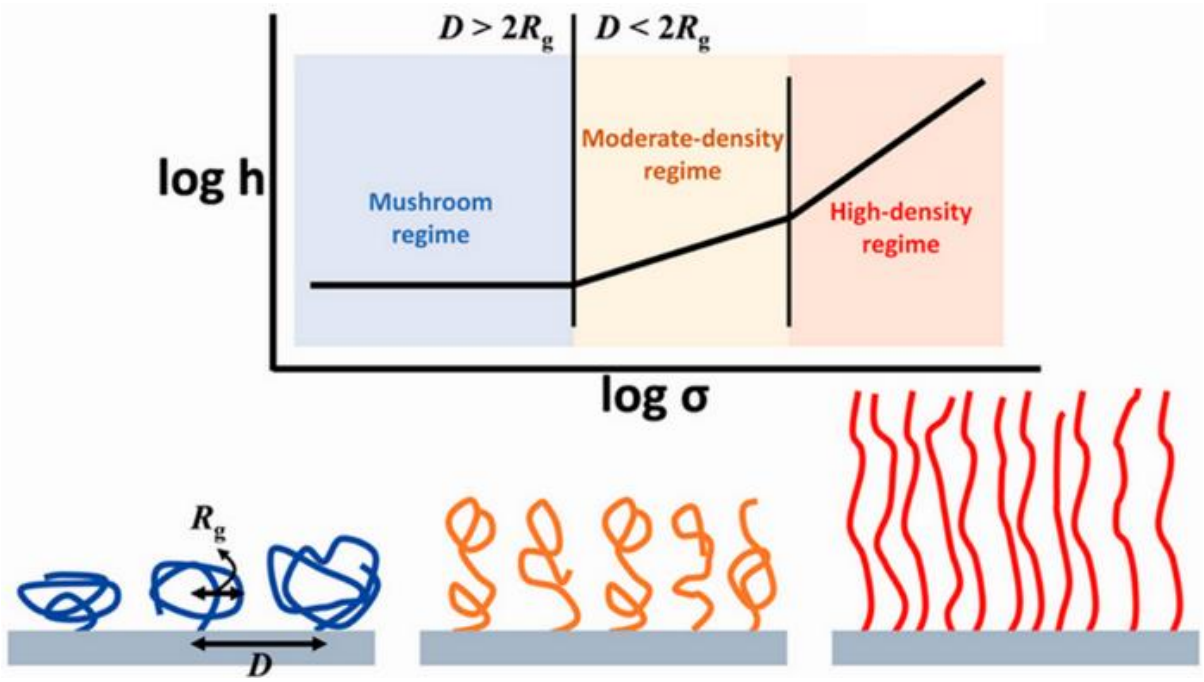

Figure 1.10. Schematic illustration of a polymer brush, with the transition from the "mushroom-like" regime to the "high-density" regime. The radius of gyration (R_g), the distance between neighbouring chains (D), the height of the brush (h) and the grafting density (σ) are depicted. Reprinted and adapted with permission from [131].

Some other approaches such as hydrogels and nanogels have also been employed to functionalize surfaces with hydrophilic polymers, as well as zwitterionic polymers and polysaccharides [37,132–135]. In these cases, the hydrophilic chains are "crosslinked" either by physical bonds (e.g. hydrogen bonds) or chemical bonds, and result in structures that can absorb large quantities of water and provide non-fouling properties. Polymers such as PEG, poly(2-hydroxyethyl methacrylate) (PHEMA) or poly(acrylic acid) (PAA) have been used as hydrogels for pharmaceutical applications [136].

1.3.2.1.1 Addition of surface-active "oils" to functionalize polymeric coatings

One of the main methods to functionalize coatings (and other polymeric materials) is the addition of the so-called "oils". These are typically non-reactive surface-active block copolymers, which are added to the coating mixture in small amounts (<10%). When the coatings are applied and cured, the copolymers can segregate to the surface of the film, thus modifying the physicochemical properties of the surface with negligible influence on the bulk properties of the coating [88,89]. Because these additives are added in small amounts and directly mixed without further preparation, they are an economical solution suitable for most applications. The functionalization of polymeric surfaces by addition of small amount of surface-active additives was introduced in the 1960s by Zisman and coworkers [137].

These surface-active copolymers generally consist of different blocks that impart various properties. One of the blocks is usually used as "anchor", which has a high affinity for the coating binder and provides adhesion. The other block(s) is often extended inside the water phase and provides the desired non-fouling properties, though other qualities such as wettability and lubricity have been likewise achieved [138,139]. Copolymers possessing different structures have been employed (e.g. ABA and grafted).

For example, Martinelli et al. [103] synthesized acrylate copolymers with pendant PDMS and PEG groups, as well as acrylate copolymers with pendant PDMS and PTFE groups of different lengths. They added these copolymers to PDMS-based coatings as non-reactive “oils”. Both the settlement of cyprids and the removal of *Ulva linza* sporelings could be improved by the addition of the oils. Likewise, Kavanagh et al. [89] added “fluid additives” (i.e. “oils”) with different chemistries and molecular weights to PDMS coatings for fouling-release purposes with positive results. Moreover, PEG-poly(propylene glycol)-PEG triblock copolymers have been used to suppress non-specific protein adsorption on PDMS-based microfluidic systems [140]. In addition to PDMS, other polymeric coatings have been functionalized by this method. Berndt et al. [141] synthesized acrylate copolymers containing bactericidal pendant groups and added them as “oils” to poly(n-butyl methacrylate) coatings. The addition of these “oils” resulted in a reduction of colonization of *Staphylococcus aureus* bacterium of up to 99.2% after 2 hours of exposure. Finally, fluorinated additives have been successfully used to modify the surface properties of styrene–(ethylene-co-butene)–styrene (SEBS) elastomers [88].

The amount of “oil” necessary to modify the surface properties of a polymeric material has also been studied. Significant differences can readily be observed when 1 wt% of these additives are added, though higher amounts (2-10 wt%) are required to reach saturation levels at the surface [88,142]. These “oils” are retained on the surface of the coating by physical forces between one of the blocks of the copolymer, known as “anchor” and the coating binder. The copolymer molecules sitting on the surface can be in principle removed, displaced or dissolved by hydrodynamic forces or by dissolution into seawater. When a copolymer molecule is “washed away”, another molecule can segregate from the bulk of the coating to replace it, in a “self-healing” process. This process can only be effective as long as there is copolymer in the bulk of the coating. Therefore, it has been suggested that these systems might not be suitable for long-term applications, if the release/loss of copolymer occurs at a fast pace. To overcome this limitation, the use of “reactive oils” has been explored [79,104,143]. These copolymers contain reactive end-groups that can covalently react with the binder, thus increasing their long-term stability. Webster and coworkers [97,144,145] have used this approach to functionalize PU-based coatings for fouling-release purposes. Reactive surface-active additives containing PDMS chains modified with acidic and PEG groups, as well as PDMS-based copolymers containing zwitterionic groups, have been added as reactive-oils to polyurethane mixtures with successful results. Nonetheless, the fact that the copolymer is covalently bonded can completely hinder its segregation to the surface, thus impeding the self-healing process previously described.

Different groups have studied the phenomena behind the segregation of these surface-active additives in different polymeric matrices. Lee and Archer [142,146] studied the diffusion of PS-PDMS and PS-PMMA polymers in PS hosts. They reported that differences in surface free energy and molecular weight have an influence on the segregation of these additives. In other words, the segregation of these additives to the surface of the polymeric materials results in a decrease of the energy of the system. Moreover, the effect of differences in chain-end entropy and the formation copolymer micelles in the host were discussed [142,146,147]. Bodkhe et al. [97] also attributed the segregation of PDMS copolymers in PU coatings to the difference in surface energy. Inutsuka [138] studied the diffusion of

PDMS-PEG-based block copolymers in a PDMS elastomer and attributed it to the enthalpic gain associated with the solvation of the PEG block when this segregates to the PDMS-water interface. Finally, Marabotti et al. [105] mentioned the incompatibility between the copolymer and the polymer matrix as a trigger for surface segregation.

1.3.2.2 Hydrophilic polymers

One group of surfaces capable of withstanding biofouling is polymeric surfaces. It has namely been shown that some polymer chains impart non-fouling properties when these are present on the surface of immersed materials, with hydrophilic polymers providing superior properties. In the 1980s, Vroman et al. [148] and E. W. Merrill [149] already found that hydrophilic substrates and polymers prevented protein and platelet adhesion for blood-contact materials. With regards to marine biofouling, Callow et al. [150] and Schilp et al. [151] found an inverse correlation between water wettability (i.e. hydrophilicity) and adhesion of proteins, cells and algal zoospores .

The fouling-inhibition properties of hydrophilic polymers involve different mechanisms related to the interaction of the polymeric chains with the foulants and the water molecules of the medium. Polymers with long, flexible chains have shown prevention of proteins and cells, and this has been attributed to steric hindrance. Moreover, hydrophilic polymers are known to interact with water by hydrogen bonding or electrostatic forces. It has been shown [115] that a layer of “ordered water” is formed at the surface of these polymers. This “bound-water” layer has some specific properties. As example, it does not freeze at 0°C due to the strong binding to the hydrophilic polymers and the surrounding water molecules [115]. The energy penalty associated with the displacement of this layer of ordered water molecules has been pointed as one of the main reasons of the biofouling-inhibition properties of these polymers [113,115]. The effect of the interfacial water molecules at the surface of these polymers and the influence on adsorption of proteins was already observed in the 1970s [117] and has been extensively studied [115,152,153].

One of the first polymers that was reported as potential biomaterial was polyethylene glycol (PEG). Salzman et al. [154] described already in 1981 its use as biomaterial, and in 1989 Tay [134] reported that the low non-specific protein adsorption of PEG was practically unique, when compared to all other synthetic polymers and hydrogels known at that time. Later, Whitesides and coworkers [35,113,155] showed that these properties were not unique for PEG, but other polymers and chemical moieties displayed similar characteristics. After reviewing up to 48 different chemistries, Ostuni et al. [113] found that the chemistries that provided the best properties (i.e. inertness) were characterized by 4 properties: polar (i.e. hydrophilic), presence of hydrogen bond acceptors, absence of hydrogen bond donors and electrical neutrality. These properties are very similar to those described by E. W. Merrill [149] in 1987. Merrill studied polymeric surfaces to diminish protein adsorption for biomedical purposes, and reported that the best-performing polymers were non-ionic, solvated by water and with hydrogen bonding accepting groups. Some other inert chemistries, however, have challenged these results. For example, some cationic and anionic chemistries have been successfully used to supress protein adsorption, as well as moieties with hydrogen bond donors (e.g. mannitol) [118,156].

The mostly utilized polymers for non-fouling purposes are briefly presented below.

1.3.2.2.1 Poly(ethylene glycol) – "The golden standard"

Poly(ethylene glycol) (PEG), also known as oligo(ethylene glycol) (OEG) or poly(ethylene oxide) (PEO) depending on the molecular weight, is a linear hydrophilic polymer which has been extensively used to prevent cell and non-specific protein adsorption on a range of surfaces in biomedicine and the marine environment. Some biocompatible polymers modified with PEG comprise PDMS and PU [8,140,157]. PEG has a surface energy >43 mN/m, much higher than the polymers used for fouling release-purposes, which are in the range of 15-25 mN/m. It has been demonstrated that surfaces functionalized with PEG provide resistance against the settlement of proteins, cells, bacteria and marine biofouling organisms [8,46,118]. These properties have been attributed to different reasons, mainly related to the characteristic of the PEG structure and its interaction with water molecules [9,46].

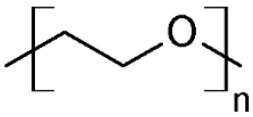

Figure 1.11. Chemical structure of the repeating unit of poly(ethylene glycol) (PEG).

Regarding the characteristics of the PEG backbone, it has been reported that the PEG chains are very mobile in water, when compared to other polymers. This has been attributed to: (1) its electrical neutrality, (2) the lack of bulky side-groups and (3) the properties of the C-O bond [9]. The mobility and flexibility of the chain on the interface with seawater shortens the contact time between the settling protein/cell and the surface, thereby decreasing the probability of settlement. Moreover, the presence of a protein or cell approaching the surface would result in the compression of the otherwise extended PEG chains in water. The compression of the chains results in a repulsive steric force that also hinders the settlement of foulants. Regarding the flexibility of PEG, Benhabbour et al. [158] functionalized some surfaces with PEG, and further modified the end-groups of the PEG chains with hydroxyl-terminated polyester dendrons. In spite of increasing the hydrophilicity of the surfaces, the adsorption of proteins increased. This fact was attributed to the reduced flexibility of the PEG chains due to the presence of the dendrons. Regarding the interaction with water, PEG is well-known for being very water soluble and strongly interacting with water via hydrogen bonding, in comparison to polyethers with similar structures [9]. PEG-functionalized surfaces have shown that the absorption of water can reach 80 vol% [46]. Moreover, PEG has a very low interfacial energy with water (~ 5 mN/m), in comparison to other polymers like PDMS (~52 mN/m) [46]. This strong interaction with water has been suggested as the main mechanism of the non-fouling properties of PEG [9,46]. For a protein/cell to settle on a PEG-hydrated surface, the water molecules must be displaced. However, due to the strong hydrogen bonds and low energy of the PEG-water interface, this process is very energetically unfavourable [9,46,115,118].

Many studies have focused on optimizing the non-fouling properties of surfaces functionalized with PEG chains. The main parameters that have been modified have been: (1) the molecular weight, (2) the architecture, (3) the grafting density and (4) the end-group of the PEG chains [8,46,151]. However, it has been reported that PEG is not very stable and easily degradable in a range of conditions. PEG

suffers namely from biotic and abiotic degradation in a range of pH and temperature conditions [8]. Moreover, PEG is oxidised in the presence of O_2 and transition metals (which are usually present in FR coatings and in the marine environment) [35]. This has limited the use of PEG as a long-term solution in some fields [8,118]. Therefore, alternative polymers have been explored to substitute PEG.

1.3.2.2.2 Other hydrophilic polymers

Poly(N-vinyl pyrrolidone) (PVP) is a hydrophilic non-ionic biocompatible polymer that has been used in medicine for more than 75 years. It was discovered in Germany in 1930 and used in World War II as a substitute for blood plasma [128]. It is characterized by its chemical stability and bioinertness, which has converted PVP into a potential candidate for PEG substitution [118,128]. Regarding its non-fouling properties, it has been mainly used for separation membranes with the aim of decreasing the adsorption of proteins. In addition to its non-fouling properties against proteins, it has been shown that its cytotoxicity is negligible, making it a good candidate for non-toxic non-fouling coatings [159].

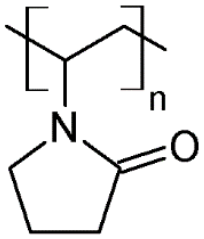

Figure 1.12. Chemical structure of the repeating unit of poly(N-vinyl pyrrolidone) (PVP).

Poly(2-hydroxyethyl methacrylate) (PHEMA) is a hydrophilic, electrically neutral polymer which has been used to provide protein repellency to silicon wafers [129]. PHEMA has also been copolymerized with PEG-based methacrylates and bactericidal peptides to obtain copolymers with thermal-responsive properties, and thus providing bactericidal and cell-repellence properties depending on the temperature of the medium [33]. Other acrylates with similar structures have also been exmployed with non-fouling purposes such as poly(2-methoxyethyl acrylate) (PMEA) or poly(2,3-dihydroxypropyl methacrylate) [119]. Sato et al. [160] functionalized PET substrates with a series of PMEA analogues with small variations in the chemical structures. They could prove that there were layers of hydrated water on the surface of the different PMEA analogues and a correlation between the amount of hydrated water and the adsorption of Bovine serum albumin (BSA) protein was found.

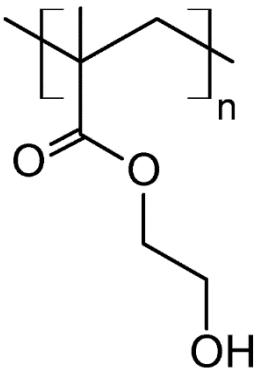

Figure 1.13. Chemical structure of the repeating unit of poly(2-hydroxyethyl methacrylate) (PHEMA).

Poly(2-methyl-2-oxazoline) (PMOXA) is a hydrophilic, non-ionic polymer that has been employed to reduce the adsorption of proteins and bacteria on immersed surfaces [118,161]. PMOXA was initially used to functionalize artificial membranes, and later other applications have been explored [161]. It was shown that the non-fouling properties of PMOXA where equal to those provided by PEG, with the advantage of superior stability in comparison to the easily degradable PEG [118]. In addition to PMOXA, other polyoxazolines have been applied with similar purposes [118]. It has been shown that PMOXA does not have cytotoxic effects, which allows the use of this polymer as environmentally friendly inert surface [118].

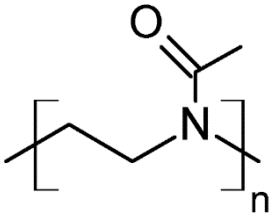

Figure 1.14. Chemical structure of the repeating unit of poly(2-methyl-2-oxazoline) (PMOXA).

Poly(vinyl alcohol) (PVA) is a hydrophilic, non-ionic polymer with high physical and chemical stability, which presents excellent integrity both in acidic and alkaline environments [162]. In 1983, Goosen and Sefton reported the use of PVA-based hydrogels functionalized with heparin due to its thromboresistant properties [163]. PVA has been additionally used to decrease the adsorption of proteins on separation membranes with successful results [162,164].

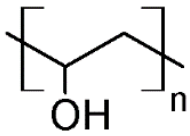

Figure 1.15. Chemical structure of the repeating unit of poly(vinyl alcohol) (PVA).

Poly(acrylic acid) (PAA) is a pH-sensitive hydrophilic polymer that has been used to reduce the amount of fouling in both organic (e.g. polyethersulfone) and inorganic (e.g. ZrO_2) separation membranes [165]. Its pH-responsiveness originates from the acidic groups in the backbone of the polymer, which can deprotonize (i.e. turn from COOH to COO^-) depending on the pH and the salinity [130,165]. Therefore, at acid pH the poly(acrylic acid) chains remain electrically neutral, while they acquire negative charge at alkaline pH, thus completely modifying their non-fouling properties.

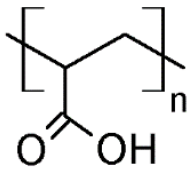

Figure 1.16. Chemical structure of the repeating unit of poly(acrylic acid) (PAA).

Poly(acrylamide) (PAM) is a hydrophilic, electrically neutral and stable polymer that has been employed to reduce protein and microbial adhesion on different substrates [166,167]. Different modified

polyacrylamides have been employed to design non-fouling brushes and nanogels. Some examples include poly[N-(2-hydroxypropyl) methacrylamide] (PHPMA) or poly(N-hydroxyethyl acrylamide) (PHEAA) [135,167]. In the case of PHEAA, it has been reported that it has almost negligible toxicity [135]. Moreover, some temperature-responsive polymers based on poly(acrylamide) have also been used with non-fouling purposes such as poly(N-isopropyl acrylamide) (PNIPAM) [168].

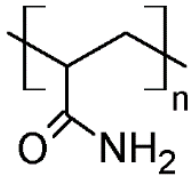

Figure 1.17. Chemical structure of the repeating unit of poly(acrylamide) (PAM).

1.3.2.3 Polyzwitterions

Polyzwitterions, also known as polybetaines, are a group of polymers whose repeating unit is characterized by its dipolar character, containing both positively and negatively charged ions depending on the dielectric permittivity, the pH and the ionic strength of the medium [132]. It should be noted that zwitterions are electrically neutral in spite of possessing both cations and anions, since both are found in the same amount in the zwitterionic polymer. Many studies have shown that zwitterions reduce the non-specific adsorption of proteins and bacteria [139]. Similar results have been achieved by use of pseudo-zwitterions (also known as polyampholites). Pseudozwitterionic brushes are surfaces grafted by anionic and cationic polymers in equal amounts, which leads to electrically neutral surfaces. The difference relies on the fact that the cation and the anion are not part of the same polymeric chain in pseudo-zwitterions [169]. Both structures can be schematically seen in Figure 1.18. It has been suggested that, similarly to PEG, zwitterions possess the hability to form layers of ordered water. In contrast with PEG, zwitterions interact with water by electrostatic (ion solvation) forces, which have been reported to be stronger than hydrogen bonds [170]. In addition, it has been shown that polyzwitterions are more stable than PEG and have therefore been explored as alternative to PEG for non-fouling purposes [41]. The three main families of polyzwitterions are briefly presented in Table 1.4.

Table 1.4. Structure, properties and applications of the main zwitterions used for fouling-release purposes.

	Poly(phosphorylcholine)	**Poly(carboxybetaine)**	**Poly(sulfobetaine)**
Structure	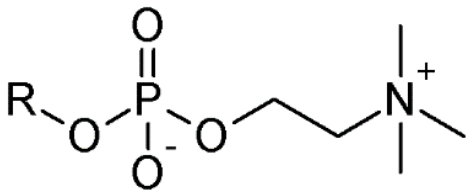	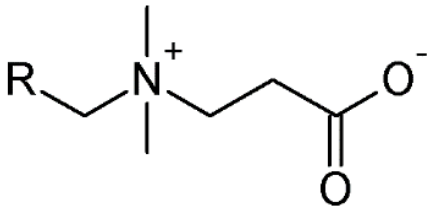	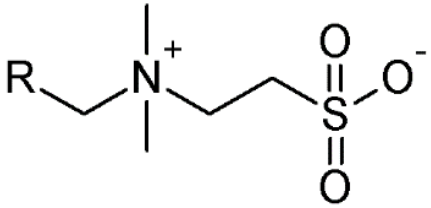
Cation / Anion	N^+ / PO_4^-	N^+ / CO_2^-	N^+ / SO_3^-
Polymer backbone	Acrylates, polyurethanes, siloxanes and vinyl polymers [132]	Acrylates [132,170]	Acrylates [132,170]
Properties and applications	Strongly affected by pH and ionic strength [41,171]. Protein-repellence [41,171]. Phospholipids (e.g. phosphatidylcholine) with similar structures are found in the outer membrane of different cells to impart non-thrombogenic properties [116,171]. Phosphatidylcholine-modified polyurethanes show blood compatibility and low levels of platelet adhesion [172].	Strongly affected by pH [41]. Protein- and cell-repellence [139]. Possibility of covalently bonding a biocide or an enzyme converting the carboxyl anion into an hydrolysable ester group [170]. The quaternary ammonium cation (N^+) of carboxybetaines can provide antimicrobial (toxic) properties if the carboxylate ion is “protected” (e.g. COOR or COOH) [173,174].	Functional under a range of pH, temperature and salt types [40]. Strongly affected by ionic strength [41]. Very hydrophilic surfaces (with contact angles as low as 12°) [40]. Protein- and bacteria-repellence [41,121]. Negligible cytotoxicity [175]. Applied to functionalize the surface of contact lenses [175].

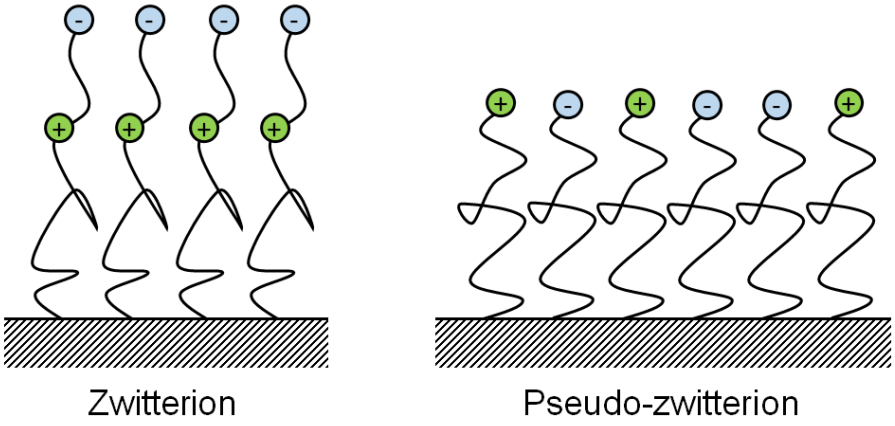

Figure 1.18. Depicted structure of zwitterionic and pseudo-zwitterionic surfaces.

1.3.2.4 Other organic moieties

1.3.2.4.1 Peptides and Peptoids

Peptides are biologically-occurring chains of aminoacids linked by amide bonds. Peptoids are synthesized structures that mimic the structure of peptides, but where the alkyl "R" group is attached to the nitrogen atom of the chain, instead of the α-carbon. The structures can be seen in Figure 1.19.

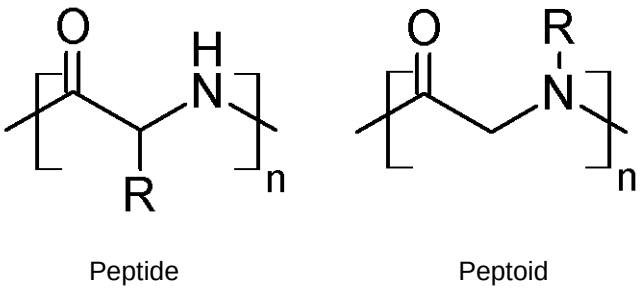

Figure 1.19. Chemical structure of the repeating unit of peptides (left) and peptoids (right).

Both peptides and peptoids have been successfully used to inhibit biofouling in different circumstances. Already in 1976 albumin peptides were employed to functionalize silicone elastomers used for blood-contact purposes with successful results [176]. In the 1990s, Lestelius and coworkers [177,178] studied the adsorption of proteins from blood plasma on monolayers of peptides (L-cysteine and glutathione) and a significant decrease in protein adsorption was observed on those surfaces. Furthermore, Bolduc and Masson [179] studied the adsorption of proteins on surfaces functionalized with single aminoacids. They reported decreased protein adsorption, with hydrophilic (i.e. polar) and ionic aminoacids performing slightly superior than the more hydrophobic ones. Statz et al. [180] reported remarkably low values of cell and protein adhesion on surfaces modified with peptidomimetic polymers when exposed to cell cultures for up to 5 months. The decrease in cell adhesion was up to 2 orders of magnitude compared to the "state-of-the-art" technologies [179,180]. Similar results have been accomplished by other groups and can be found elsewhere [169]. Calabrese et al. [120] used amphiphilic copolymers based on oligopeptides to functionalize the surface of SEBS elastomers. The settlement of spores and sporelings of *Ulva linza* on the surface was diminished by the presence of the oligopeptides-based copolymers.

1.3.2.4.2. Polysaccharides

Polysaccharides are long hydrophilic chains of monosaccharides (i.e. carbohydrates), which are linked by glycosidic bonds. Polysaccharides are hydrophilic and (usually) electrically neutral, and provide strong interactions with water, creating an hydration layer via hydrogen bonding. Polysaccharides are widely produced by marine organisms [133] and it has been shown that the external region of cell membranes is dominated by glycosylated molecules, which prevent protein and cell adhesion [181]. Moreover, it has been reported that polysaccharides generated by marine algae impart anti-viral properties and are chemically stable under a range of temperatures and pH [182]. Therefore, many have considered polysaccharides the natural substitutes for hydrophilic synthetic polymers as PEG [122]. In the 1960s Salzman and coworkers [183–185] functionalized surfaces with polysaccharides such as heparin and cellulose for the biomedicine industry due to their non-thrombogenic properties. In the early 80s it was reported that surfaces functionalized with polysaccharides such as heparin and dextran could decrease the amount of protein adsorption (e.g. fibrinogen) on surfaces exposed to blood plasma [186,187]. In 1991, Prime and Whitesides [155] demonstrated that surfaces coated with argarose could prevent protein adsorption, though PEG moieties provided superior results. Conversely, Österberg et al. [122] compared the resistance to protein adsorption of PEG and polysaccharides and did not find significant differences. In addition, saccharide moieties have been used to functionalize polymers for non-fouling purposes. For example, Chen et al. [188] reported a preparation method for polyurethanes containing glucose groups, which were oriented at the surface of the polyurethane-base film and provided good blood compatibility and low platelet adhesion.

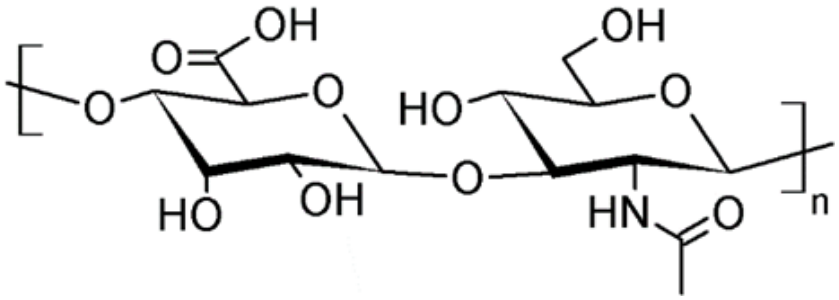

Figure 1.20. Chemical structure of the repeating unit of hyaluronic acid.

Although it has been shown that the functionalization of different surfaces with polysaccharides results in a large reduction on the adhesion of proteins and cells [37,189], the results are less promising regarding some marine organisms such as algae and barnacles [37].

1.3.2.5 Enzymes

Enzymes are proteins that have the ability of acting as macromolecular organic catalysts. Because enzymes are rapidly biodegraded, they have been explored as an environmentally friendly alternative to traditional biocides for antifouling coatings [190]. Different antifouling mechanisms have been described for enzymes, which include hydrolysis of cell tissues [190], degradation of the adhesives secreted by biofoulants [191] or production of hydrogen peroxide [190], which has toxic effects on some fouling species. The different mechanism are depicted in Figure 1.21.

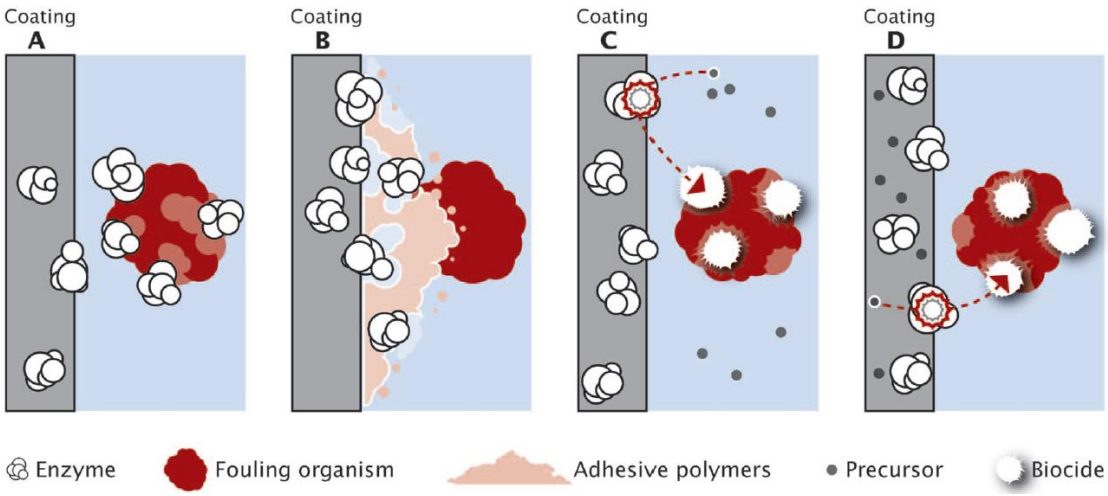

Figure 1.21. Schematic illustration of some antifouling mechanisms provided by enzymes. Reprinted with permission from [190].

To functionalize coatings with enzymes, different strategies have been used. S. M. Olsen [28] dispersed enzymes within a rosin-acrylic matrix, while Vaterrodt et al. [192] functionalized the surface of PDMS coatings with enzymes by embedding them in a zwitterionic polymer brush by electrostatically driven (i.e. ionic) interactions. Moreover, Zanoni et al. [5] covalently attached Proteinase K to the surface of silica-based nanobeads. Finally, Kristensen et al. reported a method to encapsulate hydrogen peroxide producing enzymes in silica capsules, and dispersing the capsules in a coating matrix as a replacement for traditional biocides [193]. In addition, the antimicrobial properties of some enzymes have been exploited for coatings in the food-packaging industry [194].

1.3.2.6 Biocides

In spite of the drawbacks associated with the use of biocides, some research has been focused on employing biocidal compounds in a more environmentally friendly manner. It is believed that the gains associated with the use of biocides in terms of decreased fuel consumption and CO_2 emissions can outweigh its toxicity-related drawbacks. The current development of biocides has focused on developing a more environmentally friendly use of biocides by:

1) Decreasing the environmental consequences for non-targeted species [52,54].
2) Finding biocidal compounds with low inhibition/effective concentration (EC50) but high lethal concentrations (LC50) [48,49].
3) Optimizing the release profile of the biocide (e.g. decrease the release rate of biocides when it is not required) [48].
4) Decreasing its bioaccumulation and/or increase its degradation rate [195].

Some successful examples of new biocides include Econea, that has low hydrolytic stability, and Selektope, that is effective at very low concentrations by causing hyperactivity in barnacle larvae [48,196]. Some other examples of novel strategies regarding the use of biocides in non-fouling coatings are reviewed in Table 1.5.

Table 1.5. Summary of some novel environmentally friendly use of biocides in fouling-control coatings

Strategy	Examples	References
Natural biocidal compounds	Furans and lactones	[24,42,48,195,197]
	Peptides	[6,198]
	Peptides in combination with hydrophilic polymers (e.g. PEG and PHEMA)	[33]
Decrease release rate of biocides	Covalently bonding biocides to different polymers such as PDMS and polyacrylamide	[84,199]
	Use of antimicrobial quaternary ammonium compounds (QAC)-based polymers	[200,201]
	QAC in combination with hydrophilic polymers (e.g. PEG)	[202]
	QAC in combination with zwitterionic polymers (e.g. polysulfobetaine)	[203]
	QAC in combination with enzymes	[192]
	Exploiting interaction of some biocides with different molecules and polymers (for example, by coordination chemistry)	[195,204]
	Immobilized biocides in a polymeric matrix, which are reached by biofoulants which penetrate inside the coating (e.g. barnacles)	[48]
Others	Compounds with toxic effects at very low concentrations	[3,49]
	Ammonium salt-based acrylic binders, where the ammonium salts released have low toxicity (low EC50[a] and high LC50[b]) and are readily biodegraded	[205]
	Fillers that generate compounds that inhibit bacterial adhesion (e.g. singlet oxygen and nitric oxide)	[5]

[a] EC50 – Effective concentration that inhibits 50% of biofouling growth
[b] LC50 – Lethal concentration that kills 50% of the biofouling organism

1.3.2.7 Topographies

Some studies have obtained inspiration from the strategies followed by some marine organisms that are able to completely suppress biofilm growth due to the physical properties of their surfaces [114,206,207]. Because these coatings solely rely on the topography of the surface to provide non-fouling properties, they are excellent potential solutions as environmentally friendly coatings. For example, Sharklet AF™ has been developed inspired by shark skin topography and applied for catheters and films. Some studies have shown that the settlement of *Ulva spores* on Sharklet AF™ was reduced by 86% due to topographical effects [207].

Different mechanisms have been suggested to impart non-fouling properties to surfaces with topographical features:

- Changes in wettability of the surface [207].
- Influence on the dynamics of water flow near the surface [2].
- Reduced contact area due to the presence of “walls” and “valleys” (depending on the size and spacing of the topographical features), which hinders the settlement of biofouling [46].
- Presence of trapped air on the cavities of superhydrophobic topographical surfaces [208].

One of the most studied strategies is the presence of certain topographies or textures on the surfaces of marine organisms. For example, the skin of sharks is well-known for exhibiting a surface texture that inhibits biofouling. Similarly, marine mammals, echinoderms, algaes or molluscs exhibit special surface topographies that can resist biofouling. It should be noted that the topographical elements on the surface of these marine organisms vary both in size and shape. For example, molluscs present ripples on their surfaces usually in the order of 1 µm, while sharks present scale riblets with sizes ranging between 50 and 300 µm [114]. Some examples can be seen in Figure 1.22.

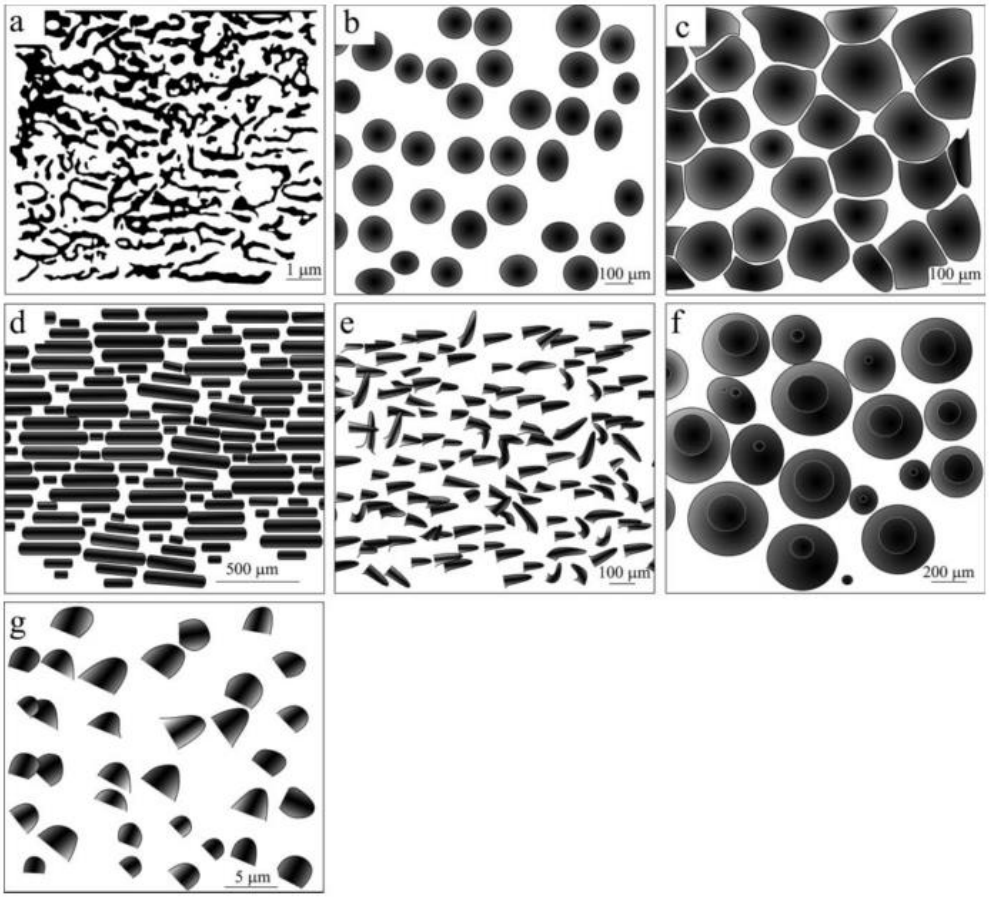

Figure 1.22. Schematic illustration of some surfaces microtopographies from different marine animals. Reprinted with permission from [114].

Different groups have fabricated artificial surfaces with topographical features to supress biofouling. For instance, Schumacher et al. [108,206] fabricated PDMS-based surfaces with specific microtopographies to supress the settlement of *Ulva spores* with successful results. A relationship between the aspect ratio (height/width) of the features and the settlement of *Ulva* and *B. amphitrite* barnacle was found.

1.3.2.8 Others

Ambiguous or amphiphilic surfaces, with nanodomains of both hydrophilic and hydrophobic character have also been shown to provide non-fouling properties [120,209]. In addition, superhydrophobic polymers have been also employed to provide inert surfaces [208]. Finally, Duong et al. [210] and Pavlovic [211] have recently reported the use of biocide-free hybrid antifouling-fouling-release coatings. These hydrophobic coatings are based on copolymers containing PDMS and silyl-acrylate-based blocks

and its inhibition properties against the settlement of marine bacteria has been shown, both in the laboratory and in static immersion in the Mediterranean Sea [210].

1.4 Conclusions

The settlement of biofouling on ship hulls has been a problem since ancient times. The addition of toxic compounds to keep the hulls fouling-free was the most extended approach in the shipping industry. However, evidence of serious environmental consequences for the marine environment resulted in significant changes in this field. As a result, the development of environmentally friendly coatings to protect ship hulls has experienced a significant increase in the last decades. Although the first solutions relied on hydrophobic PDMS surfaces, the functionalization of PDMS and other substrates by a variety of hydrophilic polymers, peptides, polysaccharides, zwitterions, enzymes and biocides has proven to impart biofouling-inhibition properties. It is clear from this chapter that a great number of solutions have been explored in laboratory experiments to decrease the settlement of proteins, cells and organisms on immersed surfaces. However, not all the presented approaches might be suitable for the inhibition of marine biofouling on ship hulls due to the severe requirements associated with the shipping industry in terms of ease of application, low cost and extended lifetime.

1.5 References

[1] D.M. Yebra, S. Kiil, K. Dam-Johansen, Antifouling technology—past, present and future steps towards efficient and environmentally friendly antifouling coatings, *Prog. Org. Coatings*. **50** (2004) 75–104.

[2] M. Lejars, A. Margaillan, C. Bressy, Fouling release coatings: A nontoxic alternative to biocidal antifouling coatings, *Chem. Rev.* **112** (2012) 4347–4390.

[3] S. Dobretsov, M. Teplitski, M. Bayer, S. Gunasekera, P. Proksch, V.J. Paul, Inhibition of marine biofouling by bacterial quorum sensing inhibitors, *Biofouling*. **27** (2011) 893–905.

[4] A. Heyer, Microbiollogically influenced corrosion in ship ballast tanks, Delft University of Technology, Alblasserdam, The Netherlands (2013).

[5] M. Zanoni, O. Habimana, J. Amadio, E. Casey, Antifouling activity of enzyme-functionalized silica nanobeads, *Biotechnol. Bioeng.* **113** (2016) 501–512.

[6] R. Trepos, G. Cervin, C. Pile, H. Pavia, C. Hellio, J. Svenson, Evaluation of cationic micropeptides derived from the innate immune system as inhibitors of marine biofouling, *Biofouling*. **31** (2015) 393–403.

[7] I. Fitridge, T. Dempster, J. Guenther, R. de Nys, The impact and control of biofouling in marine aquaculture: a review, *Biofouling*. **28** (2012) 649–69.

[8] A. Camós Noguer, S.M. Olsen, S. Hvilsted, S. Kiil, Long-term stability of PEG-based antifouling surfaces in seawater, *J. Coatings Technol. Res.* **13** (2016) 567–575.

[9] J. Lee, H. Lee, J. Andrade, Blood compatibility of polyethylene oxide surfaces, *Prog. Polym. Sci.* **20** (1995) 1043–1079.

[10] I. Szleifer, Protein adsorption on surfaces with grafted polymers: A theoretical approach, *Biophys. J.* **72** (1997) 595–612.

[11] R.O. Darouiche, Treatment of infections associated with surgical implants, *N. Engl. J. Med.* **350** (2002) 1422–1429.

[12] R.D. Scott, The direct medical costs of healthcare-associated infections in U.S. hospitals and the benefits of prevention, *Natl. State Heal. Infect. Prog. Rep.* (2009) 13.

[13] (Woods Hole Oceangraphic Institute) WHOI, Marine fouling and its prevention, US Naval Institute Press, Annapolis, Maryland, US (1952).

[14] R.L. Townsin, D.S. Spencer, M. Mosaad, G. Patience, Rough Propeller Penalties, *Soc. Nav. Archit. Mar. Eng. Trans.* **93** (1985) 165 – 187.

[15] H.M. Horbund, A. Freiberger, Slime films and their role in marine fouling: a review, *Ocean Engng.* **1** (1970) 631–634.

[16] A. Lindholdt, K. Dam-Johansen, S.M. Olsen, D.M. Yebra, S. Kiil, Effects of biofouling development on drag forces of hull coatings for ocean-going ships: a review, *J. Coatings Technol. Res.* **12** (2015) 415–444.

[17] Y. Hiraga, Experimental investigations on the resistance of long planks and ships, *Zosen Kiokai*. **55** (1934) 159–199.

[18] R.L. Townsin, The Ship Hull Fouling Penalty, *Biofouling*. **19** (2003) 9–15.

[19] M.P. Schultz, Effects of coating roughness and biofouling on ship resistance and powering, *Biofouling*. **23** (2007) 331–341.

[20] M.P. Schultz, J.A. Bendick, E.R. Holm, W.M. Hertel, Economic impact of biofouling on a naval surface ship, *Biofouling*. **27** (2011) 87–98.

[21] M. Salta, J.A. Wharton, P. Stoodley, S.P. Dennington, L.R. Goodes, S. Werwinski, U. Mart, R.J.K. Wood, K.R. Stokes, Designing biomimetic antifouling surfaces, *Philos. Trans. A. Math. Phys. Eng. Sci.* **368** (2010) 4729–4754.

[22] M.E. Callow, R.L. Fletcher, The influence of low surface energy materials on bioadhesion-a review, *Int. Biodeterior. Biodegradation*. **34** (1994) 333–348.

[23] A. Garg, A. Jain, N.B. Bhosle, Chemical characterization of a marine conditioning film, *Int. Biodeterior. Biodegrad.* **63** (2009) 7–11.

[24] S. Abarzua, S. Jakubowski, Biotechnological investigation for the prevention of biofouling. 1. Biological and biochemical principles for the prevention of biofouling, *Mar. Ecol. Prog. Ser.* **123** (1995) 301.

[25] P.J. Molino, R. Wetherbee, The biology of biofouling diatoms and their role in the development of microbial slimes, *Biofouling*. **24** (2008) 365–379.

[26] D.J. Crisp, G. Walker, G.A. Young, A.B. Yule, Adhesion and substrate choice in mussels and barnacles, *J. Colloid Interface Sci.* **104** (1985) 40–50.

[27] K. Kamino, Mini-review: barnacle adhesives and adhesion, *Biofouling*. **29** (2013) 735–49.

[28] S.M. Olsen, Controlled release of environmentally friendly antifouling agents from marine coatings, Technical University of Denmark, Kongens Lyngby, Denmark (2009).

[29] R.Y. Morita, R.D. Haight, Temperture Effects on the Growth of an Obligate Psychrophilic Marine Bacterium, *Limnol. Oceanogr.* **9** (1964) 103–106.

[30] D.J.S. Montagnes, M. Franklin, Effect of temperature on diatom volume, growth rate, and carbon and nitrogen content: Reconsidering some paradigms, *Limnol. Oceanogr.* **46** (2001) 2008–2018.

[31] D.M. Yebra, S. Kiil, C.E. Weinell, K. Dam-Johansen, Dissolution rate measurements of sea water soluble pigments for antifouling paints: ZnO, *Prog. Org. Coatings*. **56** (2006) 327–337.

[32] S. Kiil, C.E. Weinell, M.S. Pedersen, K. Dam-Johansen, Analysis of self-polishing antifouling paints using rotary experiments and mathematical modeling, *Ind. Eng. Chem. Res.* **40** (2001)

3906–3920.

[33] X. Laloyaux, E. Fautré, T. Blin, V. Purohit, J. Leprince, T. Jouenne, A.M. Jonas, K. Glinel, Temperature-responsive polymer brushes switching from bactericidal to cell-repellent, *Adv. Mater.* **22** (2010) 5024–5028.

[34] S.O. Stanley, R.Y. Morita, Salinity effect on the maximal growth temperature of some bacteria isolated from marine enviroments, *J. Bacteriol.* **95** (1968) 169–173.

[35] R.G. Chapman, E. Ostuni, M.N. Liang, G. Meluleni, E. Kim, L. Yan, G. Pier, H.S. Warren, G.M. Whitesides, Polymeric thin films that resist the adsorption of proteins and the adhesion of bacteria, *Langmuir*. **17** (2001) 1225–1233.

[36] P. Landini, G. Jubelin, C. Dorel-Flamant, The molecular genetics of bioadhesion and biofilm formation, in: A.M. Smith, J.A. Callow (Eds.), Biol. Adhes., Springer, Berlin (2006) pp. 21–40.

[37] X. Cao, M.E. Pettit, S.L. Conlan, W. Wagner, A.D. Ho, A.S. Clare, J.A. Callow, M.E. Callow, M. Grunze, A. Rosenhahn, Resistance of polysaccharide coatings to proteins, hematopoietic cells, and marine organisms, *Biomacromolecules*. **10** (2009) 907–915.

[38] M. Camps, A. Barani, G. Gregori, A. Bouchez, B. Le Berre, C. Bressy, Y. Blache, J.-F. Briand, Antifouling Coatings Influence both Abundance and Community Structure of Colonizing Biofilms: a Case Study in the Northwestern Mediterranean Sea, *Appl. Environ. Microbiol.* **80** (2014) 4821–4831.

[39] S.M.M. Gutierre, PH tolerance of the biofouling invasive hydrozoan Cordylophora caspia, *Hydrobiologia*. **679** (2012) 91–95.

[40] Y. Chang, S.C. Liao, A. Higuchi, R.C. Ruaan, C.W. Chu, W.Y. Chen, A highly stable nonbiofouling surface with well-packed grafted zwitterionic polysulfobetaine for plasma protein repulsion, *Langmuir*. **24** (2008) 5453–5458.

[41] R.E. Holmlin, X. Chen, R.G. Chapman, S. Takayama, G.M. Whitesides, Zwitterionic SAMs that Resist Nonspecific Adsorption of Protein from Aqueous Buffer, *Langmuir*. **17** (2001) 2841–2850.

[42] N. Fusetani, Biofouling and antifouling, *R. Soc. Chem.* **21** (2004) 94–104.

[43] W. Admiraal, H. Peletier, Influence of Seasonal Variations of Temperature and Light on the Growth Rate of Cultures and Natural Populations of Intertidal Diatoms, *Mar. Ecol. Prog. Ser.* **2** (1980) 35–43.

[44] K.A. Zargiel, G.W. Swain, Static vs dynamic settlement and adhesion of diatoms to ship hull coatings, *Biofouling*. **30** (2014) 115–129.

[45] K. Thomas, K. Raymond, J. Chadwick, M. Waldock, The effects of short-term changes in environmental parameters on the release of biocides from antifouling coatings - cuprous-oxide and tributyltin, *Appl. Organomet. Chem.* **13** (1999) 453–460.

[46] A.G. Nurioglu, A.C.C. Esteves, G. de With, Non-toxic, non-biocide-release antifouling coatings based on molecular structure design for marine applications, *J. Mater. Chem. B*. **3** (2015) 6547–6570.

[47] A. Milne, G. Hails, Marine Paint, US4021392 (1977).

[48] E. Pinori, M. Berglin, L.M. Brive, M. Hulander, M. Dahlström, H. Elwing, Multi-seasonal barnacle (Balanus improvisus) protection achieved by trace amounts of a macrocyclic lactone (ivermectin) included in rosin-based coatings, *Biofouling*. **27** (2011) 941–953.

[49] K. Kon-ya, N. Shimidzu, W. Miki, M. Endo, Indole Derivatives as Potent Inhibitors of Larval Settlement by the Barnacle, Balanus amphitrite, *Biosci. Biotechnol. Biochem.* **58** (1994) 2178–2181.

[50] C. Alzieu, P. Michel, I. Tolosa, E. Bacci, L.D. Mee, J.W. Readman, Organotin compounds in the

Mediterranean: A continuing cause for concern, *Mar. Environ. Res.* **32** (1991) 261–270.

[51] B. -m. Z. Newby, M.K. Chaudhury, H.R. Brown, Macroscopic Evidence of the Effect of Interfacial Slippage on Adhesion, *Science*. **269** (1995) 1407–1409.

[52] E. Pinori, H. Elwing, M. Berglin, The impact of coating hardness on the anti-barnacle efficacy of an embedded antifouling biocide, *Biofouling*. **29** (2013) 763–773.

[53] J.W. Readman, B. van Hattum, D. Barcelo, T.A. Albanis, B. Riemann, H. Blanck, K. Gustavson, J. Tronczynski, A. Jacobson, Assessment of antifouling agents in coastal environments, European Commission, (2002).

[54] N. Voulvoulis, M.D. Scrimshaw, J.N. Lester, Review Alternative Antifouling Biocides, *Appl. Organomet. Chem.* **143** (1999) 135–143.

[55] D.M. Yebra, P. Català, Antifouling Coating Technology — Part 2, *Mater. Perform.* **50** (2011) 42–46.

[56] M.A. Champ, A review of organotin regulatory strategies, pending actions, related costs and benefits, *Sci. Total Environ.* **258** (2000) 21–71.

[57] R. Robert, E. His, Action de l'acetate de tributyle-étain sur les oeufs et les larves D de deux mollusques d'interêt commercial : Crassostrea Rigas (Thunberg) et Mytilus galloprovincialis (Lmk), *Com. La Maric.* **42** (1981) 1–16.

[58] E. His, R. Robert, Action d'un sel organo-métallique, l'acétate de tributyle-étaine sur les oeufs et les larves D de Crassostrea gigas (Thunberg), (1980) 1–10.

[59] E. His, R. Robert, Development des Véligères de Crassostrea gigas dans le basin d'Arcachon études sur les mortalités larvaires, *Rev. Trav. Inst. Pêches Marit.* **47** (1985) 63–88.

[60] C. Alzieu, M. Heral, Y. Thibaud, M.J. Dardignac, M. Feuillet, Influence des peintures antisalissures à base d'organostanniques sur la calcification de la coquille de l'huître *Crassostrea gigas*, *Rev. Des Trav. l'Institut Des Pêches Marit.* **45** (1981) 101–116.

[61] C. Alzieu, Y. Thibaud, M. Heral, B. Boutier, Evaluation des Risques dus a l'emploi des Peintures Anti-Salissures Dans les Zones Conchylicoles, *Rev. Des Trav. l'Institut Des Pêches Marit.* **44** (1980) 305–348.

[62] C. Alzieu, Environmental problems caused by TBT in France: Assessment, regulations, prospects, *Mar. Environ. Res.* **32** (1991) 7–17.

[63] C.L. Alzieu, J. Sanjuan, J.P. Deltreil, M. Borel, Tin contamination in Arcachon Bay: Effects on oyster shell anomalies, *Mar. Pollut. Bull.* **17** (1986) 494–498.

[64] S. Kiil, K. Dam-Johansen, C.E. Weinell, M.S. Pedersen, S.A. Codolar, Estimation of Polishing and Leaching Behaviour of Antifouling Paints Using Mathematical Modelling: A Literature Review, *Biofouling*. **19** (2003) 37–43.

[65] A.M. Rouhi, The squeeze on tributyltins, *Chem Eng News Arch.* **76** (1998) 41–42.

[66] D.E. Wendt, G.L. Kowalke, J. Kim, I.L. Singer, Factors that influence elastomeric coating performance: the effect of coating thickness on basal plate morphology, growth and critical removal stress of the barnacle Balanus amphitrite, *Biofouling*. **22** (2006) 1–9.

[67] R.E. Baier, Surface behaviour of biomaterials: The theta surface for biocompatibility, *J. Mater. Sci. Mater. Med.* **17** (2006) 1057–1062.

[68] R.E. Baier, Influence of the initial surface contidition of materials on bioadhesion, in: Third Int. Congr. Mar. Corros. Fouling, (1972) pp. 633–639.

[69] R.E. Baier, Adhesion in Biological Systems, Academic Press, New York, US (1970).

[70] M.E. Schrader, On adhesion of biological substances to low energy solid surfaces, *J. Colloid Interface Sci.* **88** (1982) 296–297.

[71] S.C. Dexter, J.D. Sullivan, J. Williams, S.W. Watson, Influence of substrate wettability on the attachment of marine bacteria to various surfaces, *Appl. Microbiol.* **30** (1975) 298–308.

[72] A. Becka, G. Loeb, Ease of removal of barnacles from various polymeric materials, *Biotechnol. Bioeng.* **26** (1984) 1245–1251.

[73] S.C. Dexter, Influence of substratum critical surface tension on bacterial adhesion-in situ studies, *J. Colloid Interface Sci.* **70** (1979) 346–354.

[74] R.F. Brady, Properties which influence marine fouling resistance in polymers containing silicon and fluorine, *Prog. Org. Coatings*. **35** (1999) 31–35.

[75] B.A. Jucker, H. Harms, A.J.B. Zehnder, Adhesion of the Positively Charged Bacterium, *Microbiology*. **178** (1996) 5472–5479.

[76] M.C.M. van Loosdrecht, J. Lyklema, W. Norde, G. Schraa, A.J.B. Zehnder, M.C. van Loosdrecht, Electrophoretic mobility and hydrophobicity as a measure to predict the initial steps of bacterial adhesion, *Appl. Environ. Microbiol.* **53** (1987) 1898–1901.

[77] R.F. Brady, I.L. Singer, Mechanical factors favoring release from fouling release coatings, *Biofouling*. **15** (2000) 73–81.

[78] J.G. Kohl, I.L. Singer, Pull-off behavior of epoxy bonded to silicone duplex coatings, *Prog. Org. Coatings*. **36** (1999) 15–20.

[79] S.K. Thanawala, M.K. Chaudhury, Surface modification of silicone elastomer using perfluorinated ether, *Langmuir*. **16** (2000) 1256–1260.

[80] R.F. Brady, Fluoropolymers, *Chem. Br.* (1990) 427–430.

[81] D.E. Field, Fluorinated polyepoxy and polyurethane coatings, *J. Coatings Technol.* **48** (1976) 43–47.

[82] E. Robbart, Ship's hull coated with anti-fouling silicone resin and method of coating, US2986474 (1961).

[83] B. Watermann, H. Berger, H. Sönnichsen, P. Willemsen, Performance and effectiveness of non-stick coatings in seawater, *Biofouling*. **11** (1997) 101–118.

[84] J. Thomas, S.-B. Choi, R. Fjeldheim, P. Boudjouk, Silicones Containing Pendant Biocides for Antifouling Coatings, *Biofouling*. **20** (2004) 227–236.

[85] J.K. Pike, T. Ho, K.J. Wynne, Water-induced surface rearrangements of poly (dimethylsiloxane-urea-urethane) segmented block copolymers, *Chem. Mater.* **8** (1996) 856–860.

[86] J.E. Mark, Polymer Data Handbook, 2nd ed., Oxford University Press, New York (2009).

[87] A. Milne, Anti-fouling marine compositions, US4025693 (1977).

[88] A.P. Narrainen, L.R. Hutchings, I. Ansari, R.L. Thompson, N. Clarke, Multi-End-Functionalized Polymers: Additives to Modify Polymer Properties at Surfaces and Interfaces, *Macromolecules*. **40** (2007) 1969–1980.

[89] C.J. Kavanagh, G.W. Swain, B.S. Kovach, J. Stein, C. Darkangelo-Wood, K. Truby, E. Holm, J. Montemarano, A. Meyer, D. Wiebe, The Effects of Silicone Fluid Additives and Silicone Elastomer Matrices on Barnacle Adhesion Strength, *Biofouling*. **19** (2003) 381–390.

[90] A. Meyer, R. Baier, C.D. Wood, J. Stein, K. Truby, E. Holm, J. Montemarano, C. Kavanagh, B. Nedved, C. Smith, G. Swain, D. Wiebe, Contact angle anomalies indicate that surface-active eluates from silicone coatings inhibit the adhesive mechanisms of fouling organisms, *Biofouling*.

22 (2006) 411–423.

[91] M. Berglin, P. Gatenholm, The nature of bioadhesive bonding between barnacles and fouling-release silicone coatings, *J. Adhes. Sci. Technol.* **13** (1999) 713–727.

[92] Y. Sun, Z. Zhang, Anti-biofouling property studies on carboxyl-modified multi-walled carbon nanotubes filled PDMS nanocomposites, *World J. Microbiol. Biotechnol.* **32** (2016) 148.

[93] R.M. Barrer, J.A. Barrie, N.K. Raman, Solution and Diffusion in Silicone Rubber. II. Influence of Fillers, *Rubber Chem. Technol.* **36** (1963) 651–659.

[94] S.S. Idrus, H. Ismail, S. Palaniandy, The Effects of Silanized Ultrafine Silica on the Curing Characteristics, Tensile Properties, and Morphological Study of Natural Rubber Compounds, *Polym. Plast. Technol. Eng.* **50** (2011) 1–7.

[95] C.F. Most, Some filler effects on diffusion in silicone rubber, *J. Appl. Polym. Sci.* **14** (1970) 1019–1024.

[96] R.R. Brooks, Process for inhibiting fouling of an underwater surface, US5017322 (1991).

[97] R.B. Bodkhe, S.J. Stafslien, N. Cilz, J. Daniels, S.E.M. Thompson, M.E. Callow, J.A. Callow, D.C. Webster, Polyurethanes with amphiphilic surfaces made using telechelic functional PDMS having orthogonal acid functional groups, *Prog. Org. Coatings*. **75** (2012) 38–48.

[98] D.C. Webster, A. Ekin, S. Sommer, Anchored polysiloxane-modified polyurethane coatings and uses thereof, US2013041099 (2013).

[99] M. Tullberg, Fouling release coatings, EP2617778 (2013).

[100] S. Marceaux, C. Bressy, F.-X. Perrin, C. Martin, A. Margaillan, Development of polyorganosilazane–silicone marine coatings, *Prog. Org. Coatings*. **77** (2014) 1919–1928.

[101] M.A. Brook, Silicon in organic, organometallic, and polymer chemistry, John Wiley & Sons, New York (2000).

[102] X.W. He, J.M. Widmaier, J.E. Herz, G.C. Meyer, Competition between polycondensation of alfa,gamma-dihydroxy polydimethylsiloxane and its condensation with alkoxy silane: A kinetic approach, *Eur. Polym. J.* **24** (1988) 1145–1148.

[103] E. Martinelli, D. Gunes, B.M. Wenning, C.K. Ober, J.A. Finlay, M.E. Callow, J.A. Callow, A. Di Fino, A.S. Clare, G. Galli, Effects of surface-active block copolymers with oxyethylene and fluoroalkyl side chains on the antifouling performance of silicone-based films, *Biofouling*. **32** (2016) 81–93.

[104] M.A. Grunlan, N.S. Lee, G. Cai, T. Gädda, J.M. Mabry, F. Mansfeld, E. Kus, D.E. Wendt, G.L. Kowalke, J.A. Finlay, J.A. Callow, M.E. Callow, W.P. Weber, Synthesis of α,ω-bis epoxy oligo (1′H,1′H,2′ H,2′H-perfluoroalkyl siloxane)s and properties of their photo-acid cross-linked films, *Chem. Mater.* **16** (2004) 2433–2441.

[105] I. Marabotti, A. Morelli, L.M. Orsini, E. Martinelli, G. Galli, E. Chiellini, E.M. Lien, M.E. Pettitt, M.E. Callow, J. a Callow, S.L. Conlan, R.J. Mutton, A.S. Clare, A. Kocijan, C. Donik, M. Jenko, Fluorinated/siloxane copolymer blends for fouling release: chemical characterisation and biological evaluation with algae and barnacles, *Biofouling*. **25** (2009) 481–493.

[106] H.S. Sundaram, Y. Cho, M.D. Dimitriou, C.J. Weinman, J.A. Finlay, G. Cone, M.E. Callow, J.A. Callow, E.J. Kramer, C.K. Ober, Fluorine-free mixed amphiphilic polymers based on PDMS and PEG side chains for fouling release applications, *Biofouling*. **27** (2011) 589–602.

[107] D. Bodas, C. Khan-Malek, Hydrophilization and hydrophobic recovery of PDMS by oxygen plasma and chemical treatment—An SEM investigation, *Sensors Actuators B Chem.* **123** (2007) 368–373.

[108] J.F. Schumacher, M.L. Carman, T.G. Estes, A.W. Feinberg, L.H. Wilson, M.E. Callow, J.A.

Callow, J.A. Finlay, A.B. Brennan, Engineered antifouling microtopographies - effect of feature size, geometry, and roughness on settlement of zoospores of the green alga Ulva, *Biofouling*. **23** (2007) 55–62.

[109] B.T. Watermann, B. Daehne, S. Sievers, R. Dannenberg, J.C. Overbeke, J.W. Klijnstra, O. Heemken, Bioassays and selected chemical analysis of biocide-free antifouling coatings, *Chemosphere*. **60** (2005) 1530–1541.

[110] J. Karlsson, B. Eklund, New biocide-free anti-fouling paints are toxic, *Mar. Pollut. Bull.* **49** (2004) 456–464.

[111] R. Hamilton, Hydrolysis of Silicone Polymers in Aqueous System, Lakehead University, Thunder Bay, Ontario (2001).

[112] K.J. Wynne, T. Ho, E.E. Johnston, S.A. Myers, Surface Science and Stability of Networks Prepared from Hydroxy-Terminated Polydimethylsiloxane and Methyltriethoxysilane, *Appl. Organomet. Chem.* **12** (1998) 763–770.

[113] E. Ostuni, R.G. Chapman, R.E. Holmlin, S. Takayama, G.M. Whitesides, A Survey of Structure−Property Relationships of Surfaces that Resist the Adsorption of Protein, *Langmuir*. **17** (2001) 5605–5620.

[114] A.J. Scardino, R. de Nys, Mini review: Biomimetic models and bioinspired surfaces for fouling control, *Biofouling*. **27** (2011) 73–86.

[115] M. Tanaka, T. Hayashi, S. Morita, The roles of water molecules at the biointerface of medical polymers, *Polym. J.* **45** (2013) 701–710.

[116] P. Vermette, L. Meagher, Interactions of phospholipid- and poly(ethylene glycol)-modified surfaces with biological systems: Relation to physico-chemical properties and mechanisms, *Colloids Surfaces B Biointerfaces*. **28** (2003) 153–198.

[117] W. Drost-Hansen, Role of water structure in cell-wall interactions, *Fed. Proc.* **5** (1971) 1539–1548.

[118] R. Konradi, C. Acikgoz, M. Textor, Polyoxazolines for nonfouling surface coatings - A direct comparison to the gold standard PEG, *Macromol. Rapid Commun.* **33** (2012) 1663–1676.

[119] G. Robert-Nicoud, R. Donno, C.J. Cadman, M.R. Alexander, N. Tirelli, Surface modification of silicone via colloidal deposition of amphiphilic block copolymers, *Polym. Chem.* **5** (2014) 6687–6701.

[120] D.R. Calabrese, B. Wenning, J.A. Finlay, M.E. Callow, J.A. Callow, D. Fischer, C.K. Ober, Amphiphilic oligopeptides grafted to PDMS-based diblock copolymers for use in antifouling and fouling release coatings, *Polym. Adv. Technol.* **26** (2015) 829–836.

[121] S.-W. Hsiao, A. Venault, H.-S. Yang, Y. Chang, Bacterial resistance of self-assembled surfaces using PPOm-b-PSBMAn zwitterionic copolymer – Concomitant effects of surface topography and surface chemistry on attachment of live bacteria, *Colloids Surfaces B Biointerfaces*. **118** (2014) 254–260.

[122] E. Österberg, K. Bergström, K. Holmberg, J.A. Riggs, J.M. Van Alstine, T.P. Schuman, N.L. Burns, J.M. Harris, Comparison of polysaccharide and poly(ethylene glycol) coatings for reduction of protein adsorption on polystyrene surfaces, *Colloids Surfaces A Physicochem. Eng. Asp.* **77** (1993) 159–169.

[123] J.M. Berg, L.G.T. Eriksson, P.M. Claesson, Three-Component Langmuir-Blodgett Films with a Controllable Degree, *Langmuir*. (1994) 1225–1234.

[124] E.P.K. Currie, W. Norde, M.A. Cohen Stuart, Tethered polymer chains: surface chemistry and their impact on colloidal and surface properties, *Adv. Colloid Interface Sci.* **100-102** (2003) 205–265.

[125] T.-S. Wong, S.H. Kang, S.K.Y. Tang, E.J. Smythe, B.D. Hatton, A. Grinthal, J. Aizenberg, Bioinspired self-repairing slippery surfaces with pressure-stable omniphobicity, *Nature*. **477** (2011) 443–447.

[126] P.F. Holmes, E.P.K. Currie, J.C. Thies, H.C. Van Der Mei, H.J. Busscher, W. Norde, Surface-modified nanoparticles as a new, versatile, and mechanically robust nonadhesive coating: Suppression of protein adsorption and bacterial adhesion, *J. Biomed. Mater. Res. - Part A*. **91** (2009) 824–833.

[127] W.J. Yang, K.-G. Neoh, E.-T. Kang, S.S.C. Lee, S.L.-M. Teo, D. Rittschof, Functional polymer brushes via surface-initiated atom transfer radical graft polymerization for combating marine biofouling, *Biofouling*. **28** (2012) 895–912.

[128] Z. Wu, H. Chen, X. Liu, Y. Zhang, D. Li, H. Huang, Protein adsorption on poly(N-vinylpyrrolidone)-modified silicon surfaces prepared by surface-initiated atom transfer radical polymerization, *Langmuir*. **25** (2009) 2900–2906.

[129] C. Yoshikawa, A. Goto, Y. Tsujii, T. Fukuda, T. Kimura, K. Yamamoto, A. Kishida, Protein repellency of well-defined, concentrated poly(2-hydroxyethyl methacrylate) brushes by the size-exclusion effect, *Macromolecules*. **39** (2006) 2284–2290.

[130] T. Røn, I. Javakhishvili, S. Hvilsted, K. Jankova, S. Lee, Ultralow Friction with Hydrophilic Polymer Brushes in Water as Segregated from Silicone Matrix, *Adv. Mater. Interfaces*. **3** (2016) 1500472.

[131] M. Kim, S. Schmitt, J. Choi, J. Krutty, P. Gopalan, From Self-Assembled Monolayers to Coatings: Advances in the Synthesis and Nanobio Applications of Polymer Brushes, *Polymers (Basel).* **7** (2015) 1346–1378.

[132] S. Kudaibergenov, W. Jaeger, A. Laschewsky, Polymeric betaines: Synthesis, characterization, and application, *Adv. Polym. Sci.* **201** (2006) 157–224.

[133] P. Laurienzo, Marine polysaccharides in pharmaceutical applications: An overview, *Mar. Drugs*. **8** (2010) 2435–2465.

[134] S.W. Tay, E.W. Merrill, E.W. Salzman, J. Lindon, Activity toward thrombin-antithrombin of heparin immobilized on two hydrogels, *Biomaterials*. **10** (1989) 11–15.

[135] C. Zhao, K. Patel, L.M. Aichinger, Z. Liu, R. Hu, H. Chen, X. Li, L. Li, G. Zhang, Y. Chang, J. Zheng, Antifouling and biodegradable poly(N-hydroxyethyl acrylamide) (polyHEAA)-based nanogels, *RSC Adv.* **3** (2013) 19991.

[136] N.A. Peppas, P. Bures, W. Leobandung, H. Ichikawa, Hydrogels in pharmaceutical formulations, *Eur. J. Pharm. Biopharm.* **50** (2000) 27–46.

[137] R.C. Bowers, N.L. Jarvis, W.A. Zisman, Reduction of Polymeric Friction by Minor Concentrations of Partially Fluorinated Compounds, *Ind. Eng. Chem. Prod. Res. Dev.* **4** (1965) 86–92.

[138] M. Inutsuka, N.L. Yamada, K. Ito, H. Yokoyama, High density polymer brush spontaneously formed by the segregation of amphiphilic diblock copolymers to the polymer/water interface, *ACS Macro Lett.* **2** (2013) 265–268.

[139] L. Cheng, Q. Liu, Y. Lei, Y. Lin, A. Zhang, The synthesis and characterization of carboxybetaine functionalized polysiloxanes for the preparation of anti-fouling surfaces, *RSC Adv.* **4** (2014) 54372–54381.

[140] Z. Wu, K. Hjort, Surface modification of PDMS by gradient-induced migration of embedded Pluronic, *Lab Chip*. **9** (2009) 1500.

[141] E. Berndt, S. Behnke, A. Dannehl, A. Gajda, J. Wingender, M. Ulbricht, Functional coatings for anti-biofouling applications by surface segregation of block copolymer additives, *Polymer*. **51** (2010) 5910–5920.

[142] H. Lee, L.A. Archer, Functionalizing Polymer Surfaces by Field-Induced Migration of Copolymer Additives. 1. Role of Surface Energy Gradients, *Macromolecules*. **34** (2001) 4572–4579.

[143] M. Dahling, E.M. Lien, L.M. Orsini, G. Gallli, E. Chiellini, Fouling release composition, WO2007102741 (2007).

[144] D.C. Webster, R.B. Bodkhe, Functionalized silicones with polyalkylene oxide side chains, WO2013052181 (2013).

[145] R.B. Bodkhe, S.J. Stafslien, J. Daniels, N. Cilz, A.J. Muelhberg, S.E.M. Thompson, M.E. Callow, J.A. Callow, D.C. Webster, Zwitterionic siloxane-polyurethane fouling-release coatings, *Prog. Org. Coatings*. **78** (2015) 369–380.

[146] H. Lee, L.A. Archer, Functionalizing polymer surfaces by surface migration of copolymer additives: role of additive molecular weight, *Polymer*. **43** (2002) 2721–2728.

[147] C. Huang, W. Yu, Role of block copolymer on the coarsening of morphology in polymer blend: Effect of micelles, *AIChE J.* **61** (2015) 285–295.

[148] L. Vroman, A.L. Adams, G.C. Fischer, P.C. Munoz, Interaction of high molecular weight kininogen, Factor XII and fibrinogen in plasma interfaces, *Blood*. **55** (1980) 156–159.

[149] E.W. Merrill, Distinctions and correspondences among surfaces contacting blood, *Ann. N. Y. Acad. Sci.* **516** (1987) 196–203.

[150] M.E. Callow, J.A. Callow, L.K. Ista, S.E. Coleman, A.C. Nolasco, G.P. Lopez, Use of self-assembled monolayers of different wettabilities to study surface selection and primary adhesion processes of green algal (Enteromorpha) zoospores, *Appl. Environ. Microbiol.* **66** (2000) 3249–3254.

[151] S. Schilp, A. Kueller, A. Rosenhahn, M. Grunze, M.E. Pettitt, M.E. Callow, J.A. Callow, Settlement and adhesion of algal cells to hexa(ethylene glycol)-containing self-assembled monolayers with systematically changed wetting properties, *Biointerphases*. **2** (2007) 143.

[152] Y. Cheng, H. Suhonen, L. Helfen, J.S. Li, F. Xu, M. Grunze, P.A. Levkin, T. Baumbach, Direct three-dimensional imaging of polymer-water interfaces by nanoscale hard X-ray phase tomography, *Soft Matter*. **10** (2014) 2982–2990.

[153] G. Yiapanis, S. Maclaughlin, E.J. Evans, I. Yarovsky, Nanoscale wetting and fouling resistance of functionalized surfaces: A computational approach, *Langmuir*. **30** (2014) 10617–10625.

[154] E.W. Salzman, D. Brier-Russell, J. Lindon, E.W. Merrill, Platelets and artificial surfaces: the effect of drugs, *Philos. Trans. R. Soc. Lond. B. Biol. Sci.* **294** (1981) 389–398.

[155] K. Prime, G. Whitesides, Self-assembled organic monolayers: model systems for studying adsorption of proteins at surfaces, *Science*. **252** (1991) 1164–1167.

[156] Y.Y. Luk, M. Kato, M. Mrksich, Self-assembled monolayers of alkanethiolates presenting mannitol groups are inert to protein adsorption and cell attachment, *Langmuir*. **16** (2000) 9604–9608.

[157] B. Wesslen, M. Kober, C. Freij-Larsson, A. Ljungh, M. Paulsson, Protein adsorption of poly(ether methane) surfaces modified by amphiphilic and hydrophilic polymers, *Biomaterials*. **15** (1994) 278–284.

[158] S.R. Benhabbour, L. Liu, H. Sheardown, A. Adronov, Protein resistance of surfaces prepared by chemisorption of monothiolated poly(ethylene glycol) to gold and dendronization with aliphatic polyester dendrons: Effect of hydrophilic dendrons, *Macromolecules*. **41** (2008) 2567–2576.

[159] C.R. Kinnane, G.K. Such, G. Antequera-García, Y. Yan, S.J. Dodds, L.M. Liz-Marzan, F. Caruso, Low-fouling poly(N-vinyl pyrrolidone) capsules with engineered degradable properties, *Biomacromolecules*. **10** (2009) 2839–2846.

[160] K. Sato, S. Kobayashi, M. Kusakari, S. Watahiki, M. Oikawa, T. Hoshiba, M. Tanaka, The Relationship between Water Structure and Blood Compatibility in Poly(2-methoxyethyl Acrylate) (PMEA) Analogues, *Macromol. Biosci.* **15** (2015) 1296–1303.

[161] R. Konradi, B. Pidhatika, A. Mühlebach, M. Textor, Poly-2-methyl-2-oxazoline: A peptide-like polymer for protein-repellent surfaces, *Langmuir*. **24** (2008) 613–616.

[162] L. Na, L. Zhongzhou, X. Shuguang, Dynamically formed poly (vinyl alcohol) ultrafiltration membranes with good anti-fouling characteristics, *J. Memb. Sci.* **169** (2000) 17–28.

[163] M.F.A. Goosen, M. V Sefton, Properties of a heparin-poly(vinyl alcohol) hydrogel coating, *J. Biomed. Mater. Res.* **17** (1983) 359–373.

[164] C.H. Zhang, F. lin Yang, W.J. Wang, B. Chen, Preparation and characterization of hydrophilic modification of polypropylene non-woven fabric by dip-coating PVA (polyvinyl alcohol), *Sep. Purif. Technol.* **61** (2008) 276–286.

[165] S. Zhou, A. Xue, Y. Zhao, M. Li, H. Wang, W. Xing, Grafting polyacrylic acid brushes onto zirconia membranes: Fouling reduction and easy-cleaning properties, *Sep. Purif. Technol.* **114** (2013) 53–63.

[166] I. Cringus-Fundeanu, J. Luijten, H.C. Van Der Mei, H.J. Busscher, A.J. Schouten, Synthesis and characterization of surface-grafted polyacrylamide brushes and their inhibition of microbial adhesion, *Langmuir*. **23** (2007) 5120–5126.

[167] C. Rodriguez-Emmenegger, E. Brynda, T. Riedel, M. Houska, V. Šubr, A.B. Alles, E. Hasan, J.E. Gautrot, W.T.S. Huck, Polymer brushes showing non-fouling in blood plasma challenge the currently accepted design of protein resistant surfaces, *Macromol. Rapid Commun.* **32** (2011) 952–957.

[168] X. Cheng, H.E. Canavan, D.J. Graham, D.G. Castner, B.D. Ratner, Temperature dependent activity and structure of adsorbed proteins on plasma polymerized N-isopropyl acrylamide, *Biointerphases*. **1** (2006) 61.

[169] C. Blaszykowski, S. Sheikh, M. Thompson, Surface chemistry to minimize fouling from blood-based fluids, *Chem. Soc. Rev.* **41** (2012) 5599.

[170] S. Jiang, Z. Cao, Ultralow-fouling, functionalizable, and hydrolyzable zwitterionic materials and their derivatives for biological applications, *Adv. Mater.* **22** (2010) 920–932.

[171] S. Chen, J. Zheng, L. Li, S. Jiang, Strong resistance of phosphorylcholine self-assembled monolayers to protein adsorption: Insights into nonfouling properties of zwitterionic materials, *J. Am. Chem. Soc.* **127** (2005) 14473–14478.

[172] Y.-J. Li, K.H. Matthews, M. Kodama, T. Nakaya, Novel blood compatible polyurethanes containing long-chain alkyl groups and phosphatidylcholine analogues, *Macromol. Chem. Phys.* **196** (1995) 3143–3153.

[173] G. Cheng, H. Xue, Z. Zhang, S. Chen, S. Jiang, A Switchable Biocompatible Polymer Surface with Self-Sterilizing and Nonfouling Capabilities, *Angew. Chemie Int. Ed.* **47** (2008) 8831–8834.

[174] S. Jiang, H. Xue, S. Chen, Marine Coatings, US8349966B2 (2013).

[175] S.-B. Yeh, C.-S. Chen, W.-Y. Chen, C.-J. Huang, Modification of Silicone Elastomer with Zwitterionic Silane for Durable Antifouling Properties, *Langmuir*. **30** (2014) 11386–11393.

[176] R.G. Guidoin, J. Awad, A. Brassard, D. Domurado, F. Lawny, J.N. Barbotin, C. Calvor, G. Broun, Blood compatibility of silicone rubber chemically coated with cross-linked albumin, *Biomater. Med. Devices. Artif. Organs*. **4** (1976) 205–24.

[177] M. Lestelius, B. Liedberg, I. Lundström, P. Tengvall, In vitro Plasma protein adsorption and kallikrein formation on 3-mercaptopropionic acid,L-cysteine and glutathione immobilized onto gold, *J. Biomed. Mater. Res.* **28** (1994) 871–880.

[178] M. Lestelius, P. Tengvall, I. Lundström, Features of Plasma Protein Adsorption onto Glutathione Immobilized on Gold, *J. Colloid Interface Sci.* **171** (1995) 533–535.

[179] O.R. Bolduc, J.F. Masson, Monolayers of 3-mercaptopropyl-amino acid to reduce the nonspecific adsorption of serum proteins on the surface of biosensors, *Langmuir*. **24** (2008) 12085–12091.

[180] A.R. Statz, R.J. Meagher, A.E. Barron, P.B. Messersmith, New Peptidomimetic Polymers for Antifouling Surfaces, *J. Am. Chem. Soc.* **127** (2005) 7972–7973.

[181] N.B. Holland, Y. Qiu, M. Ruegsegger, R.E. Marchant, Biomimetic engineering of non-adhesive glycocalyx-like surfaces using oligosaccharide surfactant polymers, *Nature*. **392** (1998) 799–801.

[182] D. Gourdon, Q. Lin, E. Oroudjev, H. Hansma, Y. Golan, S. Arad, J. Israelachvili, Adhesion and stable low friction provided by a subnanometer-thick monolayer of a natural polysaccharide, *Langmuir*. **24** (2008) 1534–1540.

[183] E.W. Salzman, E.W. Merrill, A. Binder, C.F. Wolf, T.P. Ashford, W.G. Austen, Protein-platelet interaction on heparinized surfaces, *J. Biomed. Mater. Res.* **3** (1969) 69–81.

[184] E.W. Salzman, W.G. Austen, B.J. Lipps, E.W. Merrill, E.R. Gilliland, J. Joison, A new antithrombotic surface: Development and in vitro and in vivo characteristics, *Surgery*. **61** (1967) 1–10.

[185] E.W. Merrill, E.W. Salzman, B.J.J. Lipps, E.R. Gilliland, W.G. Austen, J. Joison, Antithrombogenic cellulose membranes for blood dialysis, *Trans. Am. Soc. Artif. Intern. Organs*. **12** (1966) 139–150.

[186] O. Larm, R. Larsson, P. Olsson, A new non-thrombogenic surface prepared by selective covalent binding of heparin via a modified reducing terminal residue, *Biomater. Med. Devices Artif. Organs*. **11** (1983) 161–173.

[187] J.H. Elam, H. Nygren, M. Stenberg, Covalent coupling of polysaccharides to silicon and silicon rubber surfaces, *J. Biomed. Mater. Res.* **18** (1984) 953–959.

[188] Z. Chen, R.F. Zhang, M. Kodama, T. Nakaya, Preparations and properties of a novel grafted segmented polyurethane-bearing glucose groups, *J. Biomater. Sci. Ed.* **10** (1999) 901–916.

[189] M. Morra, C. Cassineli, Non-fouling properties of polysaccharide-coated surfaces, *J. Biomater. Sci. Polym. Ed.* **10** (1999) 1107–24.

[190] S.M. Olsen, L.T. Pedersen, M.H. Laursen, S. Kiil, K. Dam-Johansen, Enzyme-based antifouling coatings: a review, *Biofouling*. **23** (2007) 369–383.

[191] A.O. Christie, L. V. Evans, M. Shaw, Studies on the Ship-fouling Alga Enteromorpha II. The Effect of Certain Enzymes on the Adhesion of Zoospores, *Ann Bot*. **34** (1970) 467–482.

[192] A. Vaterrodt, B. Thallinger, K. Daumann, D. Koch, G.M. Guebitz, M. Ulbricht, Antifouling and Antibacterial Multifunctional Polyzwitterion/Enzyme Coating on Silicone Catheter Material Prepared by Electrostatic Layer-by-Layer Assembly, *Langmuir*. **32** (2016) 1347–1359.

[193] J.B. Kristensen, R.L. Meyer, C.H. Poulsen, K.M. Kragh, F. Besenbacher, B.S. Laursen, Biomimetic silica encapsulation of enzymes for replacement of biocides in antifouling coatings, *Green Chem.* **12** (2010) 387.

[194] A.L. Cordeiro, C. Werner, Enzymes for Antifouling Strategies, *J. Adhes. Sci. Technol.* **25** (2011) 2317–2344.

[195] M. Andersson Trojer, A. Movahedi, H. Blanck, M. Nydén, Imidazole and Triazole Coordination Chemistry for Antifouling Coatings, *J. Chem.* **2013** (2013) 1–23.

[196] U. Lind, M. Alm Rosenblad, L. Hasselberg Frank, S. Falkbring, L. Brive, J.M. Laurila, K. Pohjanoksa, A. Vuorenpää, J.P. Kukkonen, L. Gunnarsson, M. Scheinin, L.G.E. Mårtensson

Lindblad, A. Blomberg, Octopamine receptors from the barnacle balanus improvisus are activated by the alpha2-adrenoceptor agonist medetomidine, *Mol. Pharmacol.* **78** (2010) 237–248.

[197] A.S. Clare, D. Rittschof, D.J. Gerhart, I.R. Hooper, J. Bonaventura, Antisettlement and Narcotic Action of Analogues of Diterpene Marine Natural Product Antifoulants from Octocorals, *Mar. Biotechnol.* **1** (1999) 427–436.

[198] M. Zasloff, Antimicrobial peptides of multicellular organisms, *Nature*. **415** (2002) 389–395.

[199] S.T. Oh, B.K. Min, C.S. Ha, W.J. Cho, Synthesis and fungicidal activities of polymeric biocides. I. TBZ-containing monomer and polymers, *J. Appl. Polym. Sci.* **52** (1994) 583–589.

[200] W.J. Yang, K.G. Neoh, E.T. Kang, S.L.M. Teo, D. Rittschof, Polymer brush coatings for combating marine biofouling, *Prog. Polym. Sci.* **39** (2014) 1017–1042.

[201] T. Ikeda, S. Tazuke, Synthesis and Antimicrobial Activity of Poly(Trialkylvinylbenzylammonium Chloride)s, *Makromol. Chem*. **185** (1984) 869–876.

[202] Z.X. Voo, M. Khan, K. Narayanan, D. Seah, J.L. Hedrick, Y.Y. Yang, Antimicrobial/antifouling polycarbonate coatings: Role of block copolymer architecture, *Macromolecules*. **48** (2015) 1055–1064.

[203] S. Yan, S. Luan, H. Shi, X. Xu, J. Zhang, S. Yuan, Y. Yang, J. Yin, Hierarchical Polymer Brushes with Dominant Antibacterial Mechanisms Switching from Bactericidal to Bacteria Repellent, *Biomacromolecules*. **17** (2016) 1696–1704.

[204] T. Segura, A.M. Puga, G. Burillo, J. Llovo, G. Brackman, T. Coenye, A. Concheiro, C. Alvarez-Lorenzo, Materials with Fungi-Bioinspired Surface for Efficient Binding and Fungi-Sensitive Release of Antifungal Agents, *Biomacromolecules*. **15** (2014) 1860–1870.

[205] C. Bressy, C. Hellio, J.P. Maréchal, B. Tanguy, A. Margaillan, Bioassays and field immersion tests: a comparison of the antifouling activity of copper-free poly(methacrylic)-based coatings containing tertiary amines and ammonium salt groups, *Biofouling*. **26** (2010) 769–777.

[206] J.F. Schumacher, N. Aldred, M.E. Callow, J.A. Finlay, J.A. Callow, A.S. Clare, A.B. Brennan, Species-specific engineered antifouling topographies: correlations between the settlement of algal zoospores and barnacle cyprids, *Biofouling*. **23** (2007) 307–317.

[207] M.L. Carman, T.G. Estes, A.W. Feinberg, J.F. Schumacher, W. Wilkerson, L.H. Wilson, M.E. Callow, J.A. Callow, A.B. Brennan, Engineered antifouling microtopographies - correlating wettability with cell attachment, *Biofouling*. **22** (2006) 11–21.

[208] M. Ferrari, A. Benedetti, Superhydrophobic surfaces for applications in seawater, *Adv. Colloid Interface Sci.* **222** (2015) 291–304.

[209] J.A. Callow, M.E. Callow, Trends in the development of environmentally friendly fouling-resistant marine coatings, *Nat. Commun.* **2** (2011) 244.

[210] T.H. Duong, J.-F. Briand, A. Margaillan, C. Bressy, Polysiloxane-Based Block Copolymers with Marine Bacterial Anti-Adhesion Properties, *ACS Appl. Mater. Interfaces*. **7** (2015) 15578–15586.

[211] D. Pavlović, S. Lafond, A. Margaillan, C. Bressy, Facile synthesis of graft copolymers of controlled architecture. Copolymerization of fluorinated and non-fluorinated poly(dimethylsiloxane) macromonomers with trialkylsilyl methacrylates using RAFT polymerization, *Polym. Chem.* **7** (2016) 2652–2664.

2. The PhD project

This chapter reviews the main commercial products within the fouling-release coatings industry and sets the scope, aims and hypothesis of this project.

2.1 Commercial fouling-release coatings (FRC)

It can be clearly seen from the review presented in Chapter 1 how research in fouling-release coatings has evolved in the last decades. After the ban of TBT-SPC coatings, many efforts focused on developing hydrophobic fouling-release coatings, which allow the settlement of biofouling, but "release" it under hydrodynamic conditions. Though some used fluorine-based polymers, PDMS has been the mostly used polymer for fouling-release purposes due to its low critical values of surface energy (γ_c), elastic modulus (E), glass transition temperature (T_g) and surface roughness. The addition of oils was explored as a method to improve the properties of these coatings. Later, functionalization of FRC with (hydrophilic) polymers, enzymes and biocides has proven to provide improved biofouling-inhibition qualities. This functionalization is commonly accomplished by addition of surface-active oils. Because this method involves relatively small amounts of compounds, the advantageous bulk properties (e.g. low elastic modulus of PDMS) of the binder can be retained and only the physicochemical properties of the surface are significantly modified. This development on the scientific field has had a direct impact on the evolution of commercial fouling-release coatings, which is evident when the fouling-release products sold by some of the main suppliers are analysed, together with several patents that these companies have published in the last 5-10 years.

For example, Hempel A/S launched its first silicone product in 2000, Hempasil 77500. It was a biocide-free PDMS-based coating with low surface energy (i.e. hydrophobic). In 2008, Hempasil was substituted by Hempasil X3. Hempasil X3 is also biocide-free, but contains a hydrophilic-modified polysiloxane additive (i.e. silicone oil) in the formulation that migrates to the surface and forms a "hydrophilic hydrogel" on the surface. Finally, Hempaguard X7 was released in 2013. Hempaguard X7 is described as utilizing the "hydrogel technology" of Hempasil X3 in combination with small amounts of biocide that can boost its non-fouling properties and provide superior biofouling protection, even in idle conditions. It is reported that the amount of biocides released from Hempaguard X7 is below 10% when compared to traditional antifouling coatings. Regarding Hempel's intellectual property rights (IPR), both the use of silicone oils and biocides have been described. PDMS oils have been modified with different hydrophilic polymers to obtain surface-active hydrophilic-modified polysiloxanes with different structures. Some of the polymers previously described in Chapter 1 have been reported, such as polyethers (e.g. PEG and poly(propylene glycol) (PPG)), poly(acrylic acid) and poly(vinyl pyrrolidone). The use of these modified polysiloxanes can be combined with some organic biocides such as copper pyrithione (CuPT) and Seanine [1,2].

Similarly, Chugoku Marine Paints (CMP) based its fouling-release technology in the early 2000s on a biocide-free low surface-energy coating, Bioclean, which contained a "hydrophobic liquid" [3]. In the later version of the product, Bioclean Plus, launched in 2014, Chugoku reports the addition of a "special

synthetic polymer" and a small amount of an "active agent" (i.e. biocide). In Chugoku's IPR, the use of two different silicone oils is described, namely hydrophobic phenyl-modified polysiloxane and polyether-modified silicone oils, both with a hydrolysable end-group [4]. Later, the addition of pyrithione metal salts (i.e. biocides) has been reported together with the abovementioned oils [5].

Jotun A/S has followed a similar tendency. In 2005, Jotun released SeaLion, which relied on a smooth hydrophobic PDMS-based surface to detach biofouling by hydrodynamic forces. With the introduction of SeaLion Repulse in 2010, it has been reported that a "nano-technology" keeps the biofouling species away from the surface. This nano-technology is described as "nano-springs" of what appears to be a polymeric brush on the surface of the coating, which repels biofouling. Jotun has described in a patent from 2007 [6] the use of vinyl- and acrylate-based copolymers with PTFE and PDMS pendant groups. This oil can be end-functionalized with a silane reactive group, so it can crosslink with the PDMS binder and be therefore "further stabilized".

Finally, International Paints experienced a similar shift on their commercial FRC. A fluoropolymer additive was used in Intersleek 900 (launched in 2007), a biocide-free technology characterized by a hydrophobic surface, similar to the previous Intersleek 425 (1996) and Intersleek 700 (1999). In the following version, Intersleek 1100SR (released in 2013), the fluoropolymer was "improved" with a "hydrophilic moiety" and better fouling-release properties were claimed. Finally, Intersleek 1000 was released in 2016, where a sterol-based polymer additive is added, but still biocide-free. International Paints has been granted different patents within the FR area, and the use of both reactive [7] and non-reactive oils [8] have been described. In both cases, the oils are based on copolymers consisting of fluorinated and polyether polymers. Furthermore other oils have been described to provide fouling-release properties when mixed on PDMS-based coatings [9]. These additives consist of hydrophobic lanolin molecules modified with a hydrophilic moiety such as a hydroxyl or ester group, or a polyether chain.

2.2 The gap between science and commercial FRC

It is surprising that almost all commercial coatings follow the principle of modifying a PDMS binder with some surface-active oils (and biocides in some recent products), in spite of the large amount of different strategies developed in the scientific field. This might be attributed to different causes. For example, most scientific studies employ laboratory studies to assess the non-fouling properties of novel materials. These experiments involve short-term tests comprising the settlement of certain proteins (e.g. fibrinogen) or marine organisms (e.g. *Ulva linza* zoospores or *Balanus Amphitrite* cyprids) in well-controlled and stable conditions. However, commercial coatings are complex mixtures of compounds that are applied on top of other coatings in real (non-ideal) conditions and exposed to seawater for extended periods. Hence, solutions that provide satisfactory results in the laboratory might not perform when applied to real vessels.

2.3 Closing the gap – the PhD project

This industrial project intends to analyse simplified FRC to contribute to the development of long-lasting robust solutions.

2.3.1 Choosing a model system

A “model system” is used in this project as a simplified representation of real fouling-release coatings. This model system intends to reduce the amount of components used and thus decrease complexity, but without resulting in significant differences from real coatings.

The model system chosen can be described as the mixture of:

1) PDMS binder. PDMS is chosen because it is the most commonly used binder in commercial products, in addition to its ease of application and availability.
2) Crosslinker. Three different crosslinkers are used in this project, all following the “condensation cure” route as previously explained (see Figure 1.8). Two alkoxy-based polysilicates are used together with a Sn-based catalyst. In addition, an oxime-curing crosslinker, which does not require the addition of catalyst due to its higher reactivity, is employed.
3) Solvent. To ensure homogeneity and ease of application, xylene is added (~ 15 wt%).
4) Surface-active oil. The current commercialized FRC contain different kinds of oils that enhance the non-fouling properties of the coatings. Here, PDMS-PEG-based copolymers are chosen for different reasons.
    - PDMS is chosen as hydrophobic block to increase the compatibility of the copolymer with the PDMS binder and enhance its “anchoring” capabilities on the surface.
    - PEG is chosen as hydrophilic block due to its superior properties, which have been largely recognized in the biomedical and the marine field. Additionally, PEG is selected because most of the patents from the different suppliers describe its use, as described previously.
    - PDMS-PEG-based copolymers also have the advantage that they are readily available from different suppliers, with different structures and molecular weights. Note that copolymers with different structures (e.g. ABA, grafted) and chemical compositions have been used.

The model system is modified in most of the experiments to resemble more accurately real FRC. Therefore, two compounds are added:

5) Silica (SiO_2) is used as filler (~1 wt%) to improve the mechanical properties.
6) Iron oxide (Fe_2O_3) is employed as pigment (~5 wt%) to provide opacity and colour.

Finally, a last compound is used in Chapter 6:

7) Copper pyrithione (CuPT). This organic biocide has been added because of its introduction in some of the latest launched products.

2.3.2 Problem statement: Limitations of fouling-release technology

It has been shown that the application of PDMS-based fouling-release coatings has considerable beneficial effects due to their very low surface roughness and the release of biofouling by hydrodynamic forces. Different articles have estimated that freshly immersed FRC show friction coefficients between 1.5 and 6.1% lower than for fresh biocide-containing antifouling coatings [10]. However, the properties of FRC tend to deteriorate over time and biofouling eventually settles. The precise point at which failure occurs depends on many factors such as the activity and speed of the vessel and the biofouling pressure of the immersion area, among others.

As example, see in Figure 2.1 an experimental biocide-free PDMS coating containing a PDMS-PEG-based copolymer. This coating has been exposed to seawater in the coast of Singapore for 64 weeks (> 1 year) in static conditions. It can be seen that the non-fouling properties of the coating are exceptionally good in the first months, but these diminish over time.

Image									
time (weeks)	0	8	16	24	32	40	48	56	64

Figure 2.1. Images of a PDMS fouling-release coating containing a PDMS-PEG-based copolymer immersed in seawater in Singapore for 64 weeks. A picture of the coating was taken every 8 weeks.

2.3.3. Aims and hypotheses

It is the aim of this project to identify the limitations of current FRC. Different reasons might explain the decline in biofouling-inhibition properties of these coatings over time, which include deterioration of the PDMS matrix and/or the PDMS-PEG-based copolymer, among others.

Regarding the matrix, two different theories are hypothesized:

(1) The surface roughness of the coating significantly increases over time. This might result in:
   1.1) Increased surface area and mechanical interlocking available for the biofouling organisms.
   1.2) An irregular surface that cannot be properly functionalized (i.e. covered) by the PDMS-PEG-based copolymer.

(2) The PDMS matrix experiences “hydrophobic recovery”, which means that PDMS chains segregate to the surface of the film over time and do not allow coverage of the surface by the PDMS-PEG-based copolymer. Without the presence of these copolymers on the surface, the non-fouling properties of these coatings are greatly reduced.

Regarding the PDMS-PEG-based copolymer, different reasons are suggested:

(3) The copolymer molecules cannot diffuse to the surface of the coating because they are "trapped" in the bulk of the PDMS matrix. Under this hypothesis, the initial performance is solely provided by the molecules which are originally on the surface of the film. When these are washed away from the surface or degraded, no replenishment of molecules from the bulk of the film is possible.

(4) The copolymer molecules can readily diffuse from the bulk, when those on the surface are washed away or degraded. Therefore, the "self-healing" process takes place as long as there are molecules available in the bulk. The decline in fouling-release performance seen after several months/years responds to the shortage of copolymer molecules in the bulk of the film.

(5) The PDMS-PEG-based copolymer is degraded. It has been previously shown that both PDMS and PEG are vulnerable to degradation under a range of conditions. Therefore, the copolymer is destructed and no fouling-inhibition properties can be provided.

Other factors are as well considered:

(6) The use of biocides in PDMS-based coatings has been described in some of the current products and patents. These can provide superior properties due to their toxicity, but might also influence (positively or negatively) the behaviour of the copolymer within the coating film. For example, the presence of biocides could hinder/boost the copolymer diffusion or increase/decrease its "washing-away" rate at the surface, to mention some examples. Likewise, the presence of fillers and pigments might enhance or hinder the abovementioned phenomena.

The main objective of this work is to investigate the causes that result in deterioration of the properties of commercial FRC. Developing superior long-lasting solutions requires answering the presented questions. Confirming or disregarding the hypotheses introduced is the first step of this complex process. Therefore, developing methods to understand, visualize and quantify processes regarding the behaviour (i.e. distribution and diffusion) and fate (release and degradation) of oils in fouling-release coatings is essential. Moreover, these methods can be a great tool towards a faster and better development of commercial products in the future. In other words, this industrial project is intended to act as a bridge between science and industry in a field that has the potential of resulting in both economical (i.e. decreased fuel consumption) and environmental benefits (reduced release of biocides to seawater, gases to the atmosphere, raw materials used and residues generated).

The following chapters are hence aimed at addressing the abovementioned questions.

2.4 References

[1] P.C.W. Thorlaksen, A. Blom, U. Bork, Novel fouling control coating compositions, WO2011076856 (2011).

[2] P.C.W. Thorlaksen, Fouling control coating compositions comprising polysiloxane and pendant hydrophilic oligomer/polymer moieties, WO2013000478 (2013).

[3] B. Watermann, H. Berger, H. Sönnichsen, P. Willemsen, Performance and effectiveness of non-stick coatings in seawater, *Biofouling*. **11** (1997) 101–118.

[4] K. Amidaiji, S. Tashiro, T. Sakamoto, Curable composition, antifouling coating composition, antifouling coating film, base with antifouling coating film, and method for preventing fouling on base, EP2103655A1 (2009).

[5] S. Tanino, Antifouling coating composition, antifouling coating film, antifouling substrate, and method for improving storage stability of antifouling coating compositions, US2015299515 (2015).

[6] M. Dahling, E.M. Lien, L.M. Orsini, G. Gallli, E. Chiellini, Fouling release composition, WO2007102741 (2007).

[7] R. Lines, D.N. Willimans, S. Turri, Antifouling coating composition comprising a fluorinated resin, US2003161962 (2003).

[8] K.J. Reynolds, B.V. Tyson, Anti-fouling compositions with a fluorinated oxyalkylene-containing polymer or oligomer, WO2014131695 (2014).

[9] B.V. Tyson, K.J. Reynolds, Fouling-resistant composition comprising sterols and/or derivatives thereof, WO2013024106 (2013).

[10] K.F. Sørensen, D. Hillerup, A. Blom, S.M. Olsen, D.M. Yebra, Keeping your guard up, *Nav. Archit.* **June** (2015) 39–44.

3. Diffusivity and biofouling-inhibition properties of PEG-based amphiphiles in FRC

The biofouling-inhibition properties of FRC depend on the ability of the surface-active copolymers added as additives to diffuse and cover the surface of the coatings. This chapter investigates the diffusion properties of different PEG-based surfactants and copolymers in PDMS, and its influence on the biofouling-inhibition properties of the coatings.

The content of this chapter was submitted for publication as “Diffusion of surface-active amphiphiles in silicone-based fouling-release coatings” in Progress in Organic Coatings (authors: A. Camós Noguer, S. M. Olsen, S. Hvilsted and S. Kiil).

3.1 Introduction

The addition of different kinds of surface-active compounds to decrease the amount of biofouling on fouling-release coatings is widespread. Various patents [1–7] and articles [8–12] in the field describe the use of both reactive and non-reactive amphiphilic copolymers in fouling-release coatings, mainly based on fluorinated, siloxane and oxyalkylane moieties. Among them, poly(ethylene glycol) (PEG) has shown promising results in the biomedical field regarding fouling-resistance properties (i.e. biofouling-inhibition) [13]. Different methods have been used to functionalize surfaces with PEG. Besides adding PEG-based surface-active compounds to change the surface properties of poly(dimethylsiloxane) (PDMS) films and coatings, PEG has also been covalently grafted or physically adsorbed on different substrates [13,14]. However, these methods are more expensive and not suitable for big-scale applications like fouling-release coatings for ships. Therefore, it is believed that incorporating PEG-based copolymers and exploiting their surface-activity is the most effective way to obtain long-term effective fouling-release coatings. The proposed working mechanism for these additives is based on the coverage of the coating surface, with the hydrophobic block of the copolymer acting as an anchor on the surface, while the PEG block provides fouling-inhibition qualities [15,16]. Therefore, the long-term fouling-release protection properties of these coatings are dictated both by the hydrophobic and the hydrophilic blocks of these amphiphilic additives.

The characterization of surface segregation/enrichment in polymeric materials has been achieved by different means. Radioactive labelling [17], infrared microdensiometry [17], fluorescence tracing [18], time-of-flight secondary ion mass spectrometry (ToF-SIMS) [19] and X-ray photoelectron spectroscopy (XPS) [20] have been used with successful results. Similarly, the diffusion of different migrants in polymer hosts has also been studied by methods such as Raman spectroscopy [21], gas chromatography (GC) [21] and infrared spectroscopy (IR) [22], among others.

In this chapter, the functionalization of silicone fouling-release coatings by addition of PEG-based amphiphiles is studied. An amphiphile is a molecule having different blocks, which provide both hydrophobic and hydrophilic properties to the molecule. Amphiphiles with three different kinds of hydrophobic blocks have been used, while PEG has been kept as hydrophilic block for all of them. The three hydrophobic blocks chosen have been: (1) alkyl hydrocarbon chains, (2) alkyl hydrocarbon chains

connected to an aryl group and (3) PDMS chains, with different molecular weights and structures. A new procedure, based on a time lag method combined with an optical tensiometer, is employed to study the diffusion of these amphiphiles through crosslinked PDMS films for fouling-release purposes. The use of time lag methods has previously been reported in the literature to obtain diffusion coefficients of different compounds in films. For example, Stewart et al. [23] measured the diffusivity of acids through thin polymer films below and above the glass transition temperature (T_g). Valente et al. [24], studied the diffusion of sodium dodecyl sulphate (SDS) through cellulose esters membranes, and Faucher et al. [25] analysed diffusion phenomena of sodium lauryl sulphate (SLS) through rat stratum corneum. In contrast with other methods that usually require sample preparation, extraction methods, vacuum and/or long waiting times, diffusion coefficients for relatively high molecular weight (M_w) amphiphiles and block copolymers can be obtained in an easy and rapid way by using the method presented in this chapter. Experimental diffusion coefficients are obtained for such molecules in crosslinked PDMS films. In addition, the diffusion coefficients obtained are compared to literature values of other diffusing molecules and polymers. The effect of the diffusant chemistry and M_w on the diffusion of these compounds within the coating film and the influence on the final biofouling-inhibition properties of the coatings are discussed.

3.2 Materials and Methods

3.2.1 Materials

Silanol-terminated PDMS (4000 cSt) was received from Dow Corning and vinyl tris(methyl ethyl ketoxime) silane from Evonik. Fumed silica (SiO_2) Aerosil R8200 was received from Evonik and red iron oxide (Fe_2O_3) pigment Bayferrox 130M from Lanxess.

PEG400, Brij O10, Brij O20, Triton X-100, Igepal CO-720 and Tween 85 were obtained from Sigma-Aldrich. Sapogenat T 080 and Sapogenat T 130 were received from Clariant. Lumulse POE(7) GML was received from Lambent Corp, Serdox NES 7 from Elementis Specialities and PEG 12 stearate from A&E Connock. The three PDMS-PEG-based copolymers analysed (copolymer 1, copolymer 2 and copolymer 3) were obtained from Dow Corning, Evonik and Siltech Corp. The chemical properties of the abovementioned compounds can be found in Table 3.1.

All the materials were used as received without further purification.

Table 3.1. Chemical composition and properties of the amphiphiles used and the diffusion coefficients obtained. Structure (where A represents the hydrophilic block and B the hydrophobic block), molecular weight (M_w), number of poly(ethylene glycol) (PEG) units, hydrophilic-lipophilic balance (HLB) value and diffusion coefficient (D) are shown for each amphiphile. Note that they have been ordered according to the chemistry of the hydrophobic block of the amphiphile

Chemistry of the hydrophobic block	Amphiphile	Structure	M_w (g/mol)	Number of PEG units in the hydrophilic block	HLB[e]	D (m^2/s) · 10^{12}	Coating number (see Figure 3.10)
Alkyl	**Brij O10**	AB	720	10	12,5	15,9 ± 1,1	1
Alkyl	**Lumulse POE(7) GML**	AB	580	7	10,5	21,6 ± 8,3	2
Alkyl	**Serdox NES 7**	AB	570	7	12	35,5 ± 12,8	3
Alkyl	**Tween 85**	-	1840[b]	20[c]	11[b]	2,2 ± 0,4	4
Alkyl	**PEG 12 stearate**	AB	820	12	13	12,5 ± 0,8	5
Alkyl + Aryl	**Sapogenat T 080**	AB	620	8	11,5	19,6 ± 7,5	6
Alkyl + Aryl	**Sapogenat T 130**	AB	840	13	13,5	5,6 ± 2,4	7
Alkyl + Aryl	**Triton X-100**	AB	610	10	13,5	9,3 ± 2,3	8
Alkyl + Aryl	**Igepal CO-720**	AB	730	12	14	10,0 ± 2,6	9
PDMS	**Copolymer 1**	AB	660	8	11	8,8 ± 0,3	10
PDMS	**Copolymer 2**	Grafted	3940	10[d]	8	3,2 ± 0,5	11
PDMS	**Copolymer 3**	ABA	1960	10[d]	10,5	3,4 ± 1,6	12
-	**PEG400**	A	400	8	-	-	13[f]
-	**-[a]**	-	-	-	-	-	14[f]

[a] No additive was used for this coating
[b] The value provided by the supplier was used
[c] Total number of PEG units in the molecule, distributed in 4 different branches
[d] Number of PEG units in each block/branch
[e] Estimated using Equation 3.4
[f] Coatings only used as references for contact angle and static immersion tests

3.2.2 Preparation of coatings

The amphiphiles listed in Table 3.1 were added as additives to conventional silicone (PDMS) coatings. The coatings were prepared by mixing silanol-terminated PDMS with a trifunctional oximinosilane crosslinker (vinyl tris(methyl ethyl ketoxime) silane) using xylene as solvent. Iron oxide (Fe_2O_3) Bayferrox 130M was added as red pigment so it accounted for 5% of the dry weight of the film. Surface treated fumed silica (SiO_2) Aerosil R8200 was added so it accounted for 1% of the final weight of the film. The pigment and the silica were premixed with the PDMS binder in a pearl mill for 1 hour. The amphiphiles in Table 3.1 were added so they accounted for 4% of the total weight in the dry film. The mixtures were applied on glass slides substrates (2.5 x 7.5 cm) using a 6 cm Dr Blade applicator with a 400 µm gap and cured for a week at room temperature. These coatings were used for the study of the diffusion coefficients.

The mixtures were also applied on poly(methyl methacrylate) (PMMA) substrates (10 x 20 cm) using a 8 cm Dr Blade applicator with a 400 µm gap and cured for a week at room temperature. Then, the top half-part of the panel was protected with aluminium foil, and the bottom part was covered (spray-applied) with an additive-free PDMS coating (coating 14 in Table 3.1). The wet thickness applied was approximately 350 µm, and the panels were cured for a week at room temperature. These coatings were used to study the diffusion and fouling-resistance properties of the additives (see Figure 3.1). Note that all the analysed coatings were biocide-free, i.e. the protection against biofouling was solely provided by the amphiphilic additives investigated and the physicochemical properties of the PDMS surface.

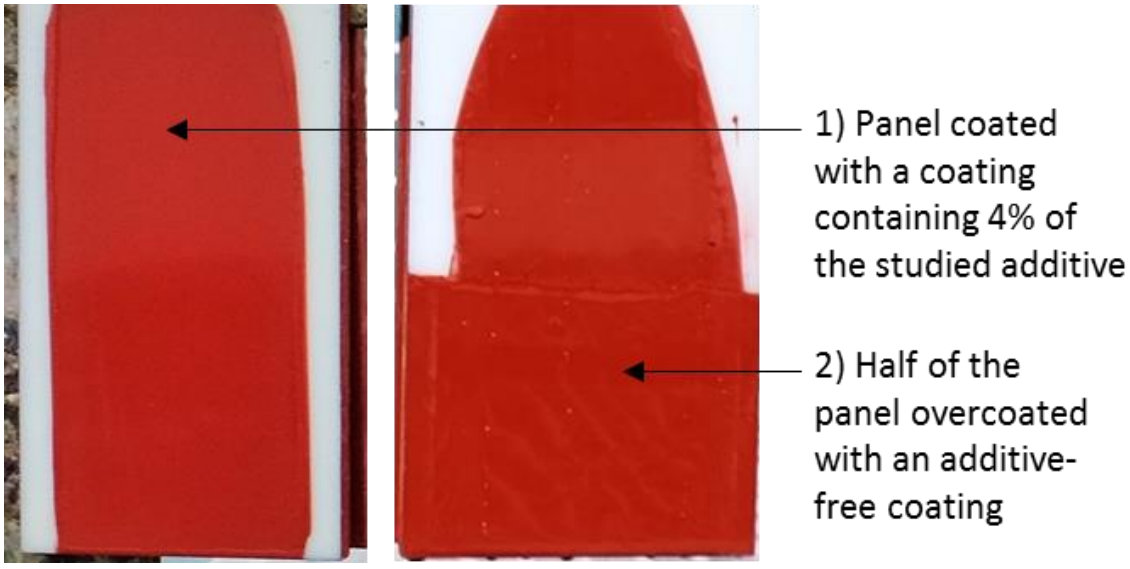

Figure 3.1. Preparation of the coatings for seawater exposure, with two layers. The first layer consisted of a coating containing 4 wt% of the studied amphiphiles, and half of the cured coating was overcoated with a layer of an additive-free coating.

Free-film coatings were applied using a 15 cm Dr Blade applicator with different gap size on poly(ethylene terephthalate) (PET) substrates, and cured for a week at room temperature. These coatings did not contain any of the studied amphiphiles (see coating 14 in Table 3.1). Three different thicknesses were applied, and the thickness of the final dry films were measured by use of optical microscopy. The coatings were cut with a scalpel and the cross-section of the coatings was analysed in

the optical microscope. The measured thicknesses were l_1 = 85 ± 2 µm, l_2 = 132 ± 3 µm and l_3 = 168 ± 16 µm (average of three measurements). These films were used as "membranes" to study the diffusion coefficients of the different PEG-based amphiphiles, as explained in the following sections.

3.2.3 Molecular weight measurements

The molecular weight of the different amphiphiles used can be found in Table 3.1. The molecular weights reported are based on Size Exclusion Chromatography (SEC) measurements calibrated with PEG standards. The molecular weight values obtained were compared with those provided by the suppliers, when available, showing differences below 5%. The only exception was Tween 85, which showed a large difference, probably due to the highly branched structure of this amphiphile. Therefore, the M_w value provided by the supplier has been used for this compound.

The molecular weight of the silanol-terminated PDMS used as binder was determined based on its viscosity. By using Equation 3.1, proposed by Barry [26] in 1950, it was estimated that the molecular weight of the PDMS binder used was 45.000 g/mol, significantly higher than the molecular weight of the studied amphiphiles. Note that for this kind of networks, the molecular weight between crosslinks (M_c) coincides with the molecular weight of the binder, and is sometimes referred to as the "molecular weight of the network". The molecular weight between crosslinks (M_c) was kept constant throughout all the experiments.

$$\log \mu = 1 + 0{,}0123 \cdot {M_w}^{1/2} \qquad \textbf{(Equation 3.1)}$$

In Equation 3.1, µ is the viscosity of the polymer in cSt (1 cSt = 10^{-6} m^2/s), and M_w is its molecular weight in g/mol.

3.2.4 The time lag method

The time lag method presented here is inspired by a methodology that was first developed by H. A. Daynes [27] in 1920, in studies of the diffusion of gases through rubber membranes. The method allowed calculation of diffusion and permeability coefficients for systems following Fick's diffusion law with negligible resistance at the interfaces. In those experiments, one side of a rubber membrane, of thickness *l*, was exposed to a gas (e.g. hydrogen) while the amount of gas released on the other side of the membrane was monitored by a katharometer. It was found that after a period where no gas was detected, the so-called time lag, the concentration of the gas started increasing at a constant rate (see Figure 3.2a).

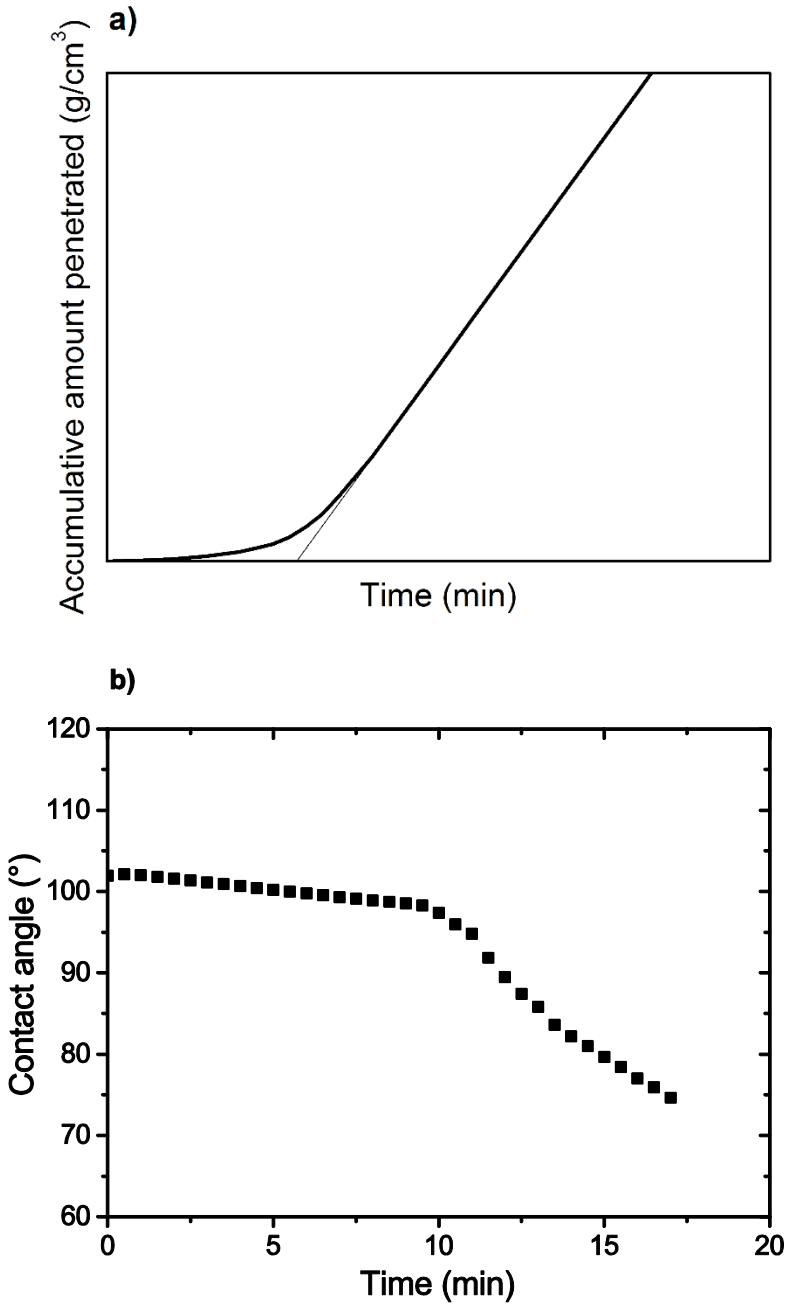

Figure 3.2. Example of results obtained with (a) original time lag method by Daynes [27] and (b) with the presented set-up.

Figure 3.3 shows a scheme of the setup used in this chapter. The original rubber membrane in the works of H. A. Daynes [27] was replaced by an additive-free PDMS coating (film). The concentration gradient of diffusant was now provided by, on one side, a PDMS film containing 4 wt% of the studied amphiphile, while a droplet of fresh water was placed on the other. To asses the presence of diffusant on the second interface, a tensiometer was used to monitor the contact angle of the water droplet. It is well-known that the presence of a surface-active additive in PDMS results in a change on the properties of the surface and, therefore, the contact angle changes [28]. An example of the results obtained by this method can be seen in Figure 3.2b, where the contact angle is plotted over time. A lag time can clearly be identified,

after which the contact angle drops due to the presence of the amphiphile. This change in slope is used here to identify the time lag L.

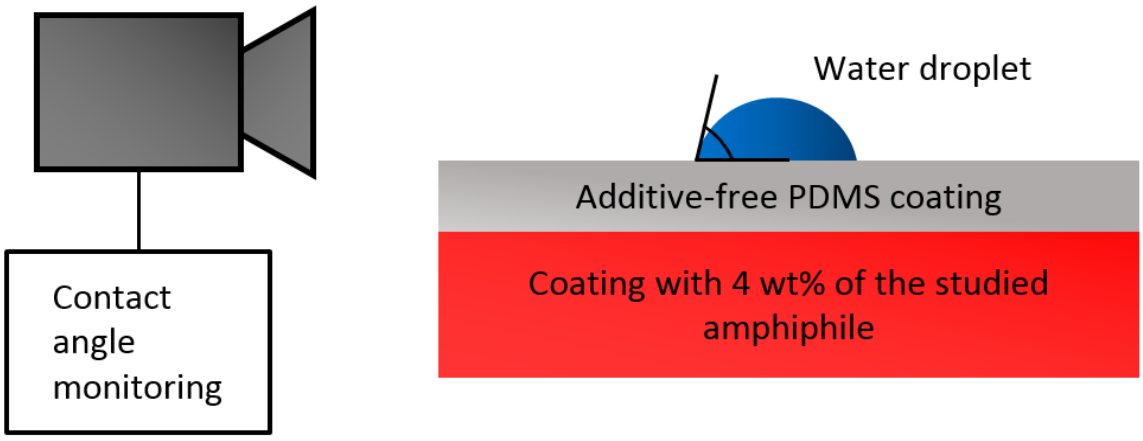

Figure 3.3. Outline of the modified time lag method used for the measurement of diffusion coefficients. An additive-free PDMS coating is placed as "membrane" between a coating containing the studied amphiphile and a water droplet. The contact angle is monitored and the time lag, L, is obtained.

Assuming that the diffusion coefficient is independent of the thickness of the membrane, the concentration of the diffusant and time, Fick's law can be solved for that system. It has been shown [27] that the diffusion coefficient can be calculated from the time lag value through Equation 3.2:

$$L = \frac{l^2}{6D} \qquad \textbf{(Equation 3.2)}$$

where L is the time lag in s, *l* is the thickness of the membrane in m and D is the diffusion coefficient in m^2/s.

Later, this model was extended to other geometries and cases, such as when the diffusion coefficient is dependent on the concentration or when there is an initial concentration (C_0) of diffusant in the membrane, to mention some examples [29,30].

However, different cases have been reported to differ from the conditions/assumptions that led to Equation 3.2. For example, systems with non-negligible entry resistance at the interfaces of the membrane and time-dependent diffusion coefficients have been reported [31,32]. Likewise, polymer membranes near or below their glass transition temperature show much larger relaxation times, having a strong influence on the diffusion processes hosted [33,34]. Some authors have referred to these deviations as "non-Fickian anomalies" and have added a term, δL, to Equation 3.2 to account for these anomalies [31,33] (see Equation 3.3). Others, however, defend that the addition of this term is not necessary and that all these "non-Fickian anomalies" can in fact be described by Fick's diffusion law if the proper boundary conditions are used [35].

$$L = \frac{l^2}{6D} + \delta L \qquad \textbf{(Equation 3.3)}$$

By assuming that the term δL is independent of the thickness of the membrane, a plot of L vs l^2 can be used to obtain D coefficients, while an ordinate intercept is obtained with value δL [31]. It is also assumed that the free volume of the films is approximately the same for all the coatings investigated. Moreover, the substrate film containing 4 wt% of the studied amphiphiles is assumed to be homogeneous with the amphiphile available on the surface, so no diffusion path is added from the lower film to the interface of the two films. Finally, due to the amphiphilic nature of the studied additives, formation of micelles is expected within the PDMS films. It has been reported elsewhere [36], that micelles lead to an important decrease of the kinetics of segregation of block copolymers in polymer hosts. It is assumed here that the diffusion is driven by unimers (amphiphile molecules which are not part of a micelle) and that the presence of micelles has a negligible effect on the diffusion process of the unimers. Under these assumptions, Equation 3.3 is used in this chapter to obtain diffusion coefficients for the studied amphiphiles.

3.2.5 Contact angle measurements

The sessile drop method was used to monitor the contact angle of a droplet of water on the different PDMS films using Dataphysics OCA20 equipment. A droplet of 25 µl of millipore water was dropped on top of the different surfaces, and the contact angle was measured every 2 seconds, so that a contact angle-time profile could be obtained. Nevertheless, in Figures 3.4 and 3.5, only one point every 30/60 seconds is plotted for clarity. Regarding the volume of the water droplet, 25 µl was chosen as a compromise: it was sufficiently large to avoid evaporation effects, but small enough, with Eötvös number below 1, so that the weight of the droplet did not have a significant influence on the contact angle [37].

3.2.6 Seawater exposure

The coatings applied on PMMA substrates (see last column in Table 3.1) were immersed in static conditions in seawater in Singapore (1° 23’ 33’’ N, 103° 58’ 34’’ E) and in Barcelona (41° 12’ 43’’ N, 1° 44’ 0’’ E). The two locations were chosen due to their difference in water temperature and biofouling pressure. Visual inspection of biofouling on the panels was undertaken after 2 months of exposure.

3.3 Results and discussion

The main aim of this chapter was to study the diffusion properties of different PEG-based amphiphiles for fouling-release coatings (listed in Table 3.1). The addition of these surface-active additives to PDMS films has an influence on their surface properties. Figure 3.4 shows how the contact angle of a water droplet changes within the first 10 minutes of contact with a PDMS film modified with some of the investigated amphiphiles. Note that a film with PEG (M_w = 400 g/mol) and a film without additives have been added as references (coatings 13 and 14 in Table 3.1 and Figure 3.10).

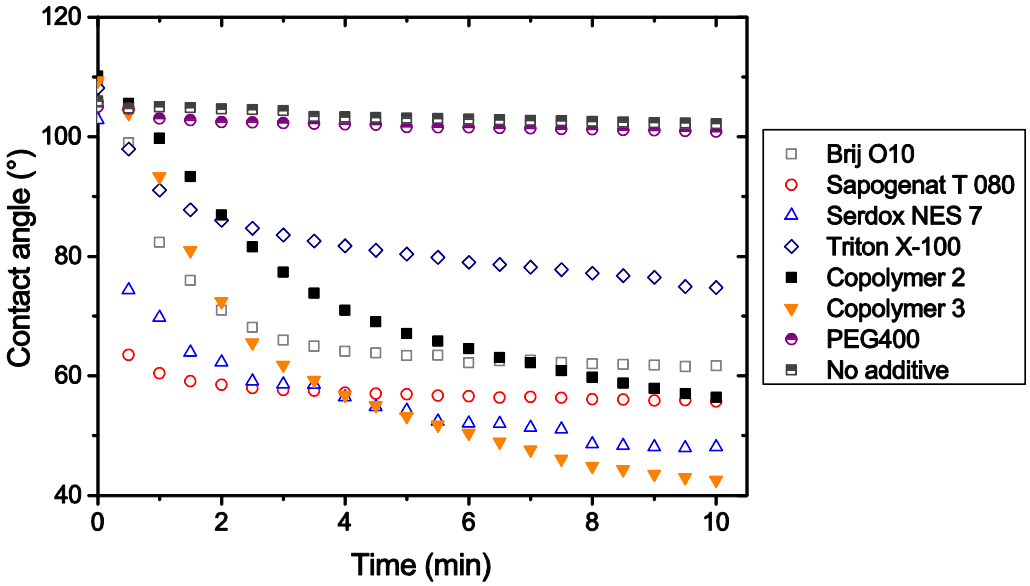

Figure 3.4. Contact angle evolution over time of a droplet of water on top of PDMS films containing some of the PEG-based additives investigated. A crosslinked PDMS film without additives and one using PEG as additive have been added as references.

In spite of some differences regarding the speed of change and the final value of the contact angle, it is clear that the addition of these amphiphilic compounds results in a change of hydrophilicity on the PDMS films' surfaces, both for alkyl-PEG, alkyl-aryl-PEG and PDMS-PEG-based amphiphiles. These surface-active additives can readily diffuse to the surface of the PDMS coatings and change the surface properties. These films have been used for the diffusion experiments (explained in a previous section) which are presented below.

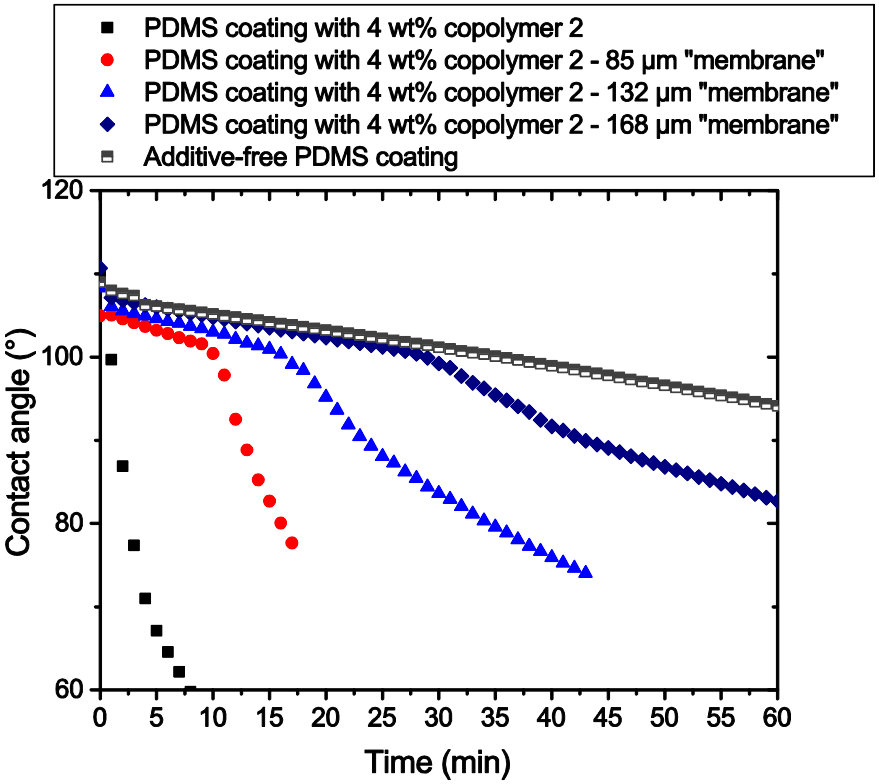

Figure 3.5. Contact angle of a droplet of water on top of PDMS films under different conditions. A PDMS film containing copolymer 2 as additive has been used, without (black squares) and with membranes of three different thicknesses, l_1 = 85 µm (red circles), l_2 = 132 µm (light blue triangles) and l_3 = 168 µm (dark blue diamonds). A PDMS film without additives is added for comparison (grey, half-filled squares).

Additive-free, PDMS films of different thicknesses have been cured separately and, after curing, placed between the additive-containing coating and the water droplet, as shown in Figure 3.3. The contact angle has been monitored by a tensiometer. An example can be seen in Figure 3.5. Due to the hydrophobic nature of the PDMS, the contact angle is initially high (~ 106°) and remains hydrophobic for some time, when the PDMS film is free of the additives used. When the added amphiphiles reach the surface, the contact angle suddenly drops. Not surprisingly, the contact angle drop time (i.e. the time lag) is dependent on thickness of the free film, as expected from Equation 3.2. For each thickness analysed (i.e. 85 µm, 132 µm and 168 µm), the time lags L_1, L_2 and L_3 have been obtained. The additive-free PDMS film used as reference remains hydrophobic throughout the experiment, though a slight decrease of the contact angle is observed, probably due to evaporation effects.

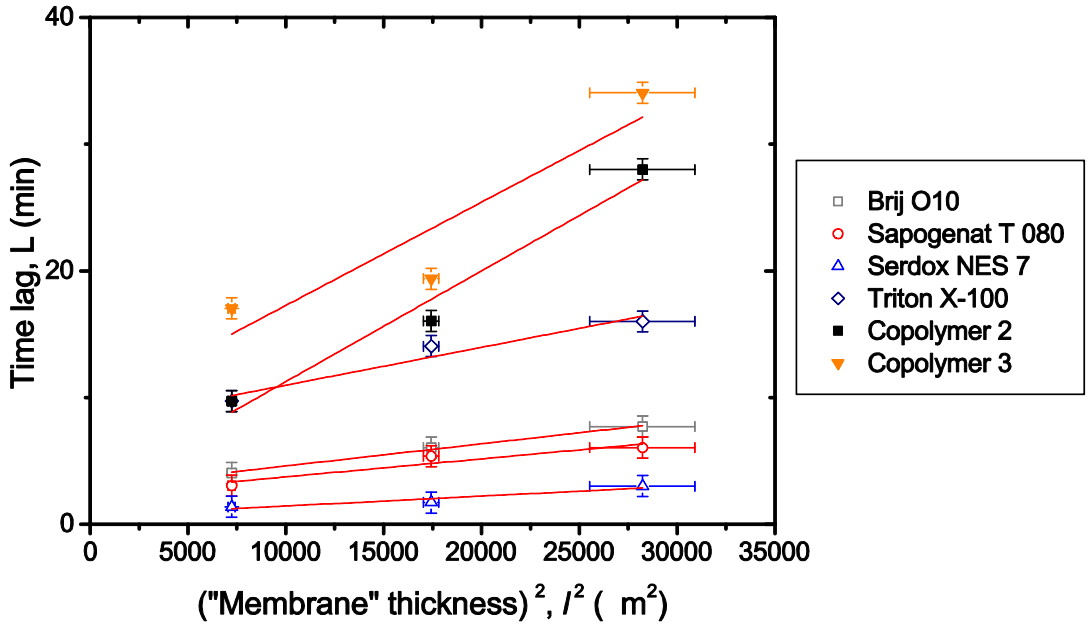

Figure 3.6. Experimental time lag (L) values against the membrane squared thickness (l^2) for some of the amphiphiles used. The linear fit for each set of three points is also shown. The slope of the curves has been used to calculate the diffusion coefficients (see Table 3.1). The y-axis error bars show the standard deviation of three repetitions of a single experiment, assuming its validity for all the experiments.

Figure 6 shows the results of plotting L vs l^2 for some of the amphiphiles studied. The three experimental values obtained for each copolymer are fitted with a straight line and the slope is used to calculate the diffusion coefficients according to Equation 3.3. The results can be found in Table 3.1. Note that all the fitting curves present R^2 values between 0.862 and 0.999. The error is mainly attributed to the variability of the thickness of the film of 168 µm (see x-axis error bar in Figure 3.6). It should also be taken into account that the high thickness films might present higher inhomogeneity due to the difference in curing time between the surface and the core of the film. This can also increase the variability of the results. Nonetheless, a clear tendency can be seen in Figure 3.6. The amphiphiles whose fitting curves present higher slopes (i.e. lower diffusion coefficients) present also the higher diffusion times (i.e. time lags) in the PDMS film.

3.3.1 Effect of the molecular weight of the diffusant

The values of the diffusion coefficients obtained range from $3.2 \cdot 10^{-12}$ to $3.5 \cdot 10^{-11}$ m^2/s. These values are compared to experimental diffusion coefficients obtained for different diffusing species through crosslinked PDMS networks. The diffusing species found in literature have been divided into two groups: (1) small molecules, with molecular weight below 1000 g/mol and (2) PDMS chains, which include both linear and cyclic oligomers and polymers of PDMS of different sizes, all of them above 1000 g/mol. Note that no gases have been included. An overview of the different diffusants, experimental conditions and D values reported in the literature can be found in Table 3.2.

Table 3.2. Experimental diffusion coefficients of different species in PDMS networks. The diffusants have been grouped in "small molecules" and "PDMS chains"

	Diffusant	$M_{w,\ diffusant}$ (g/mol)	$M_{c,\ network}$ (g/mol)	Temperature (°C)	D (m^2/s) · 10^{12}	Reference
Small molecules	Hexadecanethiol	260	-	22	59,0	[38]
	Hexadecanethiol	260	35000[a]	22	39,0	[38]
	PBDE 28	410	-	20	25,1	[39]
	PBDE 47	490	-	20	24,5	[39]
	PBDE 99	570	-	20	19,5	[39]
	PBDE 100	570	-	20	50,1	[39]
	PBDE 153	640	-	20	17,0	[39]
	PBDE 154	640	-	20	16,6	[39]
	PBDE 959	960	-	20	15,8	[39]
	PCB4	220	-	20	29,5	[40]
	PCB52	290	-	20	21,9	[40]
	PCB149	360	-	20	19,5	[40]
	PCB204	430	-	20	16,6	[40]
	Anthracene	180	-	20	37,2	[40]
	Fluorene	170	-	20	52,5	[40]
	Pyrene	200	-	20	24,0	[40]
PDMS chains	PDMS linear	4700	36000	23	1,6	[41]
	PDMS linear	11500	36000	23	1,0	[41]
	PDMS linear	3500	7400	26	6,2	[42]
	PDMS linear	3600	7400	26	5,1	[42]
	PDMS linear	5300	7400	26	3,2	[42]
	PDMS linear	6200	7400	26	3,0	[42]
	PDMS linear	3100	3700	26	6,1	[42]
	PDMS linear	3400	3700	26	5,4	[42]
	PDMS linear	4600	3700	26	3,4	[42]
	PDMS linear	5000	3700	26	3,4	[42]
	PDMS cyclic	4300	1900	23	5,5	[43]
	PDMS cyclic	4300	7400	23	7,6	[43]
	PDMS linear	4700	1900	23	4,8	[43]
	PDMS linear	4700	7400	23	6,3	[43]

[a] estimated from the reported viscosity using Equation 3.3

Although the temperature of these experiments and the molecular weight of the network (M_c) differ to some extent, they exhibit comparable values. Regarding the impact of the molecular weight of the network, it has been previously shown [41] that it has a very small influence on D ($D = k_c \cdot M_c^{0.2}$). With regards to the temperature of the experiments, all the reported values are between 20°C and 26°C, which is assumed not to have a strong effect on the results.

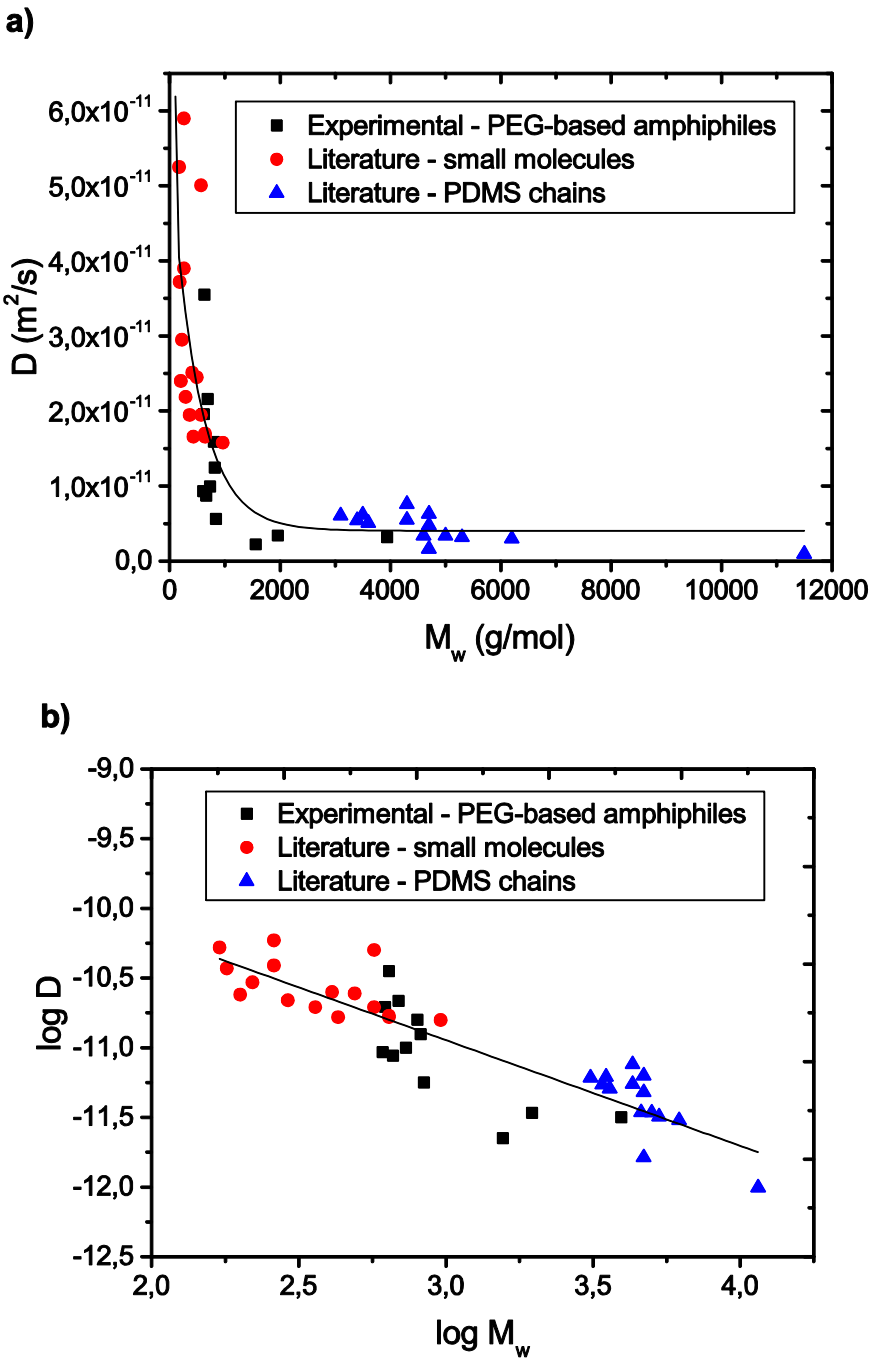

Figure 3.7. Diffusion coefficient of the studied additives and those found in the literature plotted against their molecular weights (a). A log-log plot of the diffusion data is also shown (b). A logarithimic regression has been added for visual help in (a), while a liner regression has been added in (b).

In Figure 3.7, the diffusion coefficients versus their M_w are shown for all the studied amphiphiles, together with values from the literature. It can be seen that the values obtained here are in agreement with what has been published so far, showing a power dependence of the diffusion coefficient with respect to the molecular weight of the diffusing species ($D = k_w \cdot M_w^{\alpha}$), as reported previously in the literature [34]. In this case, α has a value of -0,8 (-1 if only the experimental results obtained here are taken into account). This result is in agreement with what has been reported for PDMS diffusing through PDMS networks [41,42] with α between -1 and -1,3. These values of α are significantly lower than for other polymeric systems. For example, it has been shown that α = -1,7 for linear polyisoprene chains

into polyisoprene networks [44], in spite of both PDMS and polyisoprene networks being great above their T_g. Therefore, the molecular weight of the diffusant has a small effect on the diffusion coefficient in PDMS compared to other polymeric networks. This is reflected in the narrow range of diffusion coefficients obtained, all lying within the same order of magnitude.

Let us compare, as an example, the amphiphiles Triton X-100, Sapogenat T080, Brij O10 and Serdox NES 7, whose chemical structures are shown in Figure 3.8. In spite of having very similar molecular weights and number of PEG units, their diffusion coefficients differ up to a factor of about 4. This fact might be an indication that other parameters than the molecular weight such as the chemistry and structure of the hydrophobic block of the amphiphiles should be taken into account. It has been previously shown for small molecules diffusing in different polymer hosts like polypropylene (PP) and PDMS, that the molecular weight cannot be used as a universal parameter when comparing the diffusion coefficients of species with different chemistries and structures. Instead, other variables have been used, for example, a molecular volume corrected by a shape factor [45] or the total surface area of the molecule [40], showing much better agreement with D than the molecular weight.

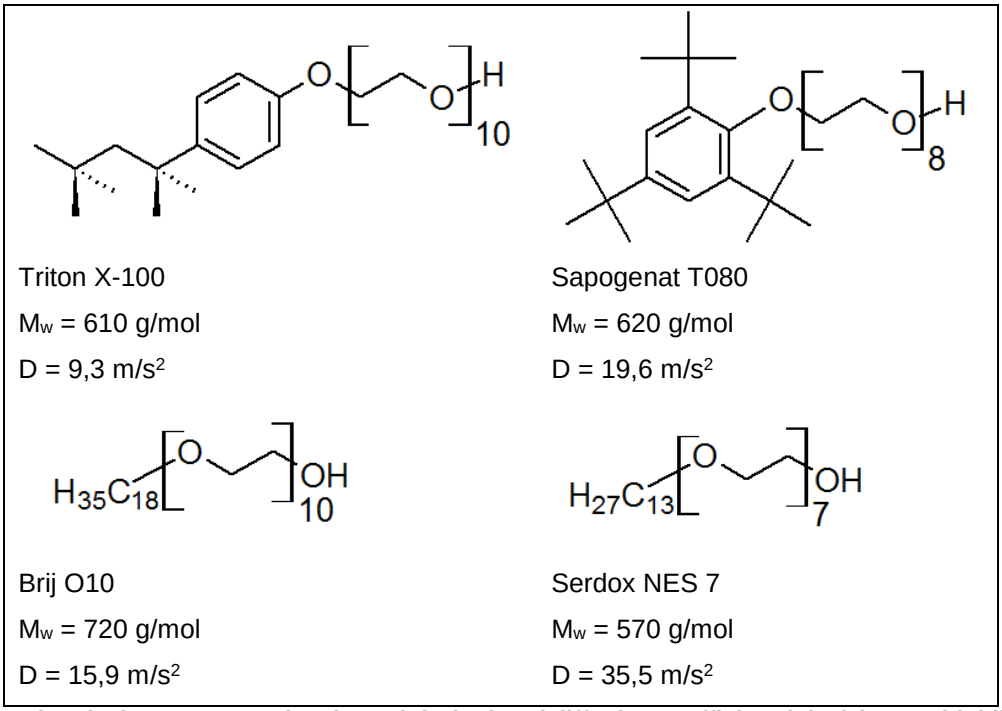

Figure 3.8. Chemical structure, molecular weight (M_w) and diffusion coefficient (D) of the amphiphiles Triton X-100, Sapogenat T 080, Brij O10 and Serdox NES 7.

3.3.2 Effect of the amphiphilicity (polarity) of the diffusant

To assess the effect of the chemistry of the studied amphiphiles on the diffusion coefficient, the hydrophilic-lypophilic balance (HLB) value is used. The HLB value has been traditionally used to characterize the solubility of surfactants, which determines their behaviour in many applications.

HLB values can be experimentally obtained or theoretically estimated. The saponification value has been extensively used to determine HLB values for different surfactants. For non-ionic surfactants,

however, Griffin [46] suggested Equation 3.4 as an easy alternative to obtain HLB values when the saponification value is not available.

$$HLB = \frac{E + P}{5} \qquad \textbf{(Equation 3.4)}$$

where E is the weight percentage of oxyethylene content, and P is the weight percent of polyhydric alcohol content (e.g. glycerol). It should be noted that Equation 3.4 only accounts for the weight fraction of the hydrophilic and hydrophobic groups, while the structure of the two blocks or the presence of aryl groups is neglected. Nonetheless, it is a broadly used formula in the industry of these kinds of amphiphiles.

Figure 3.9 shows the correlation between HLB value and the obtained diffusion coefficient for the different amphiphiles. It can be seen that no apparent relationship exists between these variables. To study the influence of the chemistry and the structure of these amphiphilic molecules, a more systematic approach should be used, with synthesis of well-defined amphiphiles, varying the length and the chemical structure of the two blocks. This is, however, outside the scope of the thesis.

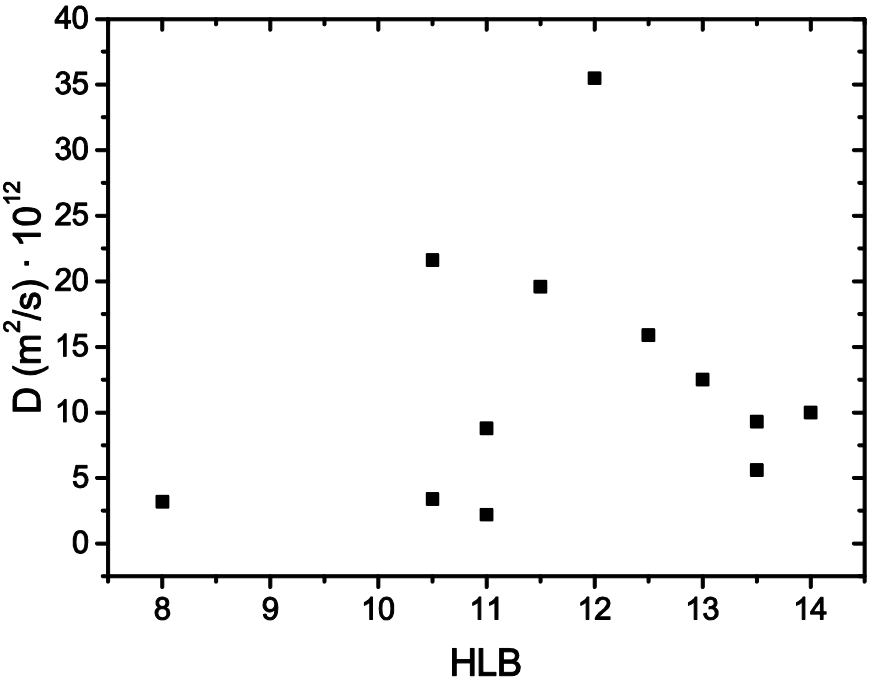

Figure 3.9. Diffusion coefficient of the studied amphiphiles against their hydrophilic-lyphophilic balance (HLB) value.

3.3.3 Effect of the studied amphiphiles on the biofouling-resistance properties of PDMS coatings

Finally, the fouling-resistance properties of these amphiphiles have been investigated. PDMS coatings containing 4 wt% of the different additives were sent to two different locations for seawater immersion, Barcelona and Singapore. Half of each coated panel was overcoated with an additive-free PDMS coating to examine the diffusion properties of these additives in real-life, seawater conditions. After 2 months of exposure, a visual inspection of the coatings was undertaken.

Figure 3.10 shows the coatings after 2 months exposure in (a) Barcelona and (b) Singapore. As shown, the biofouling community consisted mainly of slime, with some tubeworms and bryozoa being present in Singapore as well.

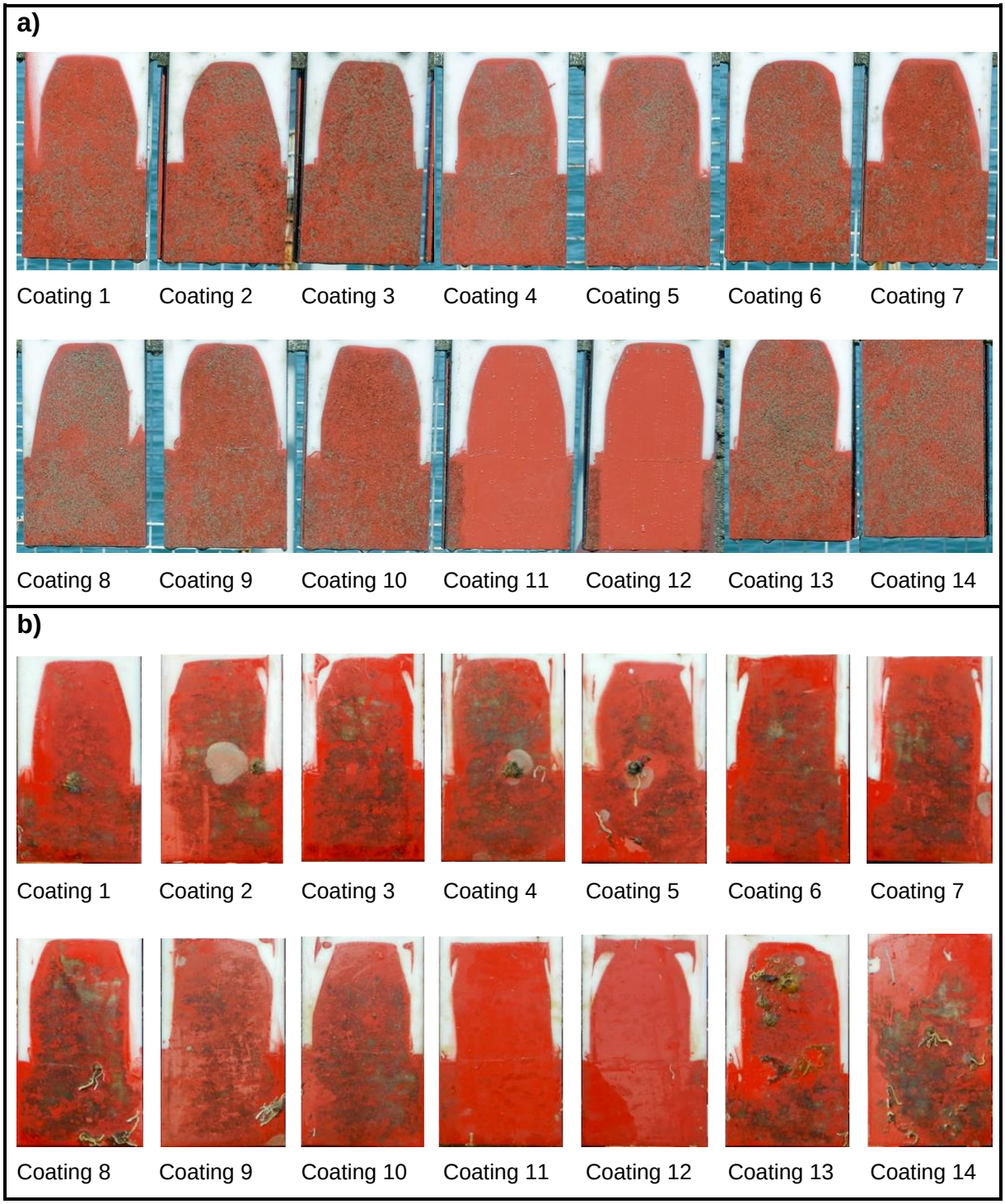

Figure 3.10. Images of the coatings immersed in seawater in Barcelona (a) and Singapore (b) after 2 months of exposure (see Table 3.1).

The two reference coatings analysed, coatings 13 and 14 (the coating containing PEG400 and the additive-free coating) show significant amounts of biofouling after 2 months of exposure, confirming their poor properties regarding biofouling-resistance in static conditions. By comparison with these two

reference coatings, the biofouling-resistance of the coatings modified with PEG-based amphiphiles is discussed below.

First of all, all the alkyl-PEG and alkyl-aryl-PEG amphiphiles investigated show poor fouling-resistance properties in the conditions studied, as the amount of biofouling on their surfaces reached the same extent as on the reference coatings (coatings 1-5 for alkyl-PEG and 6-9 for alkyl-aryl-PEG amphiphiles). This behaviour cannot be explained by a low diffusivity of these species, as it has been shown that they can diffuse through PDMS films in relatively short amounts of time, with lower diffusion coefficients than PDMS-PEG-based copolymers.

On the other hand, some of the PDMS-PEG-based amphiphiles investigated show good fouling-resistance properties, both in the overcoated and the non-overcoated area (see coatings 11 and 12). This fact proves that it is possible to functionalize PDMS surfaces by adding small amounts of amphiphiles in the uncured PDMS mixture. Moreover, these copolymers can diffuse through PDMS films, as previously shown with the time lag method, and thereby provide fouling-resistance properties to PDMS coatings that were, originally, additive-free. However, the PDMS-PEG-based amphiphile with the shortest PDMS chain did not provide fouling-resistance properties.

Amphiphiles with similar diffusion coefficients but different hydrophobic blocks (for example, Sapogenat T130 and Triton X-100 vs copolymers 2 and 3) present very different biofouling-resistance properties, with the amphiphiles containing a PDMS block exhibiting superior properties. In addition, copolymer 1, the PDMS-PEG-based amphiphile with lower molecular weight, also presents significant amounts of biofouling. These facts, together with the presence of fouling on the coatings containing alkyl-PEG and alkyl-aryl-PEG amphiphiles, shows the importance of the anchoring block of these amphiphilic molecules. However, it cannot be clarified whether it is the chemistry or the molecular weight of the anchoring group, which plays the major role in this process, because all the alkyl-PEG and alkyl-aryl-PEG amphiphiles investigated had low molecular weight hydrophobic blocks. Some previous studies have investigated the stability of different PEG-based surfactants and copolymers employed as additives in PDMS films, by soaking the films in water for different exposure times. It was reported that surfactants containing an alkyl group as hydrophobic block show poor stability, and the hydrophilicity of the PDMS films diminish upon immersion [14,47]. Conversely, copolymers using PDMS as anchoring block exhibit superior stability when compared to their alkyl-based homologues. However, only short exposure times (20 hours) were evaluated[14].

The importance of the anchoring group of the amphiphiles in fouling-release coatings can be two fold. On one hand, it can influence the surface coverage properties of the surfactant, which are crucial with regards to the protection against biofouling. On the other hand, the anchoring group controls the solubility, stability and release of the amphiphiles to seawater, dictating to a large extent the long-term stability of these additives. It has been shown, nonetheless, that it is possible to obtain fouling-resistance properties by tuning the size and structure of the hydrophobic block of the added amphiphiles without compromising their diffusion capabilities. It should be noted that, in systems with another network (with a higher α value), changing the molecular weight of the blocks of the amphiphiles will result in a M_w

increase that can have large consequences on the diffusion coefficient of the amphiphiles, and thus might compromise the final fouling-resistance properties provided.

3.4 Conclusions

The diffusion properties of different PEG-based surface-active amphiphiles have been studied in this project. A novel method has been developed for the study of the diffusion of amphiphiles in polymeric networks such as PDMS. It is based on a time lag method modified with a tensiometer, that tracks the contact angle of a water droplet on a PDMS surface. Compared to other methods used for diffusion experiments, it provides results in a much faster way without sample preparation. The method has been successfully used to study the diffusion of additives for fouling-release coatings and experimental diffusion coefficients have been estimated for PEG-based amphiphiles in crosslinked PDMS films.

The diffusion coefficient values obtained have been compared to what has been published up to date. The diffusion coefficients determined for the studied amphiphiles are in agreement with those of small diffusing molecules and polymeric PDMS chains in PDMS networks. The molecular weight of the diffusant has an influence on D following a power law, although the effect of the molecular weight is significantly lower than for molecules diffusing in other polymeric networks. In addition to the influence of the molecular weight of the molecule on the diffusion coefficient, some differences between compounds of similar molecular weight suggest that parameters like the structure and chemistry of the molecules also play a role in the diffusion process. Finally, coatings immersed in seawater have shown that copolymers with PDMS as anchoring group lead to the lowest amount of biofouling, both in the overcoated and the pristine areas. These are very interesting results from two perspectives. On one side, they confirm that PDMS surfaces can be easily functionalized by the addition of small amounts of surface-active additives in an easy and cheap way. Moreover, this process is not limited by the diffusion coefficient of these additives, in spite of the relatively high molecular weight of some of the amphiphiles investigated. Finally, the importance of the anchoring block of the amphiphilic molecules on their fouling-resistance properties has been shown. Amphiphiles with PEG blocks of the same length show very different fouling-resistance properties when the hydrophobic block is changed, with amphiphiles using PDMS as hydrophobic block showing the best performance. These large differences regarding fouling-resistance properties exist for amphiphiles that have coefficient diffusion values in the same range, confirming that the process is not diffusion-limited. Instead, the structure and chemistry of the hydrophobic block exhibit a very strong influence on the fouling-resistance properties provided by these molecules.

3.5 Nomenclature

PBDE	Polybrominated biphenyl ethers
PCB	Polychlorinated biphenyl
PDMS	Poly(dimethylsiloxane)
PEG	Poly(ethylene glycol)
PET	Poly(ethylene terephthalate)
PMMA	Poly(methyl methacrylate)
PP	Polypropylene
PPG	Poly(propylene glycol)
SDS	Sodium dodecyl sulfonate
SEC	Size exclusion chromatography
SLS	Sodium lauryl sulphate
C_0	Initial concentration of the diffusant in the membrane (g/m^3)
D	Diffusion coefficient (m^2/s)
E	Weight percentage of oxyethylene content of a surfactant (-)
HLB	Hydrophilic-lypophilic balance (-)
k_c	Constant of proportionality between M_c and D ($m^2 \cdot mol^{0,2} \cdot s^{-1} \cdot g^{-0,2}$)
k_w	Constant of proportionality between $M_{w,\ diffusant}$ and D ($m^2 \cdot mol^{\alpha} \cdot s^{-1} \cdot g^{-\alpha}$)
l	Film thickness (m)
L	Time lag (s)
M_c	Molecular weight between crosslinks (g/mol)
M_w	Molecular weight (g/mol)
P	Weight percentage of polyhydric alcohol content of a surfactant (-)
R^2	Coefficient of determination (-)
T_g	Glass transition temperature (°C)
α	Power-law dependence factor of D on the M_W (-)
δL	Non-Fickian contribution term to the time lag (s)
μ	Viscosity (cSt)

3.6 References

[1] P.C.W. Thorlaksen, A. Blom, U. Bork, Novel fouling control coating compositions, WO2011076856 (2011).

[2] P.C.W. Thorlaksen, Fouling control coating compositions comprising polysiloxane and pendant hydrophilic oligomer/polymer moieties, WO2013000478 (2013).

[3] D.C. Webster, R.B. Bodkhe, Functionalized silicones with polyalkylene oxide side chains, WO2013052181 (2013).

[4] K.J. Reynolds, B. V. Tyson, Anti-fouling compositions with a fluorinated oxyalkylene-containing polymer or oligomer, WO 2014131695 (2014).

[5] J. Stein, T.B. Brydon, J.A. Cella, Condensation curable silicone foul release coatings and articles coated therewith, US006107381 (2000).

[6] W.P. Liao, Antifouling system comprising silicone hydrogel, WO 2014126643 (2014).

[7] S. Tanino, Antifouling coating composition, antifouling coating film, antifouling substrate, and method for improving storage stability of antifouling coating composition, EP2921538 (2015).

[8] J. Dewitte, G. Piessens, R. Dams, Fluorochemical intermediates, surfactants and their use in coatings, *JOCCA - Surf. Coatings Int.* **78** (1995) 58–64.

[9] A.P. Narrainen, L.R. Hutchings, I. Ansari, R.L. Thompson, N. Clarke, Multi-End-Functionalized Polymers: Additives to Modify Polymer Properties at Surfaces and Interfaces, *Macromolecules*.

40 (2007) 1969–1980.

[10] E. Berndt, S. Behnke, A. Dannehl, A. Gajda, J. Wingender, M. Ulbricht, Functional coatings for anti-biofouling applications by surface segregation of block copolymer additives, *Polymer*. **51** (2010) 5910–5920.

[11] R.B. Bodkhe, S.J. Stafslien, N. Cilz, J. Daniels, S.E.M. Thompson, M.E. Callow, J.A. Callow, D.C. Webster, Polyurethanes with amphiphilic surfaces made using telechelic functional PDMS having orthogonal acid functional groups, *Prog. Org. Coatings*. **75** (2012) 38–48.

[12] H.S. Sundaram, Y. Cho, M.D. Dimitriou, C.J. Weinman, J.A. Finlay, G. Cone, M.E. Callow, J.A. Callow, E.J. Kramer, C.K. Ober, Fluorine-free mixed amphiphilic polymers based on PDMS and PEG side chains for fouling release applications, *Biofouling*. **27** (2011) 589–602.

[13] J. Lee, H. Lee, J. Andrade, Blood compatibility of polyethylene oxide surfaces, *Prog. Polym. Sci.* **20** (1995) 1043–1079.

[14] A. Fatona, Y. Chen, M. Reid, M.A. Brook, J.M. Moran-Mirabal, One-step in-mould modification of PDMS surfaces and its application in the fabrication of self-driven microfluidic channels, *Lab Chip*. **15** (2015) 4322–4330.

[15] N.J. Lin, H.S. Yang, Y. Chang, K.L. Tung, W.H. Chen, H.W. Cheng, S.W. Hsiao, P. Aimar, K. Yamamoto, J.Y. Lai, Surface self-assembled pegylation of fluoro-based pvdf membranes via hydrophobic-driven copolymer anchoring for ultra-stable biofouling resistance, *Langmuir*. **29** (2013) 10183–10193.

[16] T. Røn, J.B. Madsen, N. Nikorgeorgos, S. Lee, Role of Charges of the Surface-grafted Polymer Chains for Aqueous Lubrication at a Nonpolar Interface, *J. Korean Soc. Tribol. Lubr. Eng.* **30** (2014) 247–255.

[17] F.W. Wang, B.F. Howell, A novel fluorescence technique for measurements of additive migration from polymers, *Polymer*. **25** (1984) 1626–1628.

[18] V. V. Krongauz, W.F. Mooney, J.W. Palmer, J.J. Patricia, Real-time monitoring of diffusion in polymer films using fluorescent tracer, *J. Appl. Polym. Sci.* **56** (1995) 1077–1083.

[19] C.M. Mahoney, J. Yu, J.A. Gardella, Depth Profiling of Poly(L-lactic acid)/Triblock Copolymer Blends with Time-of-Flight Secondary Ion Mass Spectrometry, *Anal. Chem.* **77** (2005) 3570–3578.

[20] J. Wen, G. Somorjai, F. Lim, R. Ward, XPS Study of Surface Composition of a Segmented Polyurethane Block Copolymer Modified by PDMS End Groups and Its Blends with Phenoxy, *Macromolecules*. **30** (1997) 7206–7213.

[21] B. Martinez-Lopez, P. Chalier, V. Guillard, N. Gontard, S. Peyron, Determination of mass transport properties in food/packaging systems by local measurement with Raman microspectroscopy, *J. Appl. Polym. Sci.* **131** (2014) 40958.

[22] V. Dobbyn, R. Howley, P. Kirwan, P. McLoughlin, Measurement of the Rates of Diffusion of Halomethanes into Polymer Films Using ATR-FTIR Spectroscopy, *Int. J. Environ. Anal. Chem.* **83** (2003) 643–652.

[23] M.D. Stewards, S. V. Postnikov, H. Vi Tran, D.R. Medeiros, M.A. Nierode, T. Cao, J. Byers, S.E. Webber, C. Grant Willson, Measurement of acid diffusivity in thin polymer films above and below Tg, *ACS Polym. Mater. Sci. Eng.* **81** (1999).

[24] A.J.M. Valente, A.Y. Polishchuk, V.M.M. Lobo, H.D. Burrows, Transport Properties of Concentrated Aqueous Sodium Dodecyl Sulfate Solutions in Polymer Membranes Derived from Cellulose Esters, *Langmuir*. **16** (2000) 6475–6479.

[25] J.A. Faucher, E.D. Goddard, Diffusion and sorption phenomena in neonatal rat stratum corneum, *J. Colloid Interface Sci.* **65** (1978) 444–450.

[26] A.J. Barry, Viscometric Investigation of Dimethylsiloxane Polymers, *J. Appl. Phys.* **17** (1946) 1020.

[27] H.A. Daynes, The Process of Diffusion through a Rubber Membrane, *Proc. R. Soc. A Math. Phys. Eng. Sci.* **97** (1920) 286–307.

[28] A. Hisyam A. Razak, P. Szabo, A.L. Skov, Enhancement of dielectric permittivity by incorporating PDMS-PEG multiblock copolymers in silicone elastomers, *RSC Adv.* **5** (2015) 53054–53062.

[29] S.W. Rutherford, D.D. Do, Review of time lag permeation technique as a method for characterisation of porous media and membranes, *Adsorption*. **3** (1997) 283–312.

[30] R.M. Barrer, Diffusion in and through solids, The University Press, Cambridge, England (1941).

[31] J. Crank, The mathematics of diffusion, 2nd ed., Clarendon Press, Oxford (England) (1975).

[32] H.L. Frisch, The Time Lag in Diffusion. IV, *J. Phys. Chem.* **63** (1959) 1249–1252.

[33] H.L. Frisch, Anomalous Polymer-Penetrant Permeation, *J. Chem. Phys.* **37** (1962) 2408.

[34] L. Masaro, X.X. Zhu, Physical models of diffusion for polymer solutions, gels and solids, *Prog. Polym. Sci.* **24** (1999) 731–775.

[35] C.M. Hansen, In defense of the diffusion equation, unpublished manuscript (available at www.hansensolubility.com) (2013).

[36] K.H. Dai, J. Washiyama, E.J. Kramer, Segregation Study of a BAB Triblock Copolymer at the A/B Homopolymer Interface, *Macromolecules*. **27** (1994) 4544–4553.

[37] S. Srinivasan, G.H. McKinley, R.E. Cohen, Assessing the Accuracy of Contact Angle Measurements for Sessile Drops on Liquid-Repellent Surfaces, *Langmuir*. **27** (2011) 13582–13589.

[38] T.E. Balmer, H. Schmid, R. Stutz, E. Delamarche, B. Michel, N.D. Spencer, H. Wolf, Diffusion of Alkanethiols in PDMS and Its Implications on Microcontact Printing (μCP), *Langmuir*. **21** (2005) 622–632.

[39] J.F. Narváez Valderrama, K. Baek, F.J. Molina, I.J. Allan, Implications of observed PBDE diffusion coefficients in low density polyethylene and silicone rubber, *Environ. Sci. Process. Impacts*. **18** (2016) 87–94.

[40] T.P. Rusina, F. Smedes, J. Klanova, Diffusion coefficients of polychlorinated biphenyls and polycyclic aromatic hydrocarbons in polydimethylsiloxane and low-density polyethylene polymers, *J. Appl. Polym. Sci.* **116** (2010) 1803–1810.

[41] A.N. Gent, R.H. Tobias, Diffusion and equilibrium swelling of macromolecular networks by their linear homologs, *J. Polym. Sci. Polym. Phys. Ed.* **20** (1982) 2317–2327.

[42] L. Garrido, J.E. Mark, J.L. Ackerman, R.A. Kinsey, Studies of self-diffusion of poly(dimethylsiloxane) chains in PDMS model networks by pulsed field gradient NMR, *J. Polym. Sci. Part B Polym. Phys.* **26** (1988) 2367–2377.

[43] L. Garrido, J.E. Mark, S.J. Clarson, J.A. Semlyen, Studies of cyclic and linear poly(dimethylsiloxanes). 15. Diffusion coefficients from network sorption measurements, *Polym. Commun.* **25** (1984) 218–220.

[44] A.N. Gent, S.Y. Kaang, Diffusion of linear polyisoprene molecules into polyisoprene networks, *J. Polym. Sci. Part B Polym. Phys.* **27** (1989) 893–911.

[45] A. Reynier, P. Dole, S. Humbel, A. Feigenbaum, Diffusion coefficients of additives in polymers. I. Correlation with geometric parameters, *J. Appl. Polym. Sci.* **82** (2001) 2422–2433.

[46] W.C. Griffin, Hydrophile-lipophile balance and cloud points of nonionic surfactants, *J. Soc.*

Cosmet. Chem. **5** (1954) 249–256.

[47] H. Madadi, J. Casals-Terré, Long-term behavior of nonionic surfactant-added PDMS for self-driven microchips, *Microsyst. Technol.* **19** (2013) 143–150.

4. Visualization of PDMS-PEG-based copolymers in PDMS films

The distribution and behaviour of PDMS-PEG-based copolymers in PDMS films is a central aspect influencing the biofouling-inhibition properties of FRC. In this chapter, the synthesis of a fluorescent-labelled PEG-b-PMDS-b-PEG copolymer is described. Then, the labelled copolymer is added as additive to a PDMS film, and the distribution and diffusion of the copolymer in the film is visualized and investigated by confocal microscopy.

MSc student Rifnur Latipov contributed significantly to the chemical synthesis procedure described in this chapter, which is gratefully acknowledged. The content of this chapter was submitted for publication as “Visualization of surface-active block copolymers in PDMS films” in Journal of Materials Chemistry B (authors: A. Camós Noguer, R. Latipov, F.B. Madsen, A.E. Daugaard, S. Hvilsted, S. M. Olsen and S. Kiil).

4.1 Introduction

The hydrophobic nature of PDMS has been a drawback in areas such as microfluidics, biomedicine and marine coatings due to adsorption of proteins and cells on its surface, as well as wettability issues [1–4]. The addition of small amounts of surface-active copolymers to uncured PDMS mixtures is gaining popularity as a simple and effective method to change the surface properties of PDMS-based materials [1,3,5,6]. Upon curing, copolymer molecules migrate to the PDMS surface and provide a more hydrophilic surface [5]. This strategy has been exploited with block copolymers containing poly(ethylene glycol) (PEG) and PDMS blocks, which have been added as surface-active additives to PDMS materials.

Despite the wide use of this approach, there is a lack of knowledge regarding the distribution, mobility, behaviour and interaction of block copolymer additives in polymeric hosts. Most of the work has been focused on the final properties of the surface of these materials, studied either by direct (e.g. X-ray photoelectron spectroscopy, XPS) or indirect methods (e.g. contact angle and atomic force microscopy, AFM) [3,5]. Nonetheless, there is a lack of understanding of the processes occurring in the bulk. For example, Loh and Wang [7] reported in 2013 that the formation mechanism of polyvinylidene fluoride (PVDF) membranes when amphiphilic PEG-b-poly(propylene glycol)-b-PEG block copolymers are added is not well understood, in spite of the large number of publications reporting different properties of these membranes. Huang and Yu [8] estimated in 2015 the distribution of a copolymer and the formation of micelles in a polymeric blend by use of rheological measurements. The formation of micelles is certainly a central aspect of these systems due to the low solubility and low critical micelle concentration (CMC) of the copolymers in PDMS. It has been previously reported [9] that the formation of block copolymer micelles in polymer hosts triggers a significant decrease in the kinetics of segregation of the copolymer, which can have serious consequences in applications where the diffusion of these additives is required.

Due to the importance of these copolymers on the final properties of the polymeric materials, new methods are aimed at better understanding the distribution and behaviour of the copolymers hosted in

the bulk of these polymeric materials. The use of fluorescence-based techniques has proven to be a powerful tool to study some of these topics. For example, Kósa et al. [10] used fluorescent probes to study the morphology of interpenetrating polymer networks and the diffusion processes taking place in those networks. Martin and Webber [11] studied the behaviour and micellization of amphiphilic block copolymers labelled with different probes in solution, while Konash et al. [12] studied the distribution and interaction of enzymes incorporated into a polymer matrix. Finally, Cui et al. [13] recently used perylenediimide to label a silicone oil added to a supramolecular gel matrix, where the secretion of the silicone oil was exploited for self-healing purposes.

This chapter presents a method for visualizing the distribution of surface-active copolymers used in PDMS films, inspired by the work of Madsen et al. [14,15], where 4-methylumbelliferone, a fluorescent moiety, was used to label a crosslinker for PDMS. Here, a novel copolymer is synthesized for analytical purposes. A PEG-b-PDMS-b-PEG triblock copolymer is labelled with 4-methylumbelliferone and mixed in an uncured PDMS mixture. Upon curing, the PDMS film is analysed, and the distribution and migration of the non-crosslinked triblock copolymer within the film are studied.

4.2. Experimental

4.2.1 Materials

3-choloropropylmethyldimethoxysilane, hydride-terminated dimethylsiloxane (DMS-H11, M_w ~1500 g/mol determined by ^{1}H-NMR) and platinum-divinyl tetramethyldisiloxane (Karstedt's catalyst), with 2.1-2.4% Pt in xylene, were purchased from Gelest Inc. Mono-allyl-terminated poly(ethylene glycol), (PolyglykolA500, M_w ~500 g/mol), was purchased from Clariant. All other chemicals were acquired from Sigma-Aldrich and used as received unless otherwise stated.

Silanol-terminated poly(dimethylsiloxane) (4000 cSt) was obtained from Dow Corning and a 16-functional pre-polymerized alkoxysilane crosslinker (Dynasylan 40) was received from Evonik Industries. Dibutyltin dilaurate was received from TIB chemicals.

4-Methyl-7-(prop-2-yn-1-yloxy)-2H-chromen-2-one, an alkyne-terminated coumarin molecule, was produced using the method described by Madsen et al. [16] and will not be covered here.

All the glassware used was flame-dried prior to use, and all the reactions were carried out under a nitrogen atmosphere.

4.2.2 Synthetic procedure

4.2.2.1 Synthesis of PDMS(Cl) (1)

3-choloropropylmethyldimethoxysilane (1.00 g, 5.47 mmol) was dissolved in dry toluene (16 mL) in a three neck round-bottom flask. Hydride-terminated dimethylsiloxane (17.24 g, 16.4 mmol) was added to the mixture and stirred for 10 minutes. Tris(pentafluorophenyl) borane in dry toluene (0.7 mL, 0.002 M, 0.03 mol%) was added to the mixture. Methane gas immediately developed, and the reaction was kept under stirring for 5 minutes at RT, until no more methane formation could be observed. The product obtained was used without further purification.

IR (cm^{-1}): 2962 (C-H stretch); 1258 (Si-CH_3 deformation); 1008 (Si-O-Si stretch); 785 (Si-C stretch).

^1H NMR ($CDCl_3$, δ_H, ppm): -0.04 to 0.09 (m, 3H, Si-C*H*$_3$); 0.60 (m, 2H, Si-C*H*$_2$-CH_2); 1.80 (m, CH_2-C*H*$_2$-CH_2); 3.47 (t, J^3= 7.0 Hz, CH_2-C*H*$_2$-Cl), 4.68 (m, Si-H).

^{13}C NMR ($CDCl_3$, δ_C, ppm): 0.4 to 1.6 (Si-*C*H_3); 15.0 (Si-*C*H_2-CH_2); 26.7 (CH_2-*C*H_2-CH_2); 47.6 (CH_2-*C*H_2-Cl).

4.2.2.2 Synthesis of PEG-b-PDMS(Cl)-b-PEG (2)

Mono-allyl-terminated PEG (14.24 g, 28.4 mmol) was added to the round-bottom flask containing the PDMS(Cl) (**1**). Platinum-divinyl tetramethyldisiloxane was dissolved in dry toluene and added to the mixture (0.5 mL, 0.01 mM, 150 ppm). The reaction mixture was heated to 65°C and allowed to react for 4 hours. At the end of the reaction, the excess of allyl-PEG (insoluble in toluene) was removed by decantation. The toluene was removed by rotatory evaporation under vacuum to obtain the product in the form of a clear brown oil (**2**).

IR (cm^{-1}): 3470 (-OH stretch); 2962 (C-H stretch); 2870 (aliphatic C-H stretch); 1258 (Si-CH_3 deformation); 1070 (CH_2-O-CH_2 stretch); 1008 (Si-O-Si stretch); 785 (Si-C stretch).

^1H NMR ($CDCl_3$, δ_H, ppm): -0.02 to 0.05 (m, Si-C*H*$_3$); 0.44 (m, Si-C*H*$_2$-CH_2-); 0.56 (m, 2H, Si-C*H*$_2$-CH_2); 1.53 (m, CH_2-C*H*$_2$-CH_2); 1.76 (m, CH_2-C*H*$_2$-CH_2); 2.62 (s, C-OH); 3.34 (t, J^3= 7.1 Hz. CH_2-C*H*$_2$-Cl); 3.43 (t, J^3= 7.0 Hz, CH_2-C*H*$_2$-Cl); 3.48 to 3.69 (m, O-C*H*$_2$-C*H*$_2$-O).

^{13}C NMR ($CDCl_3$, δ_C, ppm): 0.4 to 1.6 (Si-*C*H_3); 14.0 (Si-*C*H_2-CH_2); 15.0 (Si-*C*H_2-CH_2); 23.1 (CH_2-*C*H_2-CH_2); 26.7 (CH_2-*C*H_2-CH_2); 47.6 (CH_2-*C*H_2-Cl); 70.5 (O-*C*H_2-*C*H_2-O); 74.2 (CH_2-*C*H_2-O).

4.2.2.3 Synthesis of PEG-b-PDMS(N3)-b-PEG (3)

2 was dissolved in dry tetrahydrofuran (THF, 100 mL) together with NaN_3 (1.78 g, 27.4 mmol) and tetrabutylammonium azide (0.156 g, 54.8 µmol). The reaction took place at the boiling temperature of THF (~66°C) under reflux for 72 hours. The reaction mixture obtained was filtered through a Teflon filter (pore size ~0.45 µm) and was used without further purification.

IR (cm^{-1}): 3470 (-OH stretch); 2962 (C-H stretch); 2870 (aliphatic C-H stretch); 2097 (-N_3 stretch); 1258 (Si-CH_3 deformation); 1070 (CH_2-O-CH_2 stretch); 1008 (Si-O-Si stretch); 785 (Si-C stretch).

^1H NMR ($CDCl_3$, δ_H, ppm): -0.02 to 0.05 (m, Si-C*H*$_3$); 0.44 (m, Si-C*H*$_2$-CH_2-); 0.58 (m, 2H, Si-C*H*$_2$-CH_2); 1.53 (m, CH_2-C*H*$_2$-CH_2); 1.78 (m, CH_2-C*H*$_2$-CH_2); 2.62 (s, C-OH); 3.22 (t, J^3= 7.0 Hz, N_3-C*H*$_2$-CH_2); 3.34 (t, J^3= 7.1 Hz, CH_2-C*H*$_2$-Cl); 3.45 (t, J^3= 6.9 Hz, CH_2-C*H*$_2$-Cl); 3.48 to 3.69 (m, O-C*H*$_2$-C*H*$_2$-O).

^{13}C NMR ($CDCl_3$, δ_C, ppm): -1.1 to 1.6 (Si-*C*H_3); 14.0 (Si-*C*H_2-CH_2); 15.0 (Si-*C*H_2-CH_2); 23.1 (CH_2-*C*H_2-CH_2); 26.7 (CH_2-*C*H_2-CH_2); 47.6 (CH_2-*C*H_2-Cl); 54.1 (N_3-*C*H_2-CH_2); 70.5 (O-*C*H_2-*C*H_2-O); 74.2 (CH_2-*C*H_2-O).

4.2.2.4 Synthesis of PEG-b-PDMS(coumarin)-b-PEG (4)

4-Methyl-7-(prop-2-yn-1-yloxy)-2H-chromen-2-one (1.18 g, 5.47 mmol) and CuI (77.2 mg, 0.41 mmol) were added to the reaction flask containing **3** and THF, and stirred for 15 minutes. Finally, distilled triethylamine (0.554 g, 5.47 mmol) was added dropwise. The reaction took place at RT for 17 hours. The reaction mixture was then filtered by vacuum filtering (pore size ~0.45 µm) and the THF was subsequently removed by rotatory evaporation under vacuum. The final product was purified by selective extraction with heptane and methanol to obtain the product in the form of a brown oil (7.36 g, 34.5 %, M_n = 3900 g/mol, M_w = 4500 g/mol, PDI = 1.15).

IR (cm^{-1}): 3470 (-OH stretch); 2962 (C-H stretch); 2870 (aliphatic C-H stretch); 1258 (Si-CH_3 deformation); 1070 (CH_2-O-CH_2 stretch); 1008 (Si-O-Si stretch); 785 (Si-C stretch).

^{1}H NMR ($CDCl_3$, δ_H, ppm): -0.02 to 0.05 (m, Si-C*H*$_3$); 0.44 (m, Si-C*H*$_2$-CH$_2$-); 0.59 (m, 2H, Si-C*H*$_2$-CH$_2$); 1.53 (m, CH$_2$-C*H*$_2$-CH$_2$); 1.78 (m, CH$_2$-C*H*$_2$-CH$_2$); 2.62 (s, C-OH); 3.22 (t, J^3= 7.1 Hz, N$_3$-C*H*$_2$-CH$_2$); 3.34 (t, J^3= 7.1 Hz, CH$_2$-C*H*$_2$-Cl); 3.45 (t, J^3= 7.0 Hz, CH$_2$-C*H*$_2$-Cl); 3.48 to 3.69 (m, O-C*H*$_2$-C*H*$_2$-O); 6.15 (s, 1H, O=C-CH); 6.95 (m, 2H, Ar-H); 7.50 (m, 1H, Ar-H); 7.69 (s, 1H, C=C*H*-N).

^{13}C NMR ($CDCl_3$, δ_C, ppm): 0.4 to 1.6 (Si-*C*H$_3$); 14.0 (Si-*C*H$_2$-CH$_2$); 15.0 (Si-*C*H$_2$-CH$_2$); 23.1 (CH$_2$-*C*H$_2$-CH$_2$); 26.7 (CH$_2$-*C*H$_2$-CH$_2$); 47.6 (CH$_2$-*C*H$_2$-Cl); 70.5 (O-*C*H$_2$-*C*H$_2$-O); 74.2 (CH$_2$-*C*H$_2$-O); 102.2 (Ar-C-Ar); 122.8 (Ar-C-Ar); 122.8 (C=*C*H-N).

4.2.3 Preparation of PDMS films

The PDMS films were prepared by mixing silanol-terminated poly(dimethylsiloxane) (4000 cSt, Dow Corning) (5 g, 0.11 mmol) with a 16-functional ethyl polysilicate alkoxysilane crosslinker (57 mg, 0.065 mmol), in the presence of xylene as solvent. Dibutyltin dilaurate was added as catalyst for the crosslinking reaction (~3.5 mol%).

The synthesized triblock PEG-b-PDMS-b-PEG copolymer was added so it accounted for 4 wt% of the total weight in the dry film. A Dr Blade applicator with a 480 µm gap was used to apply the mixture on a poly(ethylene terephthalate) (PET) film, and cured for a week at room temperature (RT). A film without addition of the synthesized copolymer was prepared as reference.

4.2.4 Methods

4.2.4.1 Contact angle measurements

Dataphysics OCA20 was employed to study the contact angle of a water droplet on the PDMS films by the sessile drop method. A droplet of 25 µl of millipore water was placed on the films, and the contact angle was measured every 2 seconds for 10 minutes, until it reached a stable value. Nonetheless, only one point every 30 seconds is plotted in Figure 4.3 for clarity. Three replicates were measured of each PDMS film.

4.2.4.2 Liquid Chromatography

Size-exclusion chromatography (SEC) was conducted on a SEC system consisting of three different columns, an Agilent PLgel Mixed-C (7.5 x 300 mm) + two Agilent PLgel Mixed-D (7.5 x 300 mm)

columns. Two detectors were used in this study, a UV (Ultraviolet) and an ELS (Evaporative Light Scattering) detector. Tetrahydrofuran (THF) was used as eluent at a flow rate of 1 mL/min at 22°C. The system was calibrated using PEG standards with different M_w obtained from Sigma-Aldrich.

4.2.4.3 FTIR spectroscopy

Attenuated Total Reflectance Infrared Spectroscopy (ATR-FTIR) was conducted on a PerkinElmer Spectrum One (model 2000 Fourier Transform Infrared), where spectra of the different products from the synthesis were taken with 4 cm^{-1} resolution and 32 scans in the range of 4000-650 cm^{-1} at 25°C.

4.2.4.4 NMR Spectroscopy

1-D ^{1}H-NMR and ^{13}C-NMR, and 2-D COSY and HSQC were used to analyse the chemical composition of the different products obtained during the synthetic procedure. The spectra were recorded on a 300 MHz NMR Spectrometer from Spectrospin and Bruker, using $CDCl_3$ as solvent at 25°C, which was used to reference the spectra.

4.2.4.5 Confocal Laser Scanning Microscopy (CLSM)

A 2 x 2 cm (approximately) area of the studied PDMS film was cut with a scalpel. The cut film was placed on top of a glass slide, and was covered with a cover glass. A droplet of Millipore water was placed between the two surfaces of the PDMS film and the glass substrate and cover, to ensure that no trapped air was placed between the PDMS and the glass. Then, the film between the two glass slides was placed in the confocal microscope for analysis.

A confocal laser scanning microscope (SP5-X, Leica Microsystem, Wetzlar, Germany) was used to visualize the coumarin-labelled copolymer in the PDMS film. A 355 nm ultraviolet (UV) laser was used for excitation, while the emission was collected at 420-480 nm. A 63x water immersion objective was used, and the data collected was processed in Leica LAS AF Lite (Leica Microsystems), Volocity (Perkin Elmer) and ImageJ (open source). Images of the x-y plane of the film (105 x 105 µm) were taken at different z-positions (4 µm spacing between consecutives analyses).

It is usually assumed that the fluorescence intensity and the concentration of fluorescent dyes are directly proportional. This is valid if the quantum yield of a given concentration of dye is similar in the different environments studied, that is, the PDMS phase, the labelled copolymer phase and the PDMS-water interface. In addition, no self-quenching effects should take place between dyes. It has been assumed here that the fluorescence intensity detected in the PDMS film is directly proportional to the concentration of labelled copolymer.

4.3 Results and discussion

Physical addition of amphiphilic block copolymers is one of the most used strategies to modify the surface properties of polymeric materials such as adhesion, wettability and biocompatibility. To visualize the copolymer distribution in PDMS films, a novel coumarin-labelled copolymer has been synthesized. Then, the labelled copolymer has been added to a PDMS film and confocal scanning laser microscopy has been subsequently employed to obtain information regarding the distribution of the copolymer within the PDMS film.

4.3.1 Synthesis of the coumarin-labelled PEG-b-PDMS-b-PEG copolymer

A fluorescent-labelled triblock PEG-b-PDMS-b-PEG copolymer was synthesized for visualization purposes. The synthetic procedure is shown in Figure 4.1. Briefly, the objective was to prepare a poly(dimethylsiloxane) backbone with a functional chloropropyl pendant group and reactive end-groups (**1**), to further attach PEG moieties on the end-groups of the siloxane backbone (**2**) and later modify the chloride pendant group to label the PEG-b-PDMS-b-PEG copolymer with a fluorescent dye (**4**).

In the first step of the synthesis, the Piers-Rubinsztajn reaction was used to prepare the PDMS backbone of the triblock copolymer, having two reactive hydride end-groups and a chloride pendant group in the middle of the chain (**1**). Therefore, 3-chloropropylmethyldimethoxysilane was reacted with a low molecular weight hydride-terminated dimethylsiloxane oligomer (~1500 g/mol) in each end. Under the presence of low amounts (<1 mol%) of a borane catalyst (Lewis acid), hydrosilanes and alkoxy silanes react to form a siloxane bond (Si-O-Si) and an alkane as by-product. The reaction takes place at room temperature after a short induction time. The Piers-Rubinsztajn reaction is well-known for being a mild reaction and tolerant of various functional groups. This allows coupling of the Piers-Rubinsztajn reaction with other reactions such as hydrosilylation or click chemistry to obtain complex silicon-based molecules.

Here, the purpose was to attach two siloxane oligomers to 3-chloropropylmethyldimethoxysilane supressing to the highest possible extent high molecular weight products. In polycondensation reactions, the highest molecular weight products are obtained when the reagents are mixed using stoichiometric ratios. Therefore, the hydride-terminated dimethylsiloxane oligomer was used in excess (~50% excess) to supress polymerization (i.e. obtention of long polymeric chains consisting of alternating dimethylsiloxane and 3-chloropropylmethyldimethoxysilane units). The confirmation of the reaction was provided by total disappearance of methoxy groups from 3-chloropropylmethyldimethoxysilane, as shown by the loss of resonance at δ_H = 3.32 ppm and the disappearance of the distinctive stretch peak of the -O-CH_3 group at 2832 cm^{-1} in FTIR. The advance of the reaction could also be followed by SEC, with the molecular weight showing an increase between 2 and 2.5 fold after completion of the reaction, albeit with a significant increase in the polydispesity index (PDI) (see Figure 4.7 in Supporting Information).

In the second step of the synthesis, platinum-catalysed hydrosilylation was used to react telechelic α-allyl-ω-hydroxyl-poly(ethylene glycol) (~500 g/mol) with the hydride end-groups of the PDMS backbone of **1**. The hydrosilylation addition reaction is characterized for producing Si-C bonds at moderate temperatures (~60 °C) without production of any by-product, and therefore is one of the main routes to the production of organosilicon compounds. In this step, mono-allyl-terminated PEG

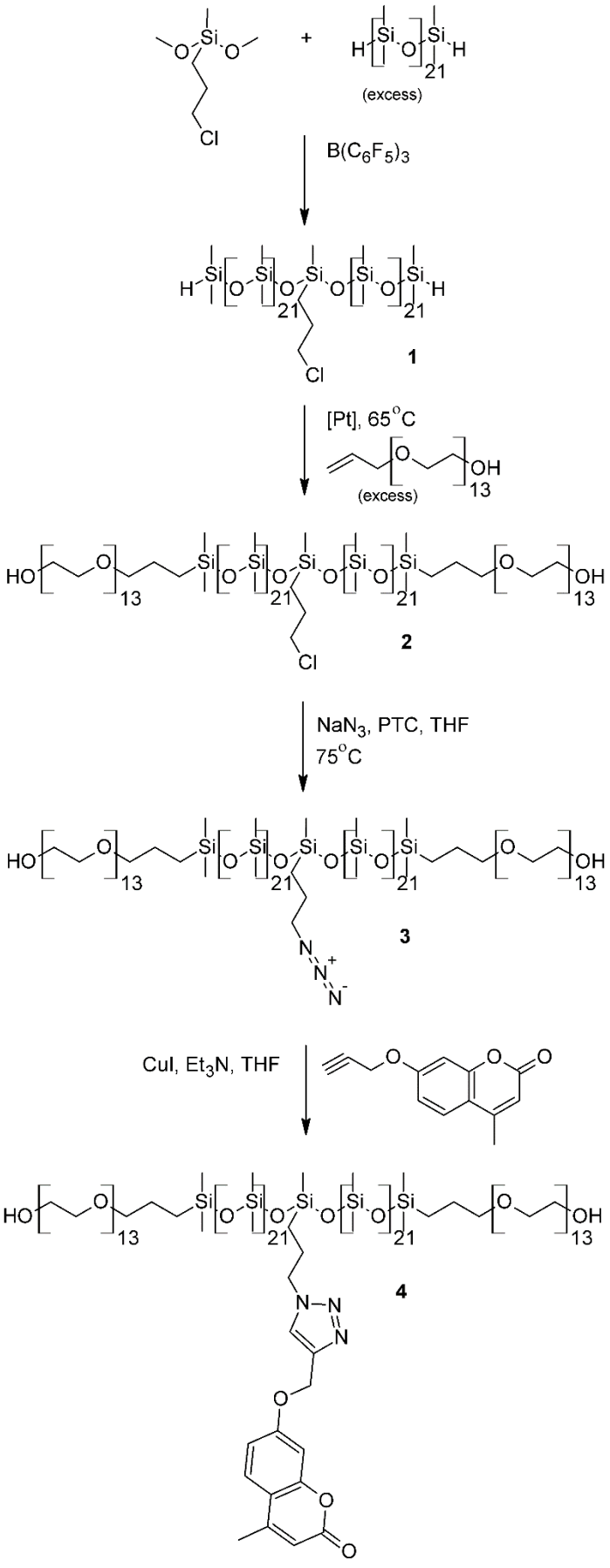

Figure 4.1. Synthesis route for the coumarin-labelled PEG-b-PDMS-b-PEG block copolymer.

was used in excess (~30% excess) to ensure that the reaction yield was as high as possible, so that full conversion of all end-groups was achieved. The appearance of the Si-C bonds with resonances at δ_H = 0.44, 1.53 and 3.34 ppm pointed to the successful formation of the propyl linkers between the allyl-terminated PEG and the PDMS backbone, in the form of Si-CH_2-CH_2-CH_2-O bonds. The reaction was further confirmed by the consumption of hydride groups, as proven by the disappearance of resonance at δ_H = 4.74 ppm. The excess of allyl-PEG was removed by decantation upon completion of the reaction, and was further removed at the last step of the synthetic pathway by selective solvent extraction in heptane.

Once the chloro-functional, triblock PEG-b-PDMS-b-PEG copolymer (**2**) was synthesized, the chloride was substituted to an azido group by nucleophilic substitution using sodium azide (NaN_3). This step of the reaction was followed by the formation of N_3-CH_2- groups, as confirmed by the appearance of resonance at δ_H = 3.23 ppm and δ_C = 53.9 ppm. FTIR corroborated it by the appearance of the characteristic peak at 2097 cm^{-1}, corresponding to the stretch of the azido group (-N_3). The SEC traces showed that the molecular weight of the product did not change in this step (see Figure 4.7 in Supporting Information).

In the last step of the synthetic pathway, click chemistry was used to functionalize **3** with a fluorescent label. The azido group of the copolymer was reacted with an alkyne-terminated coumarin molecule as shown in Figure 4.1, thereby binding the coumarin dye to the backbone of the triblock copolymer and obtaining a coumarin-labelled PEG-b-PDMS-b-PEG copolymer (**4**). The development of this reaction was followed by the appearance of a -C=CH-N- group as confirmed by the resonance at δ_H = 7.52 ppm. The successful labelling of the copolymer molecule was also proven by SEC results, with the peak corresponding to the triblock copolymer becoming visible in the UV-detector after the last synthetic step. The coumarin molecule used, 7-hydroxy-4-methylcoumarin, is a small organic fluorescent molecule (176.17 g/mol) with excitation wavelength in the UV range (λ_{ex} = 380 nm) and emition wavelength in the visible range (λ_{em} = 460 nm).

It is noteworthy that molecular weight of the pendant group of the fluorescent label (i.e. the propyl linker + the azido group + the coumarin molecule) is approximately 300 g/mol, accounting only for 7% of the total molecular weight of the copolymer molecule. However, minor traces of impurities from the synthetic procedure were observed (see the small peak at large elution time in Figure 4.7 in Supporting Information), which could not be removed from the final product.

4.3.2 PEG-b-PDMS-b-PEG block copolymer as additive in PDMS films

The purpose of this chapter was to develop a method to visualize the distribution and behaviour of surface-active additives used in PDMS films/coatings. In this case, PDMS-PEG-based copolymers used as surface-active additives in PDMS films were chosen. To that purpose, the fluorescent-labelled PEG-b-PDMS-b-PEG copolymer was successfully synthesized and added as additive (~4 wt%) to an uncured PDMS mixture. The mixture was applied on a PET film and cured for a week at room temperature. Finally, the film containing the synthesized copolymer was investigated.

The curing process of the PDMS film was carried out by a condensation reaction between α,ω-dihydroxy poly(dimethylsiloxane) (i.e. silanol-terminated PDMS) and a crosslinker containing a number of ethoxy reactive groups as schematically depicted in Figure 4.2. The process is usually known as room temperature vulcanization (RTV).

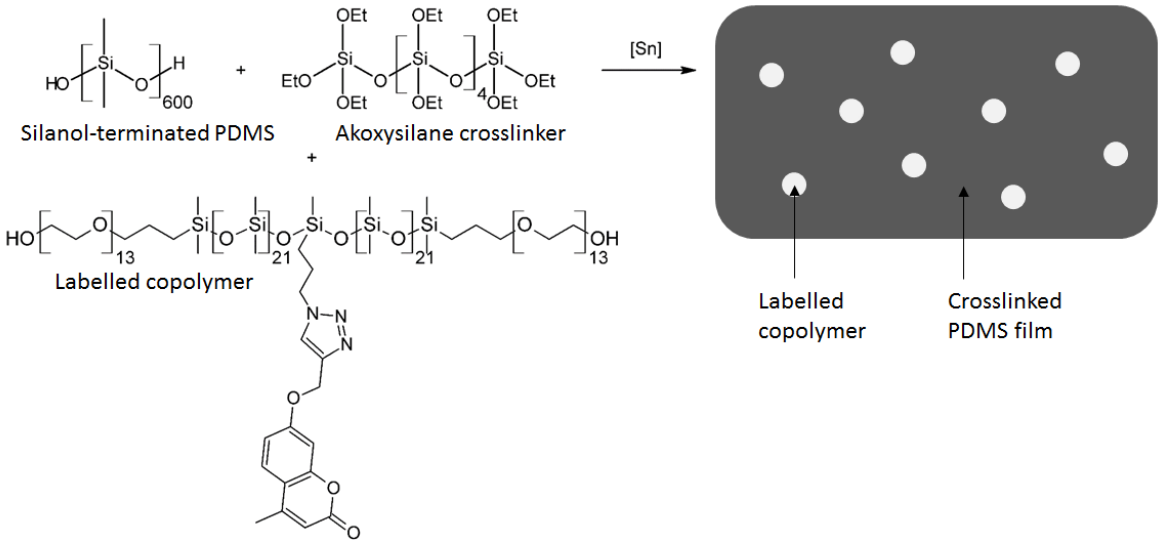

Figure 4.2. Sketch of the studied system illustrating the crosslinking of the PDMS film in the presence of the non-reactive labelled copolymer.

Under the presence of a tin-based catalyst (e.g. dibutyl tin dilaurate), the hydroxyl groups of PDMS react with the ethoxy groups of the crosslinker, producing ethanol as a side product and a siloxane bond (Si-O-Si), thereby crosslinking the PDMS film (see section 1.3.1.2.1 for further information). It is a nucleophilic substitution taking place at the silicon atom of the crosslinker, and the presence of moisture as a cocatalyst is necessary for this reaction to take place, as it activates the tin catalyst by hydrolysis. The hydroxyl end-groups of the PEG blocks of the copolymer do not react under these conditions, partly due to their significantly poorer properties as a nucleophile compared to the hydroxyl groups attached to the silicon atom of PDMS. This means that the PDMS film is formed and the solvent evaporates, but the added copolymer does not participate in the crosslinking process of the PDMS film. Instead, the copolymer molecules remain non-bonded and can diffuse to the surface of the film upon curing.

4.3.3 Diffusion and surface-activity of the synthesized PEG-b-PDMS-b-PEG copolymer

It has been previously shown in Chapter 3 that the addition of amphiphilic copolymers to PDMS films has an important effect on the surface properties of the films. In other words, these additives migrate from the bulk of the film to the surface, altering the physicochemical properties of the film surface. This phenomenon can be studied by sessile water contact angle measurements. Information regarding the energy and chemical composition of the studied surface can be obtained. Here, the migration and surface-activity of the synthesized copolymer in the PDMS film are studied by this method.

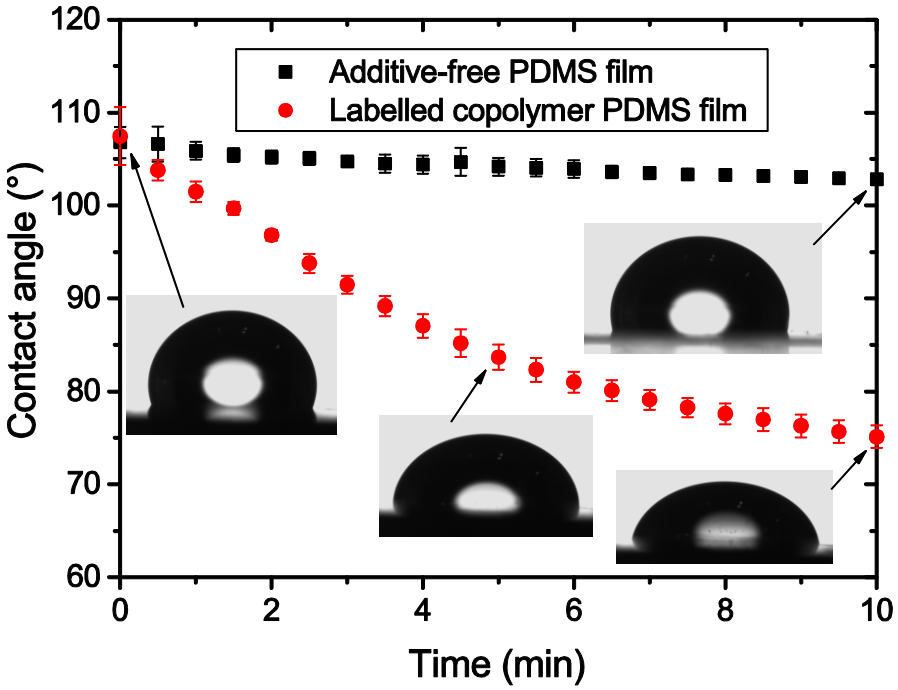

Figure 4.3. Water sessile contact angle measurements of an additive-free (black squares) and a labelled copolymer-containing (red dots) PDMS film. The average of three measurements is shown for each film, and the standard deviation is shown as error bars.

Figure 4.3 shows the contact angle of a water droplet sitting on a PDMS film containing 4 wt% of the synthesized copolymer and compared to an additive-free PDMS film. The contact angle was measured for 10 minutes for both samples (thereafter the contact angle value remained relatively stable) and a clear difference can be seen. As expected, the contact angle of the modified PDMS film decreases over time due to the presence of the labelled copolymer, confirming the diffusion capabilities and surface-activity of the synthesized copolymer. The obtained value of the contact angle after 10 minutes shown in Figure 4.3 is in agreement with what has been reported for similar PEG-based amphiphilic molecules, with contact angles between 40° and 80° approximately [17]. The results are also in agreement with the values obtained in Chapter 3 (see Figure 3.4). In contrast, the additive-free PDMS film remains hydrophobic and no changes can be observed over time.

4.3.4 Visualization of the PEG-b-PDMS-b-PEG copolymer in the PDMS film

With the aim of visualizing the distribution and the processes taking place in the bulk of the prepared PDMS film, confocal laser scanning microscopy (CLSM) has been employed to measure the distribution of the labelled triblock copolymer as a function of position and time. The PDMS film was placed on the confocal microscope, mounted between two glass slides in “wet conditions”. The fluorescence intensity emitted by the copolymer was recorded at different z-positions. Note that the position z = 0 µm was arbitrarily taken at some point far above the surface of the PDMS film where no fluorescence could be detected, and values of z > 0 indicate z-positions inside the PDMS film.

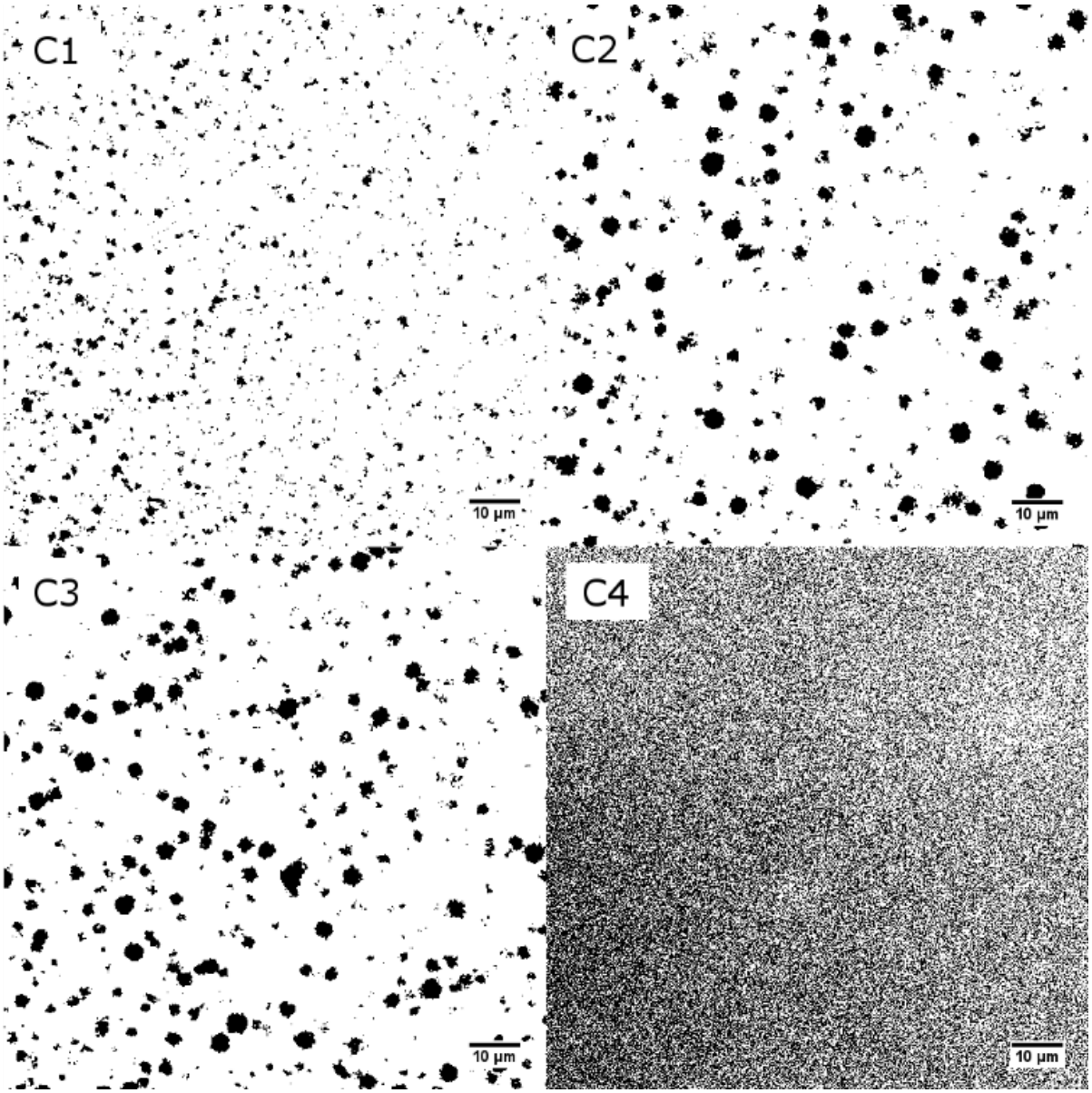

Figure 4.4. Fluorescence intensity images of the PDMS film at 4 different z-positions, 3 inside the PDMS film, C1 (z_{C1} = 90 µm), C2 (z_{C2} = 128 µm) and C3 (z_{C3} = 192 µm), and one at the PDMS-water interface, C4 (z_{C4} = 295 µm). All the measurements were undertaken at 25°C. The thickness of the PDMS film was measured by optical microscopy means in dry contiditions to be approximately 210 µm.

In Figure 4.4, images of x-y planes of the film at four different z-positions can be seen: C1 (z_{C1} = 90 µm), C2 (z_{C2} = 128 µm), C3 (z_{C3} = 192 µm) and C4 (z_{C4} = 295 µm). Some clear differences can be seen from the four images regarding the distribution of the copolymer in the PDMS film. Images at C1, C2 and C3 show that the synthesized copolymer is distributed in spherical domains inside the PDMS film. The size of these domains varies depending on the z-position, being smaller closer to the surface (C1) and bigger in the bulk of the film (C2, C3). Conversely, the image at the PDMS-water interface (C4) shows a different structure, with the triblock copolymer being homogeneously distributed within the x-y plane, without any domain formation on the micron range being detected.

The size of the spherical domains was analysed by use of image analysis software. To that purpose, Volocity and ImageJ softwares were employed. Volocity has some tools which allow for recognition and

analysis of 3-D entities in stacks of x-y (2-D) images. Volocity returns some parameters of the entities detected (the copolymer spherical domains in this case), such as position, volume and shape factor, among others. Simultaneously, ImageJ software was employed to study the size of the domains at different z-positions from images obtained at different depths (see for example the images shown in Figure 4.4). ImageJ identifies circumferences in 2-D images, and returns the area and position of each recognized circumference. The diameter of the circumference is calculated and assumed to be equal to the diameter of the spherical domain in which it is contained. The drawback of this approach is that each circumference detected is assumed to represent the largest section of a given spherical domain, which is not necessarily true. The results obtained from ImageJ are therefore expected to underestimate the real diameter of the copolymer domains. The results from both methods, however, are expected to be comparable.

Figure 4.5 shows the diameter of each individual copolymer domain inside the PDMS film against the z-position of its centre based on the results provided by Volocity. Moreover, the average of the largest 25% domains in each z-position provided by ImageJ is plotted as black dots for comparison. Note that the average of the largest 25% domains for each depth was chosen to better illustrate the importance of the large domains in each depth, and minimize to some extent the effect of the large amount of small domains detected. The small domains detected by ImageJ are a mixture of small domains and larger domains which have the center in another z-position, and therefore only a small slice of the spherical domain is visible at a certain z-position. Note also that below 60 µm and above 270 µm no domains within the detection limits of the technique could be detected.

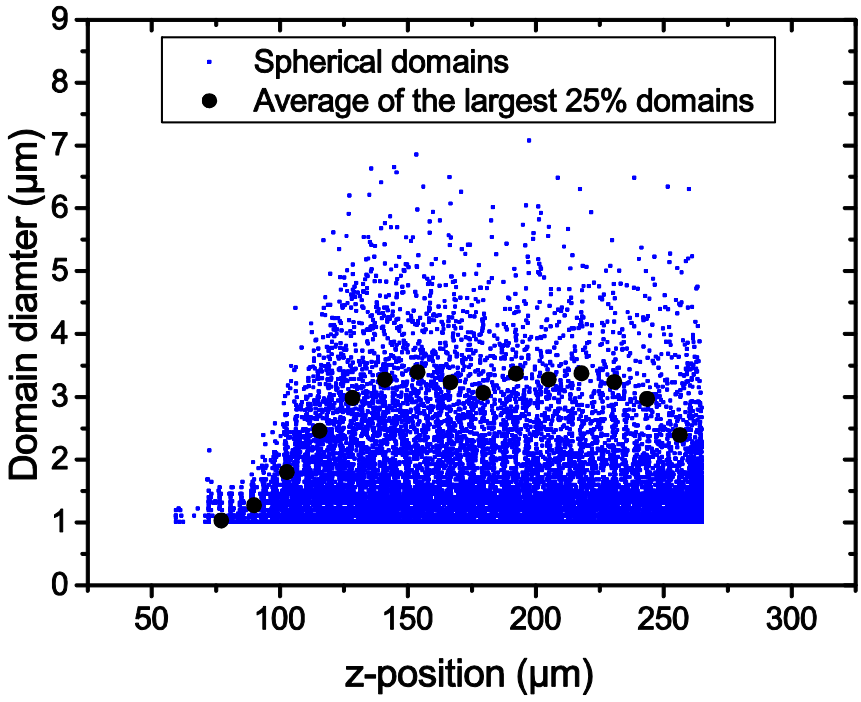

Figure 4.5. Diameter of the spherical domains of coumarin-labelled copolymer as a function of z-position (blue, obtained with Volocity) and the average of the biggest 25% domains at different z-positions (black, obtained with ImageJ).

It can be clearly seen that there is a z-position dependence of the size of the copolymer domains, with small domains being present on the surface of the film (approximately from z = 60 µm to z = 100 µm), which become larger until a maximum of around 7 microns is reached, as shown in Figure 4.5. After that, the size of the domains remains stable. These results are in agreement with the images at different depths presented in Figure 4.4. A slight decrease in size can be seen at the bottom of the film. The difference in domain size between the surface and the bulk of the film may be attributed to different reasons. Due to the higher concentration of moisture (a reactant in the PDMS crosslinking reaction) and faster solvent evaporation rates, the film is initially crosslinked on the surface, while the crosslinking in the bulk of the film takes place at a later stage. The crosslinking of the film results in a decrease in the free volume and therefore the copolymer molecules might migrate to the bulk of the film. Furthermore, the faster evaporation of xylene from the surface, together with the low solubility of the copolymer in PDMS can also be a reason for the copolymer to assemble into spherical domains in the bulk of the film and thus decrease the energy penalty associated with the interfacial area between the copolymer and the PDMS matrix.

4.3.5 Migration of PEG-b-PDMS-b-PEG copolymer in the PDMS film

To study possible variations over time in the distribution of the copolymer in the PDMS film, it was decided to analyse the PDMS film on the same spot at different times. Three measurements were undertaken with 15 minutes between consecutive scans and the results are plotted in Figure 4.6, where the fluorescence intensity vs the z-position is shown for three different times.

Three main conclusions can be drawn from Figure 4.6. Firstly, there is a significant amount of copolymer at the interfaces of the PDMS film. Assuming that the quantum yield of the fluorescent label is similar in the PDMS bulk and PDMS-water interface, the copolymer is distributed approximately equally between the top interface, the bulk of the film and the bottom interface, with one third of the copolymer molecules being present in each of these three positions (see also Figure 4.9 in Supporting Information). Secondly, the fluorescence intensity is not constant throughout the film, i.e. the synthesized copolymer has a tendency to distribute unevenly. This is in agreement with the previous results, showing that the domains vary in size with the z-position. Finally, a change in fluorescence over time can be seen if the three experiments are compared, with the fluorescence intensity decreasing in the bulk of the film, which increases at the two PDMS interfaces. Although the change in fluorescence intensity is significant in such a short amount of time, these results are in agreement with what has been shown in Chapter 3, namely that surface-active PEG-b-PDMS-b-PEG copolymers added as additives to PDMS can diffuse through PDMS films of 168 µm in approximately 30 minutes (see Figure 3.5). A plot of the accumulative fluorescence vs the z-position (see Figure 4.9 in Supporting Information) confirms that the total amount of fluorescence remains constant throughout the three measurements, confirming the migration of the synthesized triblock copolymer. By comparison of Figures 4.5 and 4.6, it can be hypothesized that the smaller domains on the surface of the PDMS film are due to depletion. That is, the copolymer molecules initially contained in the spherical domains close to the surface migrated to the surface of the film, thus leaving behind a layer of PDMS with low amounts of copolymer, contained in small-sized domains.

The results shown in Figures 4.4 and 4.5 have some similarities to those observed by Cui et al. [13], who studied the secretion of a hydrophobic silicone oil in a supramolecular polymer matrix. A PDMS oil was embedded in a PDMS-urea polymer, which was reversibly crosslinked by hydrogen bonds between the urea groups. Their results showed a system with a layer of high concentration of silicone oil on the surface, followed by a droplet-free layer and, after that, the bulk of the film with droplets of silicone oil embedded in the polymer-gel matrix.

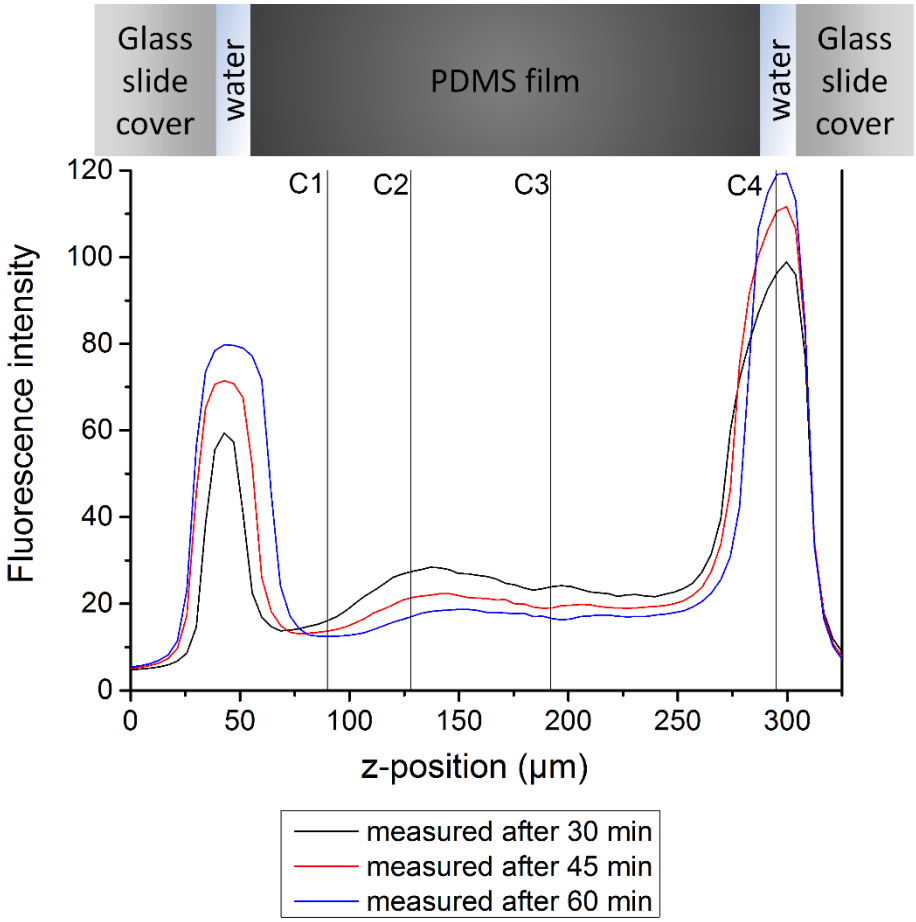

Figure 4.6. Fluorescence intensity distribution as a function of the z-position (depth) for the same PDMS film measured at three different times. The z-position of the images shown in Figure 4.4 of the PDMS film at three different depth positions (C1, C2, C3) and at one of the PDMS-water interface (C4) are marked with black solid lines. For calculation, the baseline has been established connecting the first and last points of the plot (i.e. at z = 0 and z = 325 µm).

The results shown in Figures 4.4 and 4.5 have some similarities to those observed by Cui et al. [13], who studied the secretion of a hydrophobic silicone oil in a supramolecular polymer matrix. A PDMS oil was embedded in a PDMS-urea polymer, which was reversibly crosslinked by hydrogen bonds between the urea groups. Their results showed a system with a layer of high concentration of silicone oil on the surface, followed by a droplet-free layer and, after that, the bulk of the film with droplets of silicone oil embedded in the polymer-gel matrix.

In the presented chapter, the distribution and migration of triblock PDMS-PEG-based copolymers in PDMS films have been studied. Due to the flexibility of the synthetic pathway presented, different modifications could be introduced to further improve the understanding of these systems. Hence, the

effect of the molecular weight of the copolymer and the relative molecular weight of its blocks on the distribution and migration of the copolymer could be studied. Likewise, more significant variations could be considered. The PEG block of the copolymer could be substituted by other hydrophilic polymers providing biofouling-inhibition properties such as poly(acrylic acid) or poly(vinyl alcohol) to mention some examples (see section 1.3.2.2.2), and elucidate the influence of the chemistry of the hydrophilic block on the aforementioned phenomena. Finally, different PDMS-based block copolymers could be synthesized and labelled with different dyes. In that way, all the different PDMS-based copolymers could be simultaneously added to a PDMS film and independently visualized at the same time by use of different radiation wavelengths.

4.4. Conclusions

A novel coumarin-labelled triblock PEG-b-PDMS-b-PEG copolymer has been synthesized for visualization purposes combining the Piers-Rubinstajn reaction, the hydrosilylation reaction and click chemistry in a robust and versatile synthetic pathway. The surface-activity of the synthesised copolymer has been confirmed by contact angle measurements. The labelled copolymer has been used as additive in a PDMS film, which has been studied by confocal microscopy and subsequently by image analysis software.

It has been shown that the synthesized copolymer tends to coalesce into spherical domains inside the PDMS film. Domains as large as 7 µm in diameter have been observed, and it has been found that the size of the domains depend on the z-position, with small domains being present close to the surface, while larger domains exist in the bulk of the PDMS film. Likewise, the concentration of the copolymer inside the film varies with the z-position. A significant amount of copolymer was observed homogeneously distributed in the interfaces of the film, presenting a different distribution pattern than in the bulk of the film where spherical domains could be observed. Finally, it has been shown that the distribution of the copolymer in the film changes over time, with copolymer diffusing from the bulk of the film towards its interfaces, in agreement with the expected surface-activity of these amphiphilic copolymers. In summary, the versatile method presented allows for visualization and understanding of complex systems such as the distribution and diffusion of surface-active block copolymers in PDMS films.

4.5 References

[1] J. Seo, L.P. Lee, Effects on wettability by surfactant accumulation/depletion in bulk polydimethylsiloxane (PDMS), *Sensors Actuators, B Chem.* **119** (2006) 192–198.

[2] A.G. Nurioglu, A.C.C. Esteves, G. de With, Non-toxic, non-biocide-release antifouling coatings based on molecular structure design for marine applications, *J. Mater. Chem. B*. **3** (2015) 6547–6570.

[3] Z. Wu, K. Hjort, Surface modification of PDMS by gradient-induced migration of embedded Pluronic, *Lab Chip*. **9** (2009) 1500.

[4] H. Madadi, J. Casals-Terré, Long-term behavior of nonionic surfactant-added PDMS for self-driven microchips, *Microsyst. Technol.* **19** (2013) 143–150.

[5] T. Røn, I. Javakhishvili, S. Hvilsted, K. Jankova, S. Lee, Ultralow Friction with Hydrophilic

Polymer Brushes in Water as Segregated from Silicone Matrix, *Adv. Mater. Interfaces*. **3** (2016) 1500472.

[6] H. Lee, L.A. Archer, Functionalizing Polymer Surfaces by Field-Induced Migration of Copolymer Additives. 1. Role of Surface Energy Gradients, *Macromolecules*. **34** (2001) 4572–4579.

[7] C.H. Loh, R. Wang, Insight into the role of amphiphilic pluronic block copolymer as pore-forming additive in PVDF membrane formation, *J. Memb. Sci.* **446** (2013) 492–503.

[8] C. Huang, W. Yu, Role of block copolymer on the coarsening of morphology in polymer blend: Effect of micelles, *AIChE J.* **61** (2015) 285–295.

[9] K.H. Dai, J. Washiyama, E.J. Kramer, Segregation Study of a BAB Triblock Copolymer at the A/B Homopolymer Interface, *Macromolecules*. **27** (1994) 4544–4553.

[10] C. Kósa, M. Danko, A. Fiedlerová, P. Hrdlovic, E. Borsig, R.G. Weiss, Pyrenyl Fluorescence as a Probe of Polymer Structure and Diffusion in a Polyethylene:Poly(butyl methacrylate)- co -polystyrene Interpenetrating Network and Related Polymers, *Macromolecules*. **34** (2001) 2673–2681.

[11] T.J. Martin, S.E. Webber, Fluorescence Studies of Polymer Micelles: Intracoil Direct Energy Transfer, *Macromolecules*. **28** (1995) 8845–8854.

[12] A. Konash, M.J. Cooney, B.Y. Liaw, D.M. Jameson, Characterization of enzyme–polymer interaction using fluorescence, *J. Mater. Chem.* **16** (2006) 4107–4109.

[13] J. Cui, D. Daniel, A. Grinthal, K. Lin, J. Aizenberg, Dynamic polymer systems with self-regulated secretion for the control of surface properties and material healing, *Nat. Mater.* **14** (2015) 1–6.

[14] F.B. Madsen, I. Javakhishvili, R.E. Jensen, A.E. Daugaard, S. Hvilsted, A.L. Skov, Synthesis of telechelic vinyl/allyl functional siloxane copolymers with structural control, *Polym. Chem.* **5** (2014) 7054–7061.

[15] F.B. Madsen, A.E. Daugaard, C. Fleury, S. Hvilsted, A.L. Skov, Visualisation and characterisation of heterogeneous bimodal PDMS networks, *RSC Adv.* **4** (2014) 6939–6945.

[16] F.B. Madsen, I. Dimitrov, A.E. Daugaard, S. Hvilsted, A.L. Skov, Novel cross-linkers for PDMS networks for controlled and well distributed grafting of functionalities by click chemistry, *Polym. Chem.* **4** (2013) 1700–1707.

[17] H.T. Kim, J.K. Kim, O.C. Jeong, Hydrophilicity of surfactant-added poly(dimethylsiloxane) and its applications, *Jpn. J. Appl. Phys.* **50** (2011).

4.6 Supporting Information

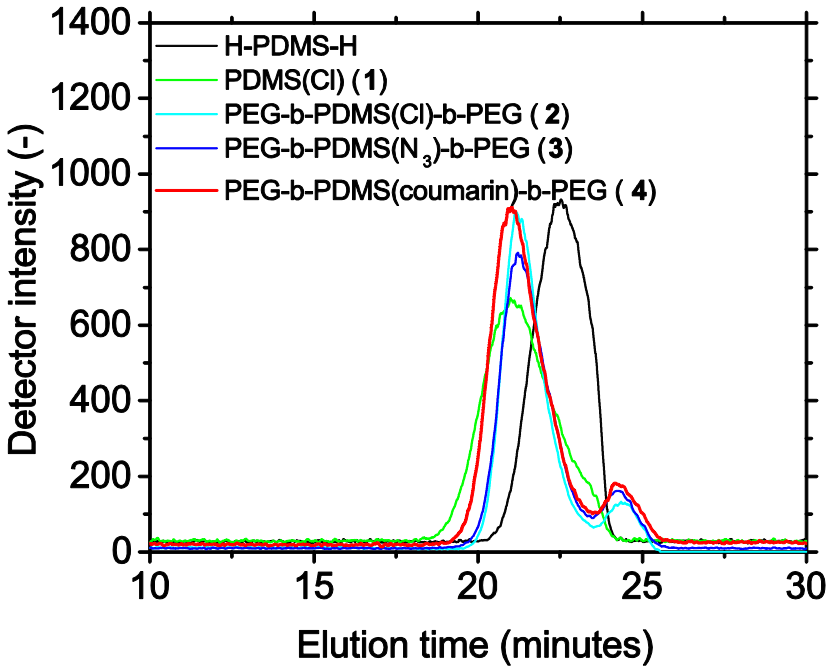

Figure 4.7. SEC chromatogram of the synthesis products from initial H-PDMS-H (black) until the final coumarin-labelled copolymer (red).

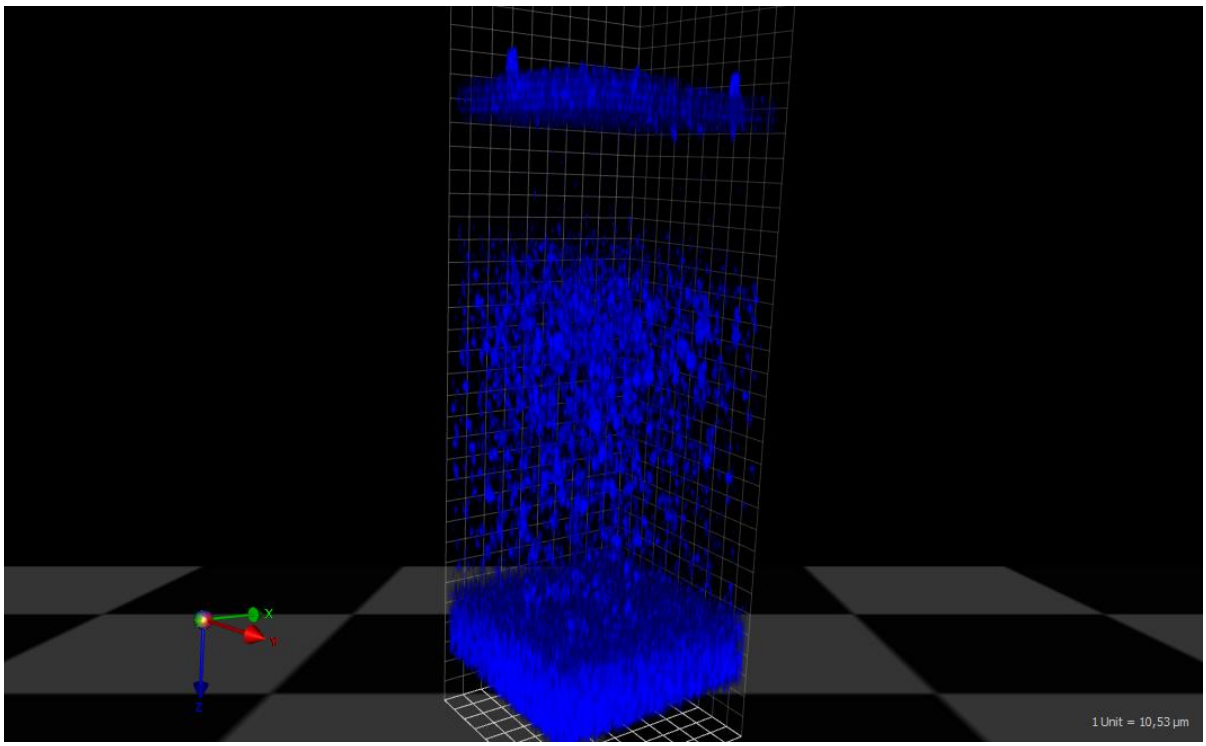

Figure 4.8. 3-D Projection obtained by confocal laser scanning microscopy (CLSM). The blue colour represents fluorescent activity of the cuomarin molecule. Formation of spherical domains of coumarin-labelled copolymer inside the PDMS film can be observed.

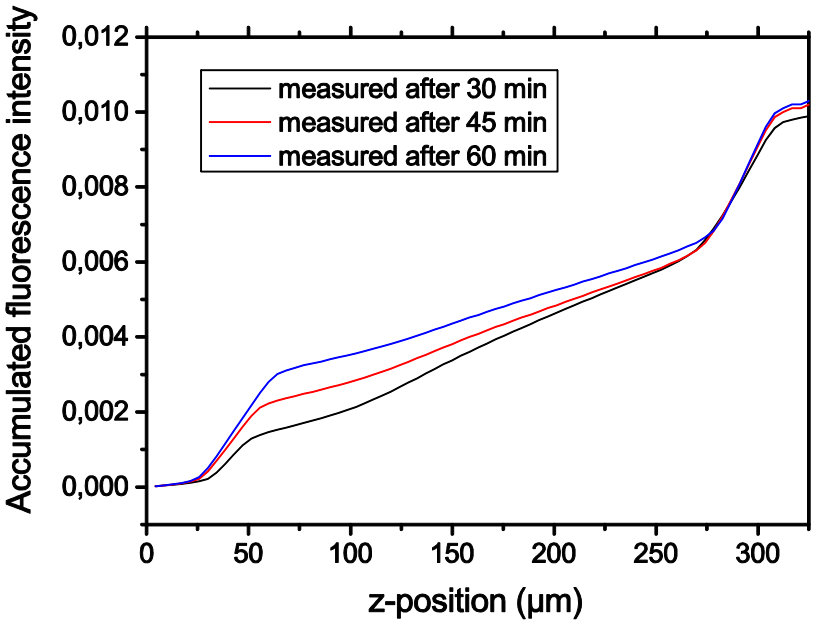

Figure 4.9. Total accumulated fluorescence for the three coatings as a function of z-position that shows that the total amount of fluorescence intensity is constant within the three measurements.

5. Long-term chemical stability of PDMS-PEG-based copolymers in FRC

For PDMS-PEG-based copolymers to be a long-term solution in FRC, the chemical stability of these copolymers in FRC immersed in seawater is essential. This chapter investigates the long-term chemical stability and degradation of different PDMS-PEG-based copolymers in PDMS coatings immersed in seawater for 2.5 years, and the results are compared to copolymers degraded in the laboratory under a range of conditions.

The content of this chapter was published as “Long-term stability of PEG-based antifouling surfaces in seawater” in Journal of Coatings Technology and Research (2016) (authors: A. Camós Noguer, S. Hvilsted, S. M. Olsen and S. Kiil).

5.1 Introduction

Polyethylene glycol (PEG) has been extensively employed to functionalize surfaces in the biomedical field due to its antifouling (i.e. biofouling-inhibition) properties [1]. Many studies have focused on optimizing the antifouling behaviour of surfaces functionalized with PEG by changing different parameters, mainly: (1) the molecular weight (M_w), (2) the chemistry of the end-group and (3) the grafting density [2,3]. Over recent years, the widespread use of PEG has also reached the fouling-release coatings industry, as supported by the number of recent patents [4–10] and scientific papers [11–14]. For PEG-based surfaces to be a viable long-term solution in fouling-release coatings, it needs to be replenished and retained on the coating surface and stable in the marine environment.

PEG is a linear, hydrophilic and non-polar polymer with high resistance to cell and non-specific protein adsorption [1,15]. In spite of the unique properties of PEG, it also presents some limitations concerning its use in fouling-release coatings. Problems related to the long-term stability of PEG have been reported [2,16]. PEG has shown to undergo both biotic and abiotic degradation under different conditions [17,18]. In the case of biotic degradation, oxidation of the PEG chain is the most accepted mechanism [17], though others have found evidence of hydrolysis involved in the process [19]. The chemical pathway proposed for the biotic degradation of PEG involves the oxidation of the terminal hydroxyl group to an aldehyde and a carboxylic acid, followed by the cleavage of the ether bond and therefore reducing the length of the PEG chain by one unit [17]. Very limited research has been done with respect to the biotic degradation of PEG in seawater [20]. Regarding the abiotic degradation of PEG, others have proven both photooxidation [21] and thermal oxidative degradation [18,21,22] of PEG in air, both through a radical-based pathway. The suggested mechanism, shown if Figure 5.1, is initiated by the formation of a hydroperoxide in a α-C of the oxygen atom in the PEG chain, which is followed by a β-scission, which ends up with the formation of formates and other esters as main products, though formic acid and other products have also been observed [18,21–23]. Hassouna et al. [24] and Morlat and Gardette [25] compared the results of photooxidation of PEG in air and water. They found similar degradation products, i.e. formates and esters, with the partial hydrolysis of formates into formic acid and formate ions.

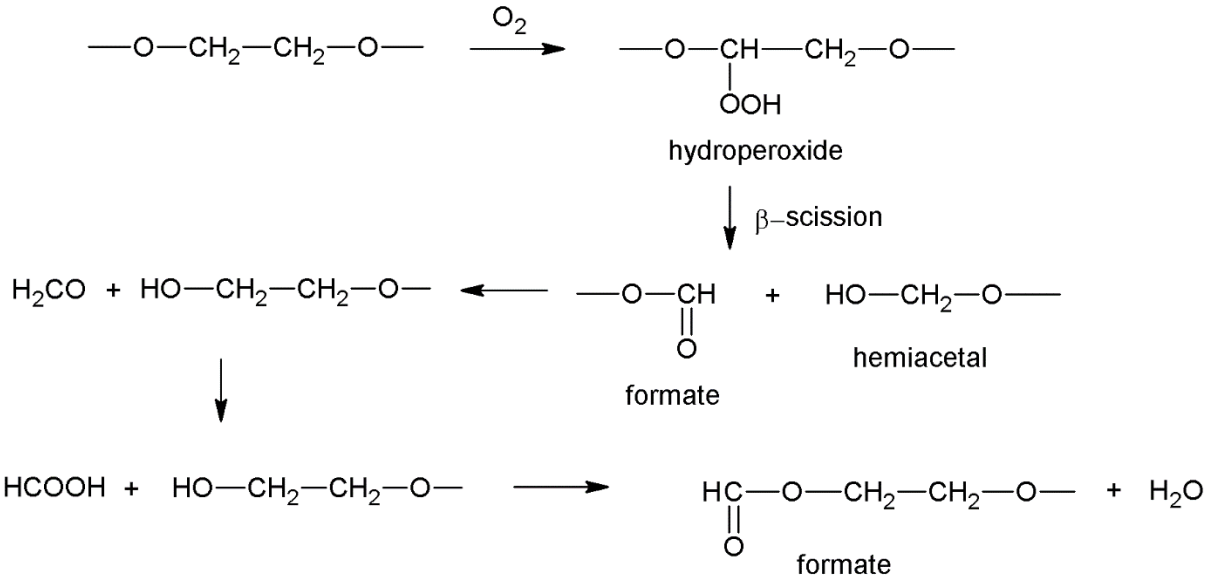

Figure 5.1. Chain scission mechanism of PEG under thermal degradation proposed by Yang et al. [22].

Non-reactive additives (usually referred to as “oils”), have been successfully added to silicone binders to enhance the biofouling-inhibition (i.e. antifouling) properties. It was first reported by Milne [26], who added a phenyl methyl silicone oil to a silicone fouling-release coating. Others [11] have followed the same strategy with different polymers. These non-reactive additives migrate to the interface upon exposure, thus changing the surface properties and providing biofouling-inhibition properties [11]. PEG has been combined/copolymerized with hydrophobic polymers like poly(dimethylsiloxane) (PDMS) and polypropylene glycol (PPG) and used likewise in different coatings. Kavanagh et al. [11] added PDMS-PEG-based copolymers as additives to fouling-release silicone coatings, while Wu and Hjort [27] employed PEG-PPG-PEG block copolymers in the same way, both with successful results in terms of antifouling properties. Kober and Wesslen [13] and Murthy et al. [14] have also used PEG-based amphiphilic copolymers to prevent protein adsorption on different coatings. Finally, Li et al. [28] adsorbed PEG homopolymers and PEG-PPG-PEG copolymers on polystyrene substrates for antifouling purposes, with the block copolymers showing superior properties compared to the PEG homopolymer, probably due to higher stability on the surface.

In spite of the promising use of PEG copolymerized with PPG, it has been reported [29,30] that PPG is even more prone to radical degradation due to the presence of the methyl side-group. The degradation mechanism proposed for PPG is very similar to PEG (see Figure 5.1), and formates, other esters and alcohols have been reported as main products too [29–32]. However, there is some discussion whether the secondary [32,33] or the tertiary [30] carbons have the major role in the degradation pathway.

In this chapter, copolymers containing PDMS, PEG and (in some instances) PPG moieties are exposed to: (1) different degrading agents in accelerated conditions in the laboratory and (2) real seawater conditions as additives for silicone coatings. The aim of this chapter is to identify the degradation pathway and products of PDMS-PEG-PPG-based copolymers under exposure to seawater.

5.2 Materials and Methods

5.2.1 Materials

Tetrahydrofuran (THF), heptane (C_7H_{16}), hydrogen peroxide (H_2O_2), hydrochloric acid (HCl) and deuterated chloroform (CCl_3D) were used as received from Sigma-Aldrich. Seawater was collected in Holmen (Copenhagen) and filtered prior to use. Tap water was treated through an osmose water system from Silhorko obtaining slightly acidic distilled water with pH=6.

5.2.2 PDMS-PEG-PPG-based Copolymers

Four different copolymers from different suppliers were used in this study. The structure is triblock X-Y-X (X: PEG / PEG-PPG ; Y: PDMS) with M_w = 1.000-10.000 g/mol (See Table 5.1). Copolymers 4, 6 and 7 were used for accelerated testing in the laboratory. Copolymers 4 and 5 were used as non-reactive additives in silicone coatings for long-term exposure in seawater.

Table 5.1. List of the copolymers studied and their chemical properties

Copolymer	PEG:PPG (weight ratio)	PEG-PPG distribution	End-group
4	2:3	Random	Methoxy
5	1:0	-	Acetate
6	1:0	-	Acetate
7	4:3	Random	Hydroxy

5.2.3 Separation of non-copolymerized PEG

In the production process of PDMS-PEG-based copolymers, most suppliers react di-hydride terminated PDMS with mono-allyl terminated PEG in the presence of a platinum catalyst, obtaining a copolymer with a propyl linker (i.e. a three carbons chain, see b), c) and d) in Figure 5.3) between both homopolymers. The reaction scheme is shown in Figure 5.2. In that process, the allyl terminated PEG is usually used in excess, which is not removed when the final product is sold. Heptane was used here prior to the use of the commercial copolymers to separate the hydrophilic PEG or PEG-PPG moieties (insoluble in heptane), which were not attached to the PDMS backbone by selective solvent extraction. The process was followed by IR spectroscopy. After degradation laboratory experiments, this separation process was repeated before NMR analysis to separate hydrophilic low molecular weight PEG/PPG degradation products. Therefore two phases were obtained for each experiment, the compounds soluble in heptane (hereafter referred to as phase 1) and the degradation products of the polyoxyalkylenes (i.e. PEG and PPG) insoluble in heptane (hereafter referred to as phase 2).

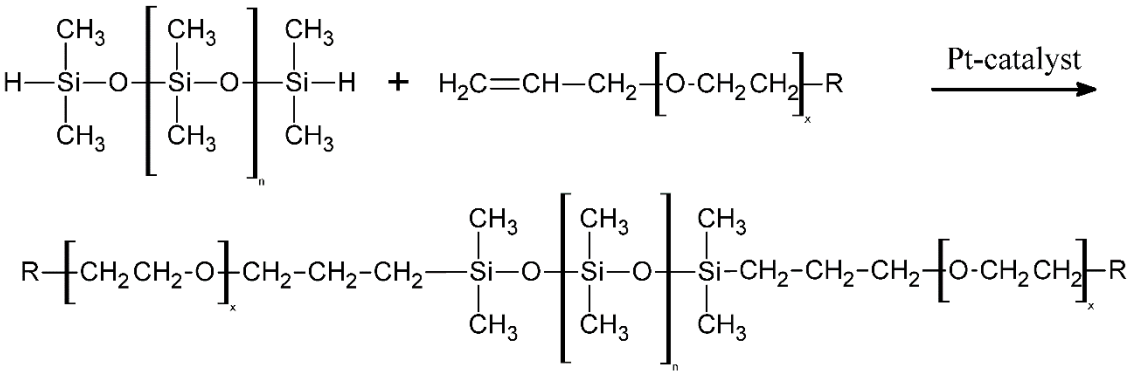

Figure 5.2. Reaction scheme for triblock PEG-b-PDMS-b-PEG copolymers, with R being the end-group of the PEG block.

5.2.4 Laboratory experiments

1 g of copolymers 4, 6 and 7 was exposed to a range of degrading conditions in closed glass containers:

(1) 60 g of HCl solution of pH=2, (2) 60 g a H_2O_2 solution (2 wt%), (3) 60 g of seawater, (4) 60 g of distilled water and (5) ultraviolet (UV) radiation. The experiments were undertaken at 60°C and room temperature (except the experiments with UV radiation that were carried out at 50°C).

Samples from the different exposure conditions were obtained and analysed at different exposure times, from 0 to 105 days for copolymer 4 and from 0 to 46 days for copolymers 6 and 7.

5.2.5 Seawater experiments

Copolymers 4 and 5 were added as additives to conventional silicone (PDMS) coatings. The coatings were prepared by mixing silanol-terminated PDMS with M_w=40.000 g/mol with surface-treated silica (SiO_2) and iron oxide pigment (Fe_2O_3), which were mixed in a pearl mill for 30 minutes at approximately 3000 rpm in the presence of xylene as solvent. Then, a trifunctional oximinosilane crosslinker (vinyl tris(methyl ethyl ketoxime) silane) was added. Copolymers 4 and 5 were added so they accounted for 3% of the total weight in the dry film. The mixtures were applied on PMMA substrates (10 x 20 cm) using a 8 cm Dr Blade applicator with a 400 µm gap and cured for a week at room temperature. The panels were immersed in static conditions in seawater in Singapore (1 23’ 33 N, 103 58’ 34 E) due to the high fouling release stress of the area [34]. A sample of each coating was retrieved after 3 and 30 months of exposure.

5.2.6 Liquid Chromatography

Semi preparative size-exclusion chromatography (semi prep. SEC) was used to isolate copolymers 4 and 5 from PDMS coatings. First, the coatings were immersed in THF for 5 hours to extract the non-reacted components from the coating binder (i.e. the studied copolymers and other non-reactive compounds). Then the THF was filtered and run through the semi preparative SEC equipment. The column system consisted of two different columns, Jordi-Gel DVB 500Å (10 x 250 mm) + Jordi-Gel DVB 100Å (10 x 250 mm), followed by a refractive index detector RID-10A, using THF as eluent at a flow rate of 0.8 mL/min at 22°C. An example of the obtained chromatogram can be seen in Figure 5.8.

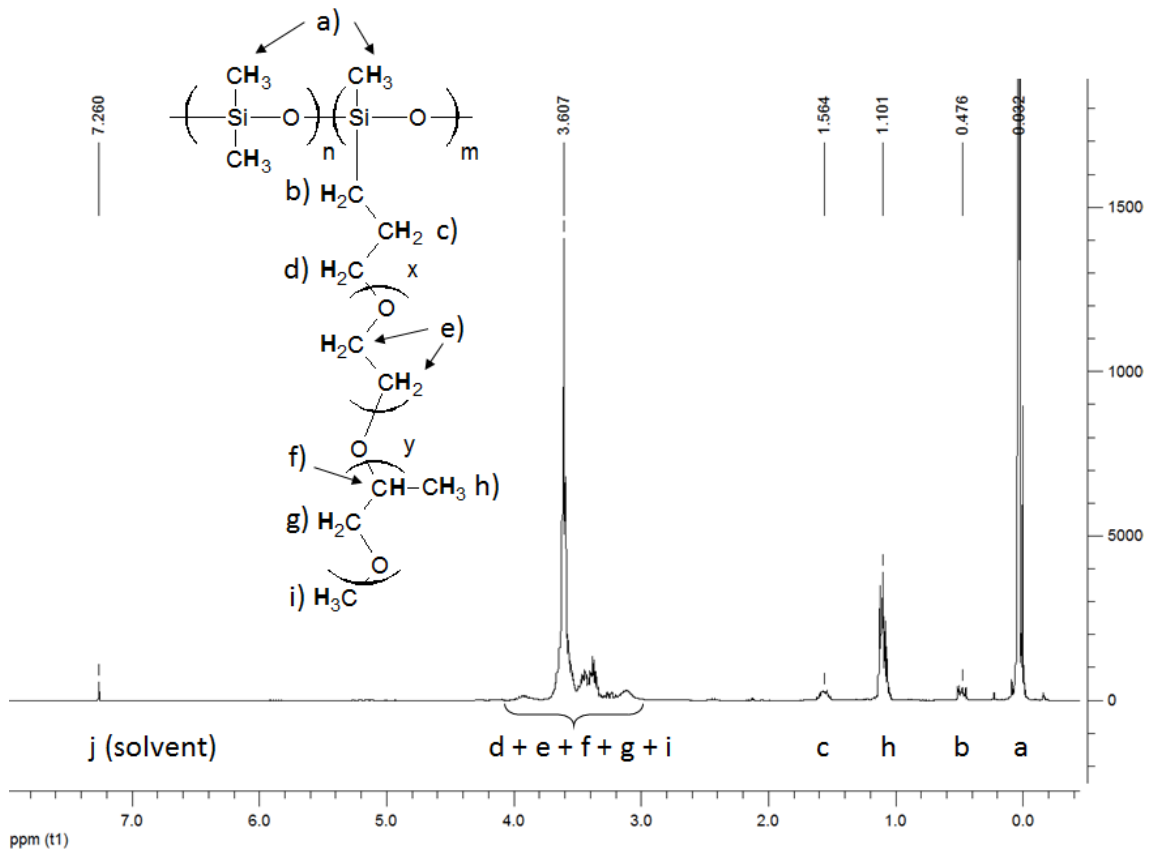

Figure 5.3. ^{1}H-NMR spectrum of copolymer 7, with the explanation of the different peaks with the corresponding chemical structure.

5.2.7 NMR

1-D ^{1}H-NMR and ^{13}C-NMR, and 2-D COSY and HSQC were used to analyse the composition of the copolymers, both in laboratory and real exposure experiments. The spectra were recorded on a 300 MHz Bruker spectrometer, using $CDCl_3$ at 25°C. One ^{1}H-NMR spectrum of the studied copolymers is shown in Figure 5.3 as example.

The loss of PEG groups (relative to the loss of PDMS groups) was calculated as follows:

$$relative\ loss\ of\ PEG(\%) = \frac{A_{e,t}/A_{a,t} - A_{e,t0}/A_{a,t0}}{A_{e,t0}/A_{a,t0}} \cdot 100 \qquad \textbf{(Equation 5.1)}$$

where A refers to the area in the ^{1}H-NMR spectra of hydrogens of every kind (see Figure 5.3), the subscript t refers to a certain exposure time and t0 refers to the non-exposed samples. Similarly, the relative loss of PPG groups, propyl linkers and acetate end-groups was calculated. The peak at 2 ppm corresponding to the OCOC$\underline{H_3}$ group was used to calculate the relative loss of acetate end-groups for copolymers 5 and 6.

The error bars in Figures 5.4a, 5.4b and 5.5 show the standard deviation obtained by three repetitions of a single experiment and assuming that it is representative for all the experiments undertaken.

5.2.8 FTIR spectroscopy

Attenuated Total Reflectance Infrared Spectroscopy (ATR-FTIR) was performed on a ThermoScientific Nicolet iS5 FT-IR. The spectra were recorded with 8 cm^{-1} resolution and 8 scans per sample in the range of 4000-400 cm^{-1} at room temperature.

5.2.9 UV radiation exposure

The copolymers were exposed to UV radiation in an Accelerated Weathering Tester from QUV (model QUV/se). Lamps UVA-340 were used with an irradiance of 0.89 $W/m^2/nm$ at 340 nm.

5.3 Results and discussion

5.3.1 Laboratory Accelerated Tests

Copolymers 4, 5 and 7 were exposed to accelerated laboratory tests with three main purposes: (1) to screen different degrading agents, (2) to study the effect of the propyl linker and the acetate end-group as possible vulnerable points for radical attack and (3) to compare the degradation results with copolymers in silicone coatings exposed to real-life seawater conditions.

In Figure 5.4 the relative loss of PPG groups and propyl linkers compared to the relative loss of PEG are shown for copolymers 4 and 7 for all the degrading conditions used and for different exposure times based on ^{1}H-NMR results. Both copolymer 4 and 7 show that PEG- and PPG-units are lost in equal amounts when exposed to the tested degradation conditions, as can be seen in Figure 5.4a. Since the PEG- and PPG-units are randomly copolymerized, the pattern in Figure 5.4a is in agreement with the random chain scision pathway proposed in Figure 5.1. There is, however, another degradation pathway that could explain the behaviour seen in Figure 5.4a, with the first degradation step taking place in the propyl linker with the subsequent scission of the whole polyoxyalkylane chain. That would also lead to the equal loss of PEG- and PPG-units shown in Figure 5.4a.

Figure 5.4b shows the loss of propyl linkers compared to the loss of PEG-units for the same experiments. It can be clearly seen that, though there is a certain loss of propyl linkers, there is no correlation between both variables, thus confirming that the degradation takes place through the proposed random chain scission pathway. No evidence is found that the propyl linker could be a vulnerable point under the studied degrading conditions.

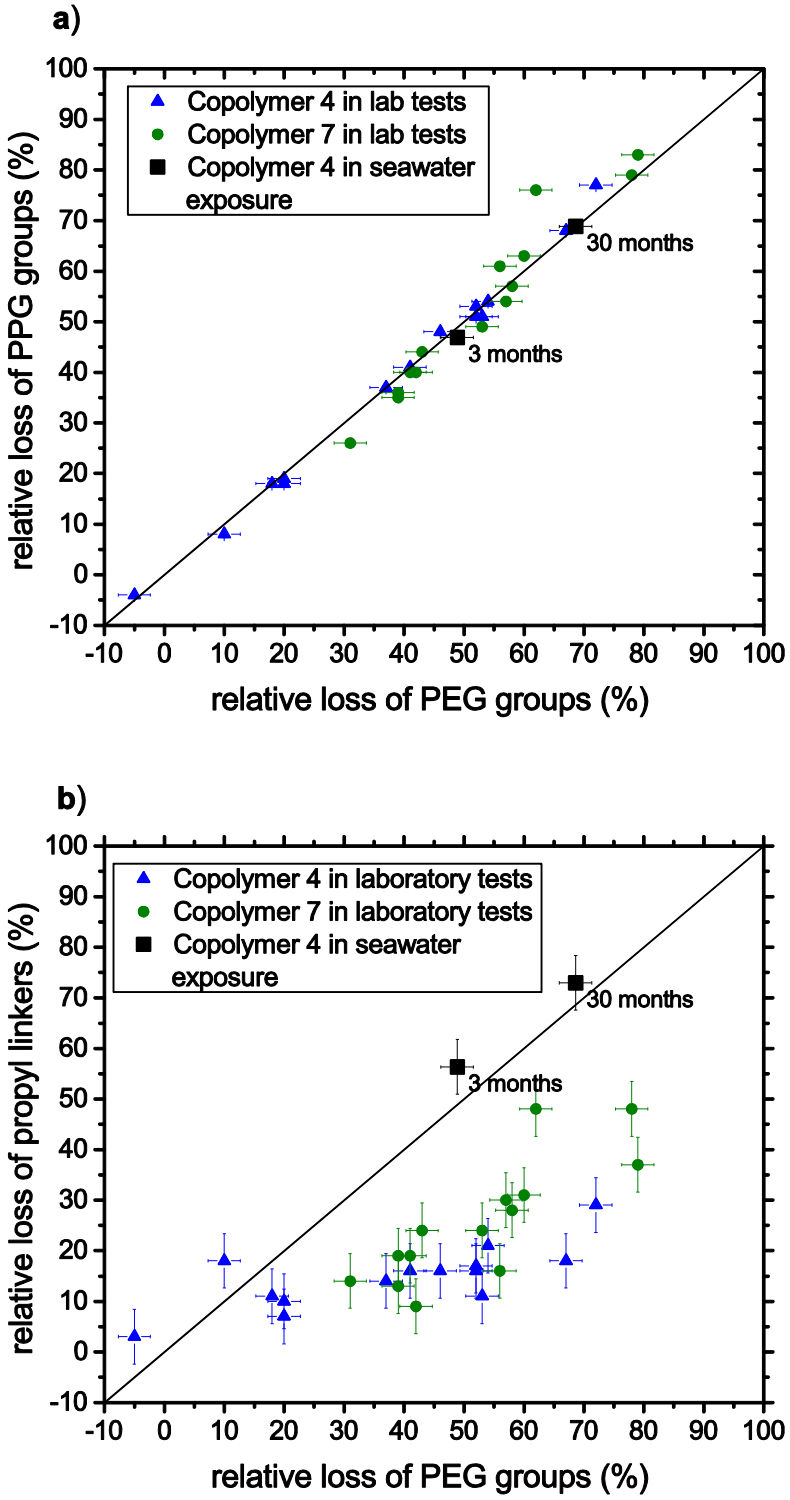

Figure 5.4. Relative loss of PPG groups (a) and propyl linkers (b) compared to the loss of PEG groups for copolymers 4 and 7 based on ^{1}H-NMR results. A black line showing an equivalent loss of the two studied groups is added for visual help.

Copolymer 6 has been used to study the degradation of the acetate end-group of the PEG chain compared to the loss of PEG units. As shown in Figure 5.5, the end-group is more prone to degradation as compared to the PEG units. More interestingly, it is possible to observe some differences depending on the degrading agents used. While at pH=2 the degradation occurs on the end-group to a very large

extent (95% of the end-groups are lost after 15 days of exposure while only 55% of the PEG groups are lost), the PEG units and end-groups seem to disappear at the same pace when exposed to UV radiation. No further experiments were undertaken with focus on other end-group chemistries in this chapter.

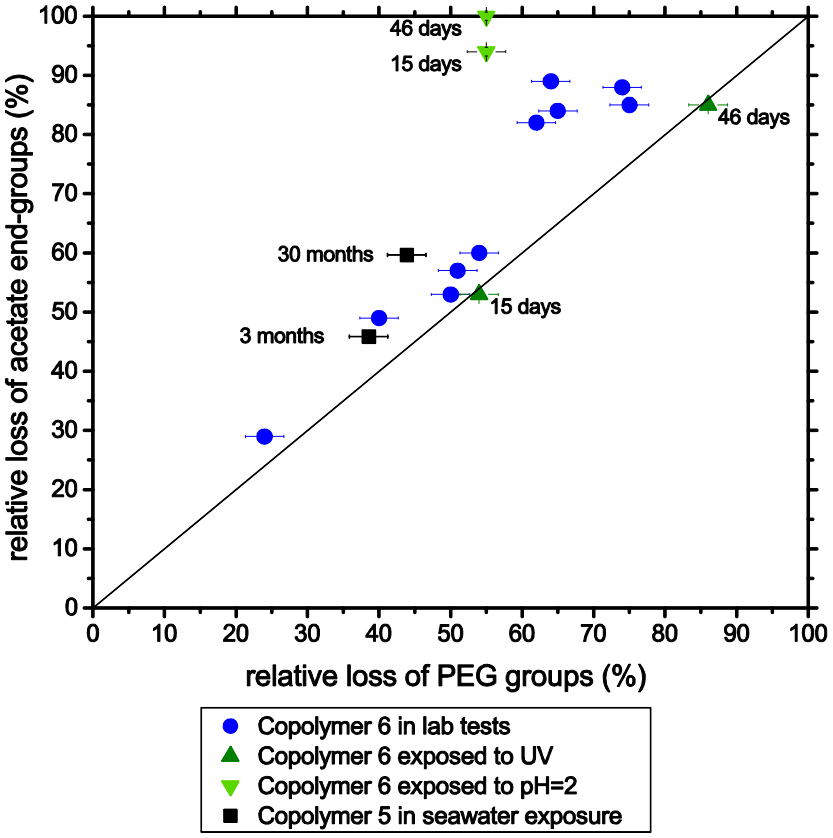

Figure 5.5. Relative loss of acetate end-groups compared to the loss of PEG groups for copolymers 5 and 6 based on ^{1}H-NMR results. A black line showing an equivalent loss of the two studied groups is added for visual help.

Some considerations should be made concerning the laboratory test results shown above:

1) Samples exposed to 60°C showed more severe degradation than the corresponding experiments at room temperature. However, no differences were seen in terms of degradation pathways and products. Hence, no differences are made in Figures 5.4 and 5.5 regarding temperature exposure. Likewise, samples exposed for longer times resulted in higher degradation yields, without further differences, and therefore exposure time is also omitted (unless otherwise stated).

2) Copolymers exposed only to seawater or distilled water at 60°C showed degradation of the PEG and PEG/PPG chains. This is in agreement with what has been reported by Morlat and Gardette [21] and Gallet et al. [31], that successfully thermodegraded PEG and PPG at 50°C in dry conditions. Therefore, the fact of accelerating the degradation tests at 60°C might not be only an acceleration method, but rather a degrading agent by itself.

5.3.2 Analysis of degradation products

Both phase 1 and phase 2 of the different experiments (see section 5.2.3) were analysed by IR and NMR means to identify the degradation products. An example is shown in Figure 5.6.

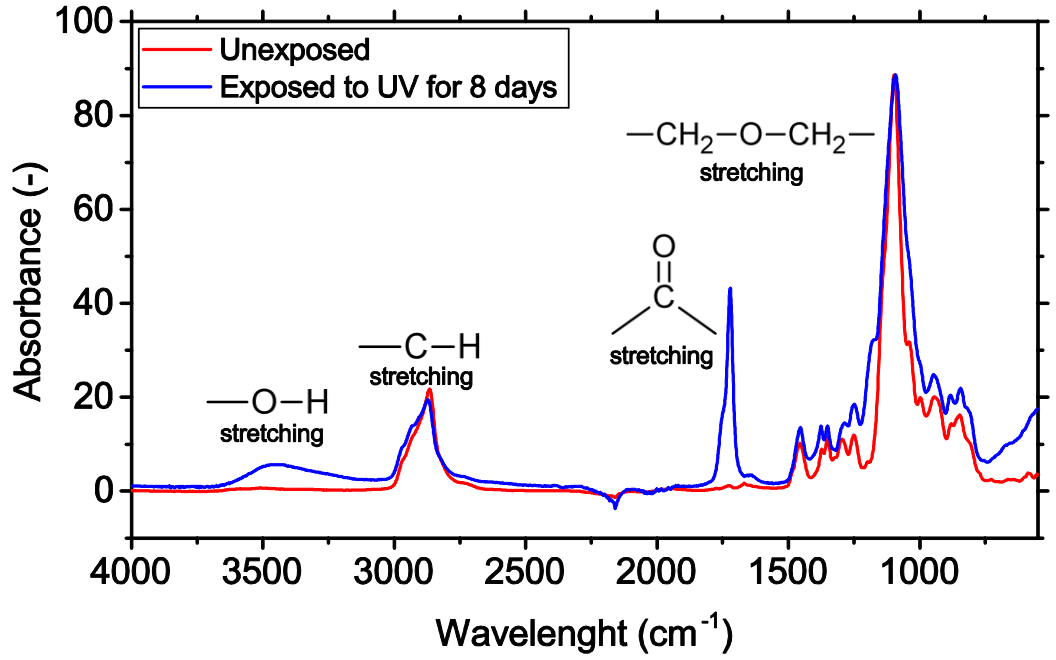

Figure 5.6. FTIR spectra of phase 2 of copolymer 7 before (red) and after (blue) exposure to UV radiation for 8 days at 50°C with the assigned chemistries of the main peaks [35].

IR and ^{1}H-NMR results show very little differences in phase 1 (not shown), mainly loss of PEG and PPG relative to the amount of PDMS. On the contrary, phase 2 shows almost no presence of PDMS and a significant change in composition (see Figure 5.6).

Peaks at 4-4.5 ppm (^{1}H-NMR), 8 ppm (^{1}H-NMR) and 1725 cm^{-1} (IR) appear during the degradation process as main degradation peaks in all the studied degradation conditions, though the shapes and sizes of the peaks differ to some extent. ^{13}C-NMR was employed to identify the degradation products. An example can be seen in Figure 5.7 for copolymer 6 exposed to UV, with the appearance of new peaks around 60-70 ppm and 160-170 ppm. Both NMR and IR results indicate that formates (esters from formic acid) are generated, in agreement with what has been observed by others [18,22,23] and as suggested in the mechanism shown in Figure 5.1. It has also been observed that the pH of the different solutions decreased over time, suggesting the formation of acids. Since the carbonyl peak at 1725 cm^{-1} shows a shoulder and the presence of –OH groups can be observed in the IR spectrum around 3400 cm^{-1} (see Figure 5.6), it cannot be disregarded that a mixture of products consisting of acids, formates and other esters is present, in agreement with what has been reported by Houssane et al. [24]. The presence of esters as degradation products is also supported by the peak at 174.2 ppm in Figure 5.7. Also in agreement with Houssane et al. [24], the degradation of the copolymers in aqueous conditions show less formates and more esters as degradation products compared to the samples exposed in dry conditions, with the IR peak at 1725 cm^{-1} shifting towards 1735 cm^{-1}. The presence of hydroxyl groups in the IR spectrum, together with the peaks at to 61.5 and 72.5 ppm in ^{13}C-NMR could

also be an indiciation of the presence of alcohol groups, in agreement with what has been found by Mortensen [36].

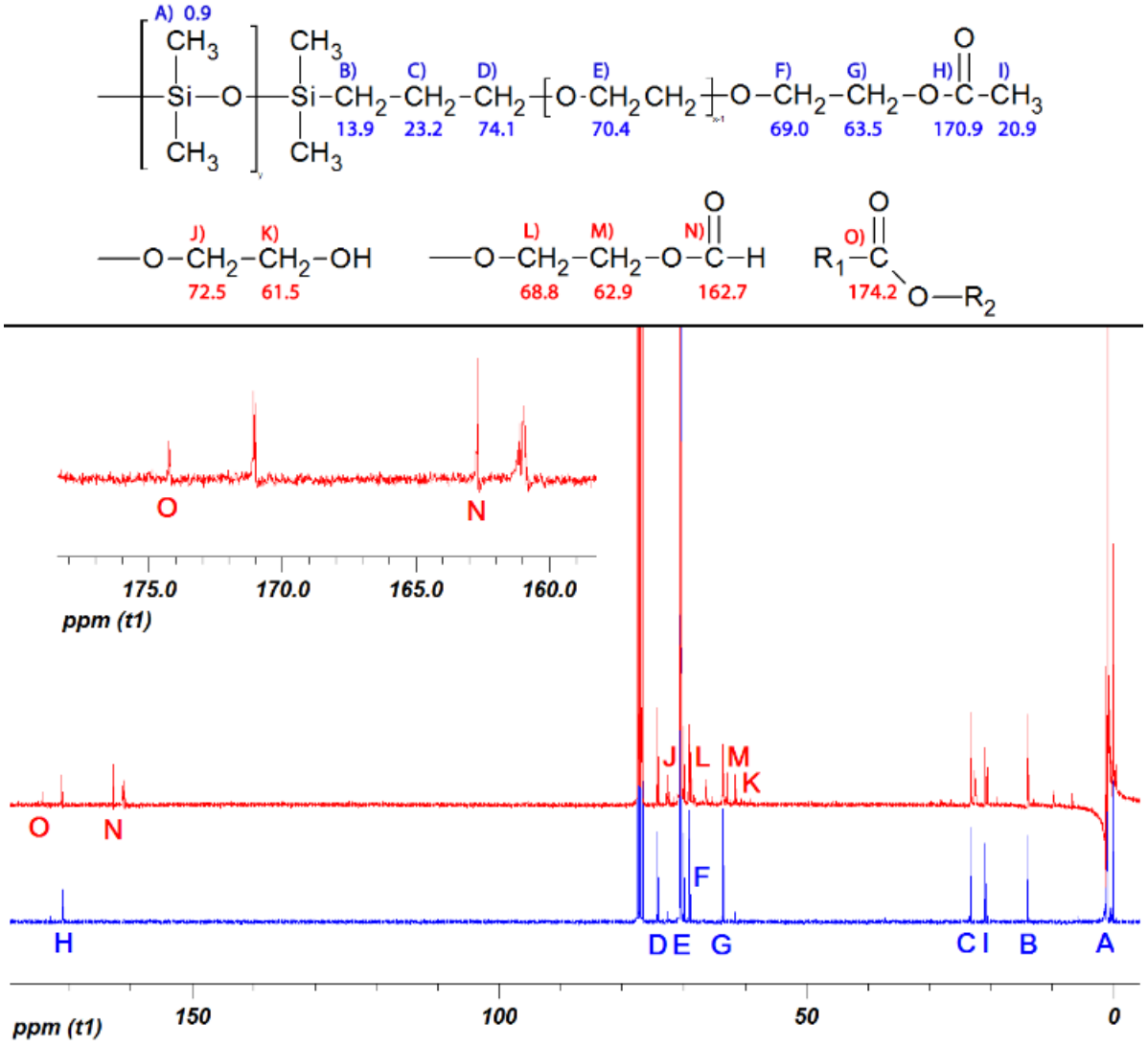

Figure 5.7. ^{13}C-NMR spectra of copolymer 6 unexposed (blue) and exposed to UV radiation for 8 days (red). An ampliation of the 160 - 180 ppm region is shown for the exposed sample. On top, the assignment of the different peaks annotated in the spectra of the unexposed (blue) copolymer and the formed degradation products (red). The values of the chemical shifts are expressed in ppm.

5.3.3 Seawater Experiments

Copolymers 4 and 5 were extracted from silicone coatings which had been immersed in seawater as previously explained. After successful isolation of the copolymers using semi prep. SEC (see Figure 5.8), IR and ^{1}H-NMR analysis were undertaken and compared to the unexposed (i.e. pristine) copolymers.

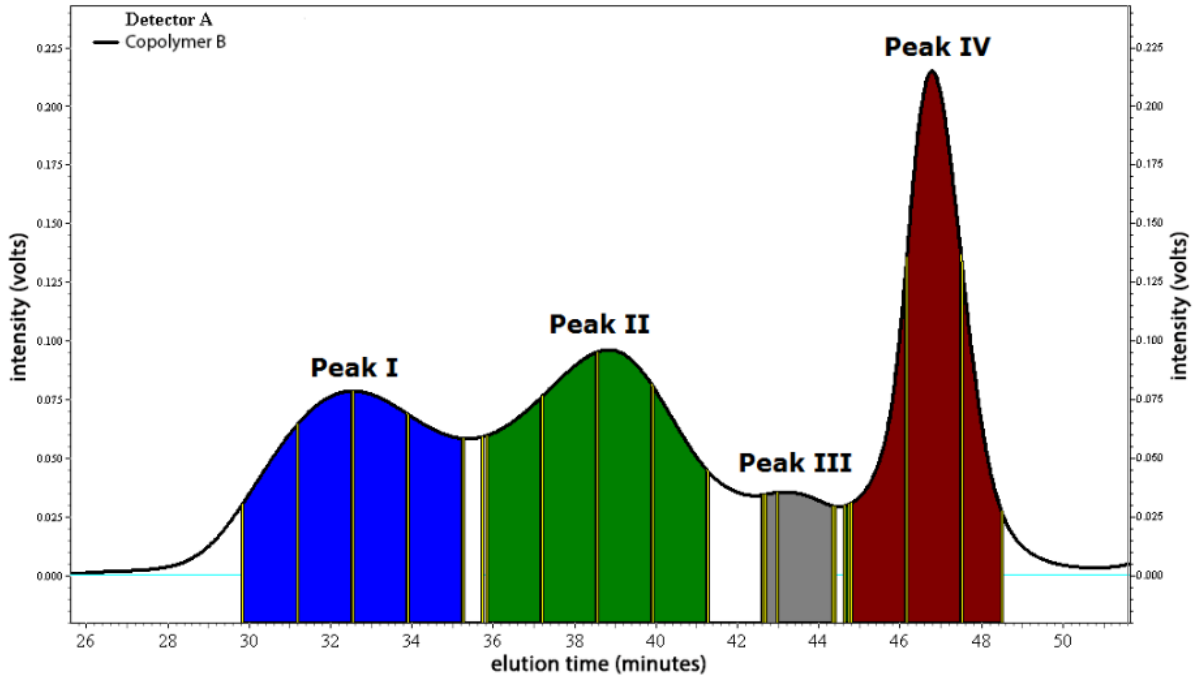

Figure 5.8. Size-exclusion chromatogram for the isolation of copolymer 5 after 30 months exposure. FTIR and NMR analysis revealed the composition of the different peaks: copolymer 5 (peak I), non-crosslinked PDMS from the binder system (peak II) and low M_w non-crosslinked PDMS chains and residues from the curing system (peak III and peak IV).

Note that the isolation of the studied copolymer (peak I in Figure 5.8) is not complete. This means that some amounts of compounds from peak II might be present when analysing the isolated copolymers.

The results of the seawater tests are shown as black squares in Figures 5.4 and 5.5, where the loss of PEG, PPG and propyl linkers for copolymer 4 and PEG and acetate end-groups for copolymer 5 after 3 and 30 months of exposure are shown. It should be noted that the apparent decrease in polyoxyalkylene units, propyl linkers and acetate end-groups found after seawater exposure may arise from an increase in the content of PDMS extracted from the binder system. An increase in PDMS content would lead to an equivalent, but false, decrease of the aforementioned groups, because the loss of all these groups is relative to the amount of PDMS. IR and NMR analysis of peak II of Figure 5.8 reveal that PDMS is the main component of this peak. The hypothesis of PDMS extracted from the binder system seems also supported by the fact that most of the "degradation" takes place in the first three months, with little further degradation occurs in the following 27 months (see figures 5.4 and 5.5). Ongoing investigations will reveal if some PDMS extracted from the binder system is altering the results of these experiments.

There is another uncertainty regarding these experiments. If the copolymers studied were degraded, it is reasonable to think that their molecular weight would decrease. Consequently, peak I would contain the copolymer that has not been degraded (or degraded to such a low extent that the change in hydrodynamic volume would be insignificant), while possible degradation products of smaller molecular weight (formates, esters, acids, etc.) would be eluted later within peaks II, III or IV. Another possibility is that, due to the high solubility of the degradation products of PEG and PPG in water, these products would be released to the seawater environment (instead of staying within the coating film). To address

this issue, IR and NMR analysis were undertaken for all the peaks shown in Figure 5.8 to look for any similarities with the degradation products described in the laboratory tests results. However, it was not possible to find any sign of those degradation products in neither IR or ^{1}H-NMR. Whether no degradation has taken place after 30 months of exposure or the degradation products have been eluted into seawater cannot be clarified at this stage (see discussion in section 5.6).

5.4 Conclusions

The degradation of PEG-based copolymers for antifouling purposes has been studied, both in accelerated laboratory conditions and in real seawater conditions. Formates and other esters have been identified as the main products for the laboratory tests, in agreement with other literature studies, though indication of other products have also been found. The relative amounts of each degradation product depend on the degradation agent used, as supported by small differences in NMR and IR results, with formates being the main product in dry conditions, while other esters and acids were found in aqueous tests. Different degradation patterns have been identified for the degradation of PEG-copolymers with acetate end-group. While the acetate end-groups were severely degraded at pH=2 compared to PEG-units, UV radiation degraded acetate- and PEG-units at the same pace.

PEG-based copolymers (4 and 5) have been exposed to seawater as additives for silicone coatings. After long-term exposure of these coatings, semi preparative SEC has been successfully used to isolate the exposed copolymers. The degradation patterns of these copolymers seem to agree with the results obtained for the accelerated laboratory conditions in terms of loss of PEG, PPG and acetate end-groups. However, unusually high amounts of degradation in the first 3 months of exposure, together with differences in the degradation behaviour of the propyl linkers leave some uncertainties regarding the isolation process. It was not possible to analyse the degradation products (if any), which were possibly eluted into seawater along the 30 months of exposure. Furthermore, the influence of the degradation of these copolymers on the biofouling-inhibition performance of the coatings should be assessed in future experiments.

5.5 References

[1] T. Ekblad, Hydrogel coatings for biomedical and biofouling applications, Linköping studies in science and technology, Linköping, Sweden (2010).

[2] E. Ostuni, R.G. Chapman, R.E. Holmlin, S. Takayama, G.M. Whitesides, A Survey of Structure−Property Relationships of Surfaces that Resist the Adsorption of Protein, *Langmuir*. **17** (2001) 5605–5620.

[3] L. Li, S. Chen, J. Zheng, B.D. Ratner, S. Jiang, Protein Adsorption on Oligo(ethylene glycol)-Terminated Alkanethiolate Self-Assembled Monolayers: The Molecular Basis for Nonfouling Behavior, *J. Phys. Chem. B*. **109** (2005) 2934–2941.

[4] P.C.W. Thorlaksen, A. Blom, U. Bork, Novel fouling control coating compositions, WO2011076856 (2011).

[5] P.C.W. Thorlaksen, Fouling control coating compositions comprising polysiloxane and pendant hydrophilic oligomer/polymer moieties, WO2013000478 (2013).

[6] D.C. Webster, R.B. Bodkhe, Functionalized silicones with polyalkylene oxide side chains,

WO2013052181 (2013).

[7] K.J. Reynolds, B. V. Tyson, Anti-fouling compositions with a fluorinated oxyalkylene-containing polymer or oligomer, WO 2014131695 (2014).

[8] J. Stein, T.B. Brydon, J.A. Cella, Condensation curable silicone foul release coatings and articles coated therewith, US006107381 (2000).

[9] S. Tanino, Antifouling coating composition, antifouling coating film, antifouling substrate, and method for improving storage stability of antifouling coating composition, EP2921538 (2015).

[10] W.P. Liao, Antifouling system comprising silicone hydrogel, WO 2014126643 (2014).

[11] C.J. Kavanagh, G.W. Swain, B.S. Kovach, J. Stein, C. Darkangelo-Wood, K. Truby, E. Holm, J. Montemarano, A. Meyer, D. Wiebe, The Effects of Silicone Fluid Additives and Silicone Elastomer Matrices on Barnacle Adhesion Strength, *Biofouling*. **19** (2003) 381–390.

[12] A.G. Nurioglu, A.C.C. Esteves, G. de With, Non-toxic, non-biocide-release antifouling coatings based on molecular structure design for marine applications, *J. Mater. Chem. B*. **3** (2015) 6547–6570.

[13] M. Kober, B. Wesslén, Surface properties of a segmented polyurethane containing amphiphilic polymers as additives, *J. Appl. Polym. Sci.* **54** (1994) 793–803.

[14] R. Murthy, C.D. Cox, M.S. Hahn, M.A. Grunlan, Protein-Resistant Silicones: Incorporation of Poly(ethylene oxide) via Siloxane Tethers, *Biomacromolecules*. **8** (2007) 3244–3252.

[15] J. Lee, H. Lee, J. Andrade, Blood compatibility of polyethylene oxide surfaces, *Prog. Polym. Sci.* **20** (1995) 1043–1079.

[16] H. Zhang, M. Chiao, Anti-fouling Coatings of Poly(dimethylsiloxane) Devices for Biological and Biomedical Applications, *J. Med. Biol. Eng.* **35** (2015) 143–155.

[17] F. Kawai, Microbial degradation of polyethers, *Appl. Microbiol. Biotechnol.* **58** (2002) 30–38.

[18] S. Han, C. Kim, D. Kwon, Thermal/oxidative degradation and stabilization of polyethylene glycol, *Polymer*. **38** (1997) 317–323.

[19] J.R. Haines, M. Alexander, Microbial degradation of polyethylene glycols, *Appl. Microbiol.* **29** (1975) 621–5.

[20] M. Bernhard, J.P. Eubeler, S. Zok, T.P. Knepper, Aerobic biodegradation of polyethylene glycols of different molecular weights in wastewater and seawater, *Water Res.* **42** (2008) 4791–4801.

[21] S. Morlat, J.-L. Gardette, Phototransformation of water-soluble polymers. I: photo- and thermooxidation of poly(ethylene oxide) in solid state, *Polymer*. **42** (2001) 6071–6079.

[22] L. Yang, F. Heatley, T.G. Blease, R.I.G. Thompson, A study of the mechanism of the oxidative thermal degradation of poly(ethylene oxide) and poly(propylene oxide) using ^{1}H- and ^{13}C-NMR, *Eur. Polym. J.* **32** (1996) 535–547.

[23] O.A. Mkhatresh, F. Heatley, A ^{13}C NMR Study of the Products and Mechanism of the Thermal Oxidative Degradation of Poly(ethylene oxide), *Macromol. Chem. Phys.* **203** (2002) 2273–2280.

[24] F. Hassouna, S. Morlat-Thérias, G. Mailhot, J.L. Gardette, Influence of water on the photodegradation of poly(ethylene oxide), *Polym. Degrad. Stab.* **92** (2007) 2042–2050.

[25] S. Morlat, J.-L. Gardette, Phototransformation of water-soluble polymers. Part II: photooxidation of poly(ethylene oxide) in aqueous solution, *Polymer*. **44** (2003) 7891–7897.

[26] A. Milne, Anti-fouling marine compositions, US4025693 (1977).

[27] Z. Wu, K. Hjort, Surface modification of PDMS by gradient-induced migration of embedded Pluronic, *Lab Chip*. **9** (2009) 1500.

[28] J.-T. Li, K.D. Caldwell, N. Rapoport, Surface Properties of Pluronic-Coated Polymeric Colloids, *Langmuir*. **10** (1994) 4475–4482.

[29] P. de Sainte Claire, Degradation of PEO in the Solid State: A Theoretical Kinetic Model, *Macromolecules*. **42** (2009) 3469–3482.

[30] P.J.F. Griffiths, J.G. Hughes, G.S. Park, The autoxidation of poly(propylene oxide)s, *Eur. Polym. J.* **29** (1993) 437–442.

[31] G. Gallet, B. Erlandsson, A.-C. Albertsson, S. Karlsson, Thermal oxidation of poly(ethylene oxide–propylene oxide–ethylene oxide) triblock copolymer: focus on low molecular weight degradation products, *Polym. Degrad. Stab.* **77** (2002) 55–66.

[32] P. Gauvin, J. Lemaire, D. Sallet, Photo-oxydation de polyéther-bloc-polyamides, 3. Propriétés des hydroperoxydes dans les homopolymères de polyéthers correspondants, *Die Makromol. Chemie*. **188** (1987) 1815–1824.

[33] Z. Barton, T.J. Kemp, A. Buzy, K.R. Jennings, Mass spectral characterization of the thermal degradation of poly(propylene oxide) by electrospray and matrix-assisted laser desorption ionization, *Polymer*. **36** (1995) 4927–4933.

[34] S.M. Olsen, Controlled release of environmentally friendly antifouling agents from marine coatings, Technical University of Denmark, Kongens Lyngby, Denmark (2009).

[35] J.M. Julian, D.G. Anderson, A.H. Brandau, J.R. McGinn, A.M. Millon, An infrared Spectroscopy Atlas for the Coatings Industry. Federation of Societies For Coatings Technology, Federation of Societies for Coatings Technology, Pennsylvania, USA (1991).

[36] M.N. Mortensen, Stabilization of polyethylene glycol in archeological wood, Technical University of Denmark, Kongens Lyngby, Denmark (2009).

5.6 Additional results

A few additional experiments were conducted involving the degradation of PDMS-PEG-based block copolymers in PDMS coatings. To that purpose, a PDMS-PEG-based copolymer of those listed in Table 5.1 was added as additive to two PDMS fouling-release coatings so it accounted for 3% of the weight of the dry films. These coatings did not contain any biocide or additive. The differences between the two coatings concerned only the physical properties and chemical composition of some the following constituents: silica, pigments, crosslinker and solvent. These two coatings (hereafter referred to as coating A and coating B) were applied on PMMA panels and immersed in seawater in Singapore in static conditions, as described in section 5.2. Two additional PMMA panels were applied with coatings A and B, which were kept in the laboratory in a closed container as “unexposed references”. The coatings immersed in seawater were retrieved and analysed after 1 year of exposure. The non-crosslinked molecules were extracted from the PDMS coating using THF, which was then analysed by size-exclusion chromatography (SEC) using a method similar to the one described in section 5.2.6 (see section 6.2.5 for a detailed description of the method). The chromatograms obtained for both coatings can be seen in Figure 5.9.

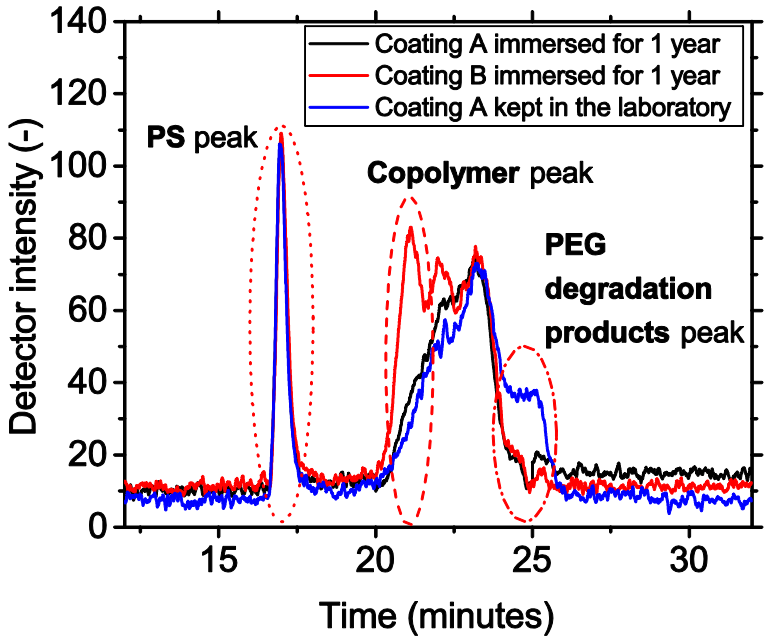

Figure 5.9. Chromatograms for the extracted molecules of Coating A (black) and Coating B (red) immersed in seawater for approximately 1 year, and for Coating A kept in the laboratory as "unexposed reference" for 1 year (blue). A red circle has been used to highlight the peaks corresponding to the PS standard (⋯), the copolymer (---) and the PEG degradation products (-·-).

Coating A shows complete loss of copolymer after one year of immersion in seawater (black curve), while a significant concentration of copolymer can be observed in Coating B after immersion (red curve). All the non-crosslinked molecules obtained from the extraction of Coating A in THF were further analysed, but none of the degradation products reported in section 5.3.2 could be observed. It was not known whether the PDMS-PEG-based copolymer was completely released/dissolved into seawater after 1 year of immersion, or the copolymer had been degraded and the degradation products eluted to seawater. To elucidate that, the unexposed coating A kept in the laboratory as reference was analysed using the same methodology, and its chromotrogram is shown in Figure 5.9 (see blue curve in Figure 5.9). No copolymer could be found in the reference coating, though a significant difference can be seen compared to Coating A immersed in seawater. The coating kept in the laboratory shows an additional peak in the low-molecular weight region of the chromatogram. The molecules corresponding to this peak were isolated and analysed by FTIR and NMR means as explained in sections 5.2.7 and 5.2.8. Chemical analysis of these molecules revealed that this peak corresponds to degradation products originating from the oxidative degradation of the PEG block of the copolymer.

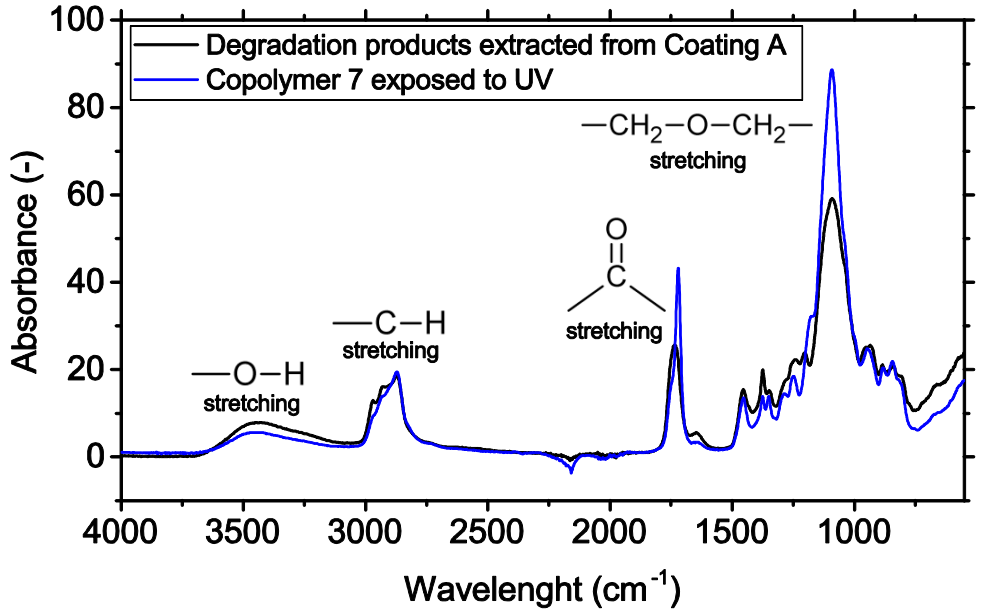

Figure 5.10. FTIR spectra of the degradation products obtained from Coating A kept in the laboratory as reference (black curve) and compared to the degradation products obtained for copolymer 7 (see Table 5.1) after exposure to UV radiation for 8 days at 50°C (blue curve, see also blue curve in Figure 5.6).

Figure 5.10 shows the IR spectrum of the isolated molecules from Coating A (blue curve), and compared to the IR spectrum obtained when a similar copolymer was degraded by UV radiation for 8 days (black curve) described previously (see Figure 5.6). A large similarity can be observed. Hence, different conclusions can be drawn:

1) PDMS-PEG-based copolymers added as additives to PDMS coatings can undergo degradation under certain conditions. Both the coating exposed to seawater and the one kept in a box in the laboratory exhibited total loss of copolymer.
2) The degradation of these copolymers takes place at the PEG block. No information is available regarding the PDMS block.
3) The physical properties and chemical composition of the coating constituents have a strong influence on the degradation of these copolymers.
4) When these copolymers undergo degradation, the molecular weight decreases and the degradation products elute at a later time when analysed by SEC (see blue curve in Figure 5.9). Therefore, it can be assumed that the molecules that appear at the same elution time as the non-degraded (i.e. pristine) copolymer have not suffered a significant degree of degradation (for example, peak I in Figure 5.8 or the copolymers analysed in the following chapter).

6. Field study of the long-term release of PDMS-PEG-based copolymers from FRC

PDMS-PEG-based copolymers must be retained to a high degree on the surface of FRC coatings, if long-term biofouling-inhibition properties are pursued. In this chapter, the long-term release/loss of copolymers from FRC immersed in seawater is studied. The influence of different variables such as seawater temperature or addition of biocides are investigated.

The content of this chapter was submitted for publication as “Field study on the long-term release of block copolymers from fouling-release coatings” in Progress in Organic Coatings (authors: A. Camós Noguer, S. Hvilsted, S. M. Olsen and S. Kiil).

6.1 Introduction

To impart biofouling-inhibition properties to poly(dimehtylsiloxane) (PDMS) fouling-release coatings (FRC), “oils” (mostly polysiloxane-based fluid additives) have been traditionally added [1,2]. These oils consist of block copolymers containing different chemical moieties. The mostly employed polymers have been fluorinated- and polyether-based polymers, as well as phenyl-modified polysiloxanes [1]. These oils segregate from the bulk and cover the surface of the coatings upon immersion. On the surface of the coatings, one of the copolymer blocks acts as an anchor to the surface and imparts stability to the copolymer molecule [3,4]. The other block(s) of the copolymer is usually extended to seawater (sometimes in the form of a polymer brush) and confers non-fouling (i.e. repellence) properties [3]. Consequently, the addition of small amounts of these additives result in the modification of the physicochemical properties of the surface with a very small influence on the bulk properties of the coating [5–7].

Nonetheless, it has been suggested that these oils can be “washed away” (i.e. released or dissolved in seawater) and/or degraded at the surface of the coating. When a molecule from the surface of the coating is removed, a new molecule diffuse from the bulk of the coating to cover the surface [5]. This “self-healing” process can take place as long as copolymer molecules are available in the bulk of the coating. The properties of these coatings are hence expected to deteriorate upon shortage of molecules in the bulk. The anchoring capabilities of this kind of surface-active copolymers on different polymeric matrices have been studied. In these investigations, different surfactants and block copolymers have been added to PDMS (or other polymeric matrices) and the wettability of the surface has been studied after soaking the samples in water for different exposure times [8–13]. For example, Seo and Lee [8] added a surfactant based on poly(ethylene glycol) (PEG) to PDMS. After immersion in water for 18 days, significant changes in wettability of the PDMS surface were observed and attributed to additive depletion. Similarly, a PDMS-PEG-based copolymer was added to PDMS by Kim et al. [9] and samples of the material were soaked in water for 35 days. Slight differences on the surface of the PDMS samples after exposure were also reported. Madadi and Casals-Terré [13] could see significant differences in hydrophilicity in PDMS samples modified with non-ionic surfactants, when the samples were exposed to contact with water for short periods. Finally, Fatona et al. [12] analysed PEG-based surfactants and

copolymers with different hydrophobic groups added to PDMS elastomers and soaked for 20 hours in water. They showed that the stability of these additives on the PDMS surface was significantly higher when copolymers containing a PDMS block were used, compared to those containing and alkyl hydrophobic group. Nonetheless, the exposure times investigated in the aforementioned studies are not representative for fouling-release coatings, which are exposed to seawater over several years. Hence, the usefulness of such experiments on the studied coatings is limited. Recently, some novel PDMS-based coatings containing both the traditional “oils” and biocides have been commercialized. The addition of small amount of biocides is suggested to improve the non-fouling properties of the coatings (specially in idle conditions). The use of organic biocides such as zinc pyrithione, Zineb and Irgarol together with fouling-release “oils” have been described in different patents [14,15]. However, the addition of biocides could significantly influence the behaviour and release of these oils, both due to the presence of biocide in the film and the leached layer that is generated upon its dissolution.

It is well recognized that addition of block copolymers (i.e. oils) to fouling-release coatings enhances the fouling-resistance of these coatings to a great extent. Therefore, being able to quantify and control the processes that dictate the release rate at the surface of the coating is crucial for the development of robust long-lasting coatings. With the aim of better understanding the stability of polymeric-based additives in silicone coatings, up to 300 experimental fouling-release coatings exposed to seawater for different periods of time have been analysed. The experimental coatings consist mainly of a PDMS binder and a surface-active additive, a PDMS-PEG-based copolymer. First, a method to quantify the amount of additive present in coatings has been developed inspired by the work of Reynier et al. [16]. Then, the experimental fouling-release coatings, exposed to seawater for different times have been analysed and compared to coatings exposed in a laboratory rotor in controlled conditions. The influence of different variables/parameters on the release of these copolymers has been studied. These variables include: (1) temperature of seawater, (2) the chemistry of the crosslinker, (3) the molecular weight (M_w) of the copolymer and the initial concentration of (4) biocide and (5) copolymer in the coating. Finally, the influence of the aforementioned variables on the release/loss of copolymer from PDMS-coatings is discussed. The results obtained from this long-term filed study are believed to provide some insights and findings, which might not be available when short-term experiments in ideal conditions are empoloyed.

6.2 Materials and Methods

6.2.1 Materials

Silanol-terminated poly(dimethylsiloxane) (4000 cSt) was purchased from Dow Corning. Vinyl tris(methyl ethyl ketoxime) silane (crosslinker I), a pre-polymerized ethoxysilane crosslinker (crosslinker II), and a methoxy functional vinyl siloxane oligomer (crosslinker III) were purchased from Evonik Industries and can be seen in Table 6.1. Surface-treated fumed silica (SiO_2, average particle size about 15 nm) was also received from Evonik and red iron oxide (Fe_2O_3) pigment Bayferrox 130M from Lanxess. Two different PDMS-PEG-based block copolymers (copolymer 8 and copolymer 9) were obtained from different suppliers with M_w = 1.000-10.000 g/mol and ABA triblock structure. The

molecular weight of copolymer 8 was ~75% larger than for copolymer 9. Copper pyrithione (CuPT), also known as copper omadine, was obtained from Lonza.

Table 6.1. Chemical structures of the three crosslinkers investigated.

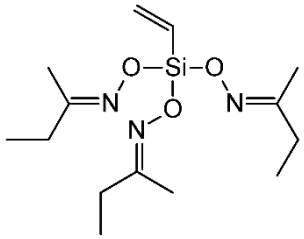	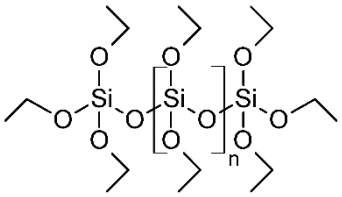	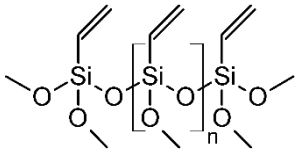
Crosslinker I (C – I)	Crosslinker II (C – II) n ~ 3 - 8 Addition of Sn-catalyst required	Crosslinker III (C – III) n ~ 2 - 6 Addition of Sn-catalyst required

6.2.2 Formulation of coatings

The coatings were prepared by mixing three components: (1) base (containing binder, solvent, silica, pigment and CuPT), (2) crosslinker (I, II or III) and (3) a PDMS-PEG-based copolymer (8 or 9). The base was prepared by mixing silanol-terminated PDMS with xylene (about 15 wt%) and with a series of components. Iron oxide (Fe_2O_3) and fumed silica (SiO_2) were added so they accounted for 5% and 1% of the dry weight of the film respectively. The organic biocide was added in different amounts, so it accounted from 0 to 7% of the dry weight of the film. The base was mixed in a pearl mill at approximately 3000 rpm for 30 minutes. Then, base, crosslinker and copolymer were mixed by hand-mixing at room temperature and applied. A small amount of tin-based catalyst was added to compositions with crosslinkers II and III to compensate for the lower reactivity of these crosslinking agents.

6.2.3 Preparation of coatings

Poly(methyl methacrylate) (PMMA) substrates (10 x 20 cm) were spray-coated with a 300 µm (wet thickness) layer of a tiecoat mainly consisting of poly(vinyl chloride)-co-poly(vinyl isobutyl ether) and cured at room temperature for 48 hours. The tiecoat was aimed at providing adhesion between the PDMS coating and the substrate. Then, the PDMS-based mixtures were applied on the coated panels using a 8 cm Dr Blade applicator with a 400 µm gap and cured for a week at room temperature. These coatings were used for static immersion tests in seawater. A similar procedure was used to apply coatings for rotary experiments on poly(ethylene terephthalate) (PET) foils.

6.2.4 Exposure of coatings

6.2.4.1 Static exposure

The coatings applied on PMMA substrates were immersed in static conditions in seawater in Barcelona (BCN) (41° 12’ 43’’ N, 1° 44’ 0’’ E) and in Singapore (SNG) (1° 23’ 33’’ N, 103° 58’ 34’’ E). Coatings were retrieved from the exposure sites and analysed after different exposure times. Significant differences in seawater temperature exist between the two locations. While seawater temperature is relatively constant throughout the year in Singapore (27-30°C), in Barcelona it can fluctuate between 13°C and 25°C depending on the season.

6.2.4.2 Rotary exposure

The coated PET films were cut in strips of 2.5 cm and mounted on the laboratory rotor. The rotor operated in artificial seawater at 25°C rotating at 20 knots. The pH was maintained at 8.2 by addition of sodium hydroxide and hydrochloric acid. A detailed description of the rotor structure and properties can be found elsewhere [17]. Samples were retrieved at different exposure times for analysis.

6.2.5 Determination of copolymer concentration in PDMS-based coatings

Size exclusion chromatography (SEC) was used to assess the concentration of copolymer in PDMS coatings. The SEC system consisted of three different columns, an Agilent PLgel Mixed-C (7.5 x 300 mm) followed by two Agilent PLgel Mixed-D (7.5 x 300 mm) columns (as described in section 4.2.4.2). An ELS (Evaporative Light Scattering) detector was employed. Tetrahydrofuran (THF) was used as eluent at a flow rate of 1 mL/min at 22°C.

A method has been developed to measure the copolymer concentration in coatings, which can be used for both freshly applied coatings, as well as those that have been immersed in seawater. Briefly, the coating analysed is immersed in THF in a closed glass container, where the non-crosslinked molecules and additives, including the studied copolymer, are extracted from the PDMS matrix by the solvent. Then, the THF phase is filtered and run through the SEC system, where the concentration of copolymer is estimated. The steps can be summarized as follows:

1) The PDMS coating is “detached” from the substrate by use of a scalpel, ensuring that no coating remains on the substrate and that no tiecoat is removed.
2) The coating obtained from (1) is immersed in a THF solution for 2 hours under stirring. The THF solvent contains a small amount of low polydispersity-index polystyrene (PS), which is later used as internal standard for quantification purposes.
3) The THF phase is separated and filtered (filter pore size = 20 µm) and run through the SEC system.
4) The area corresponding to the copolymer peak in the chromatogram obtained is measured, as well as the area corresponding to the PS peak (see Figure 6.1).
5) The measured area for the copolymer is corrected after the area of the PS peak and the amount of coating and THF used. This “corrected area” is proportional to the concentration of copolymer in the coating.

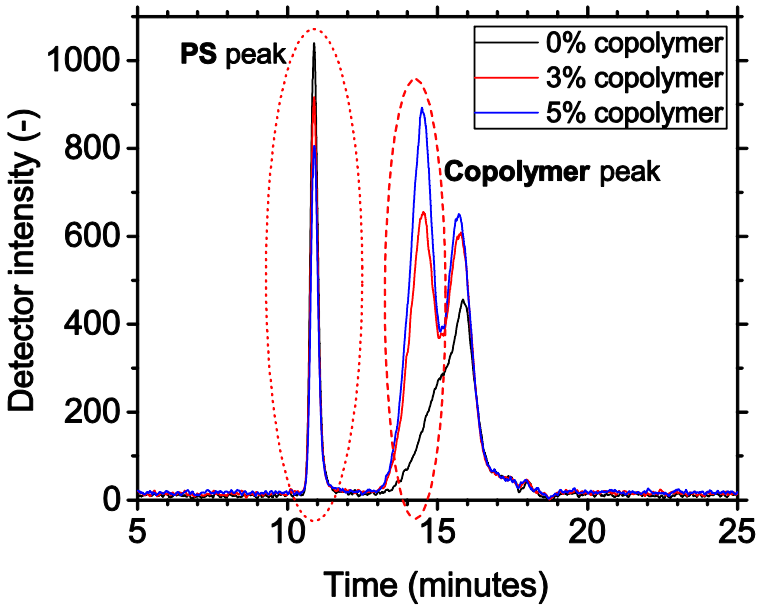

Figure 6.1. Chromatograms obtained after analysing coatings with three different copolymer concentrations (0 wt%, 3 wt% and 5 wt%). A red circle has been used to highlight the peaks corresponding to the PS standard (···) and the copolymer (---).

A series of coatings with different (well-known) copolymer concentrations were prepared, applied on PMMA substrates and cured for a week. The coatings were then analysed using the procedure described above. The "corrected area" obtained from the SEC system was plotted vs the concentration of copolymer for each coating, showing a clear correlation between both variables ($R^2 = 0.98$) as shown in Figure 6.2. The calibration curve in Figure 6.2 has been used to determine the concentration of copolymer in the analysed coatings.

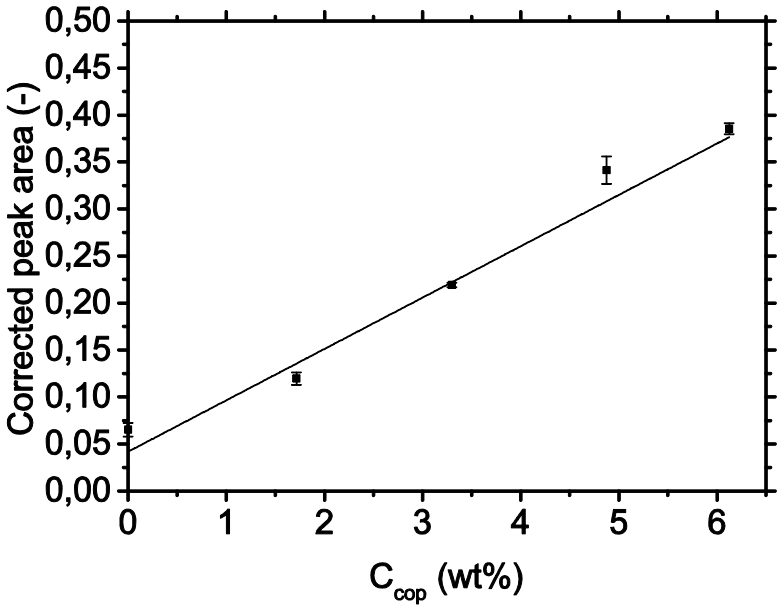

Figure 6.2. Calibration curve for copolymer 8, where the corrected area obtained from the SEC analysis of 5 different coatings is plotted against the copolymer concentration. Three independent measurements were undertaken for each point, and the error bars show the standard deviation.

It has been assumed that the silica (SiO_2) and pigment (Fe_2O_3) particles do not leach from the coating upon exposure to seawater. Likewise, non-crosslinked PDMS-chains originating from the incomplete crosslinking of the binder are also assumed to remain in the film throughout the immersion period due to their hydrophobic character.

6.2.6 Copolymer concentration and loss in PDMS-based coatings

The concentration of copolymer is defined as the weight of copolymer found in 1 gram of dry coating, and it is assumed that it is homogeneously distributed. It is expressed in weight percentage as shown in Equation 6.1. The concentration of CuPT is defined likewise. Unless otherwise stated, all biocide and copolymer concentrations are expressed in wt%.

$$C_{cop}\ (wt\%) = \frac{m_{cop}}{m_{coating}} \cdot 100 \qquad \textbf{(Equation 6.1)}$$

where C_{cop} refers to the copolymer concentration in the coating, m_{cop} is the mass of copolymer in g and $m_{coating}$ is the final dry weight of the coating in g.

The copolymer loss is then defined by Equation 6.2.

$$Copolymer\ loss\ (\%) = \frac{C_{cop}(t0) - C_{cop}(t)}{C_{cop}(t0)} \cdot 100 \qquad \textbf{(Equation 6.2)}$$

where C_{cop} refers to the copolymer concentration in the coating and t0 and t refer respectively to the unexposed and exposed coatings.

6.2.7 Uncertainty assessment

The results that are presented in this field study are subject to a series of uncertainties that should be mentioned. First, the different coatings analysed do not present the same precise composition. The particle size, composition and concentration of some constituents (e.g. silica and pigments) vary slightly among formulations. However, coatings with similar formulations have been chosen for analysis and are referred to as "*comparable*" compositions. Conversely, those with large differences have been disregarded. In addition, the coatings have been prepared by different people and exposed to seawater at different times (both seasonally and yearly). The uncertainty related to the abovementioned issues cannot be quantified, but is expected to be limited.

To account for the experimental error for each individual measurement, the series of coatings analysed in Figure 6.2 have been employed. It has been assumed that these samples are representative for all the coatings studied due to their different composition in terms of copolymer concentration. Hence, the average standard deviation of these 5 samples has been calculated and assumed representative for all the analysed coatings. Consequently, the copolymer concentrations estimated in this chapter are subject to an uncertainty of ± 0.13 wt%. To calculate the standard deviation of the copolymer loss (obtained through Equation 6.2), "propagation of error" theory has been employed, as detailed elsewhere [18].

6.3 Results and Discussion

Almost 300 experimental coatings with different compositions have been retrieved from the exposure sites in Barcelona and Singapore at different exposure times (up to 5.2 years) and analysed as previously explained.

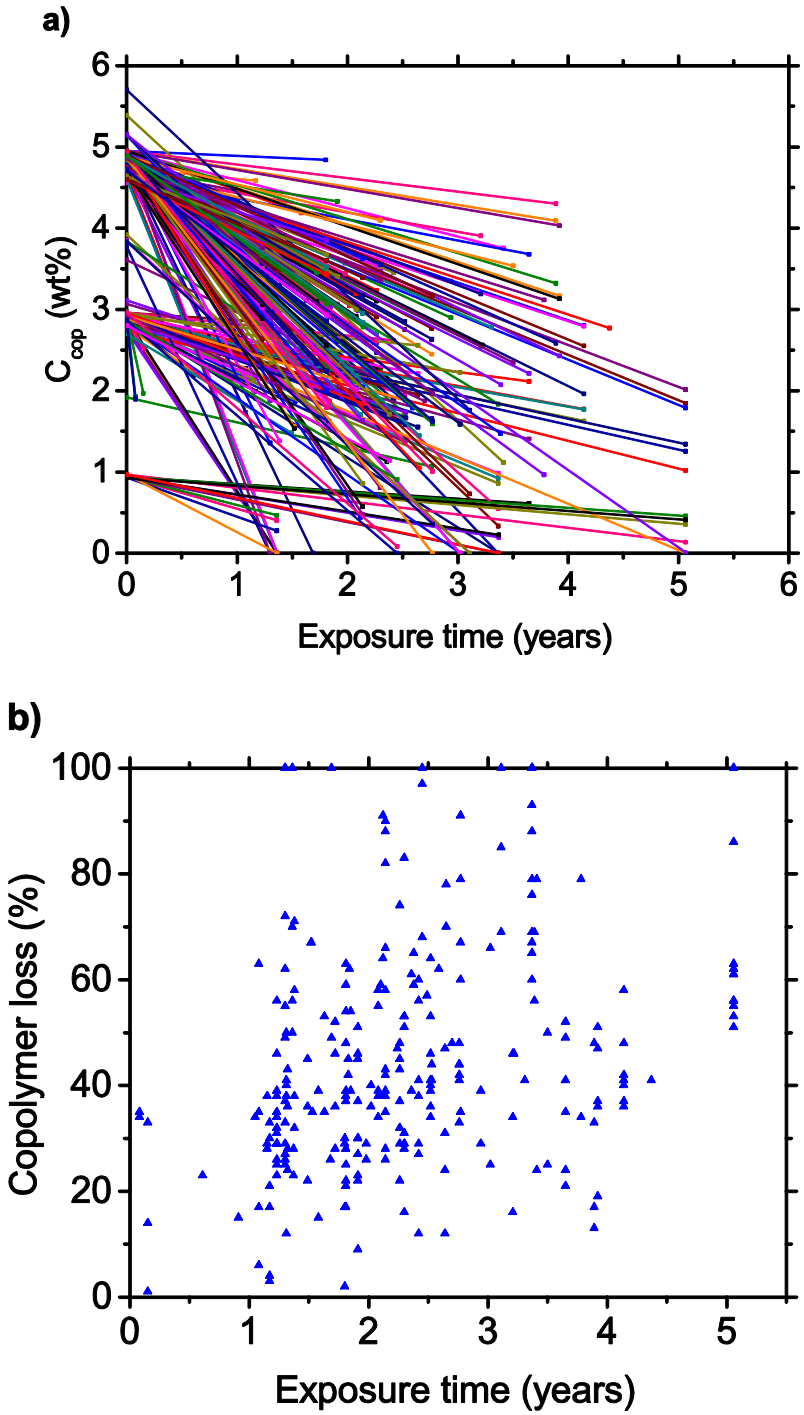

Figure 6.3. Copolymer concentration (a) and loss (b) for approximately 300 experimental coatings exposed to seawater in Singapore and Barcelona. Large differences in composition exist between the analysed coatings.

Figure 6.3a shows the initial and final copolymer concentration of all the analysed coatings. Figure 6.3b shows the copolymer loss (in %) for the same coatings. A significant scatter in the results can be clearly seen, probably due to: (1) differences in composition (including fillers, pigments, copolymer and CuPT), (2) exposure to two different locations with different seawater temperatures and (3) different starting immersion dates, among others. Therefore, specific coatings from Figure 6.3 with *comparable* compositions and exposure conditions have been selected and compared to coatings exposed in well-controlled conditions in the laboratory rotor. Details regarding the different experimental coatings analysed in this study are provided in Table 6.2.

Table 6.2. Series of coatings analysed. Details regarding the exposure site (ROT (laboratory rotor), BCN (Barcelona) and SNG (Singapore)), initial biocide (CuPT) and copolymer concentration (wt%), exposure time (years) and parameters investigated for each series are provided.

Series	Exposure site			Initial copolymer concentration (wt%)						Initial biocide concentration (wt%)						Exposure time (years)	Parameters investigated
	ROT	BCN	SNG	1%	2%	3%	5%	6%	7%	0%	0.5%	1%	3%	5%	7%		
A Fig. 6.4	x						x			x					x	1 Short-term	Biocide conc. Copolymer M_w Crosslinker
B Fig. 6.5	x				x			x		x			x		x	1 Short-term	Copolymer conc. Biocide conc.
C Fig. 6.6		x	x				x		x		x	x	x	x	X	2 Mid-term	Copolymer conc. Biocide conc. Seawater T
D Fig. 6.7		x	x	x		x	x			x			x	x	x	3,4 / 5,2 Long-term	Copolymer conc. Biocide conc. Seawater T
E Fig. 6.8			x				x								x	0 - 3,7 Long-term	Time Seawater T
F Fig. 6.9	x						x			x					x	0 - 1 Short-term	Time Biocide conc.

6.3.1 Laboratory rotary experiments

Coatings with different formulations were exposed in the laboratory rotor for 1 year to study the effect of the following variables on the loss of copolymer from fouling-release coatings:

1) The M_w of the PDMS-PEG-based copolymer used.
2) The crosslinker chosen to cure the PDMS binder.
3) The initial concentration of copolymer in the coating.
4) The initial concentration of CuPT in the coating.

The results can be seen in Figures 6.4 and 6.5. Figure 6.4 shows the loss of copolymer for eight different coatings initially containing 5 wt% copolymer (series A in Table 6.2). In these series different copolymers, crosslinkers and CuPT concentrations have been investigated. First, it can be seen that the addition of 7 wt% CuPT has a strong influence on the loss of copolymer after 1 year in the rotor, for all the conditions studied, independently of the copolymer and crosslinker used. In addition, it can be seen that the choice of crosslinker does not have a significant effect on the loss of copolymer, both for

biocide-free and biocide-containing coatings. Finally, the choice of copolymer seems to have a limited effect on the loss of copolymer, with the copolymer with lower M_w (copolymer 9) showing higher loss as expected. Due to the similar behaviour of both copolymers, copolymer 9 was disregarded and copolymer 8 has been used for the remaining experiments.

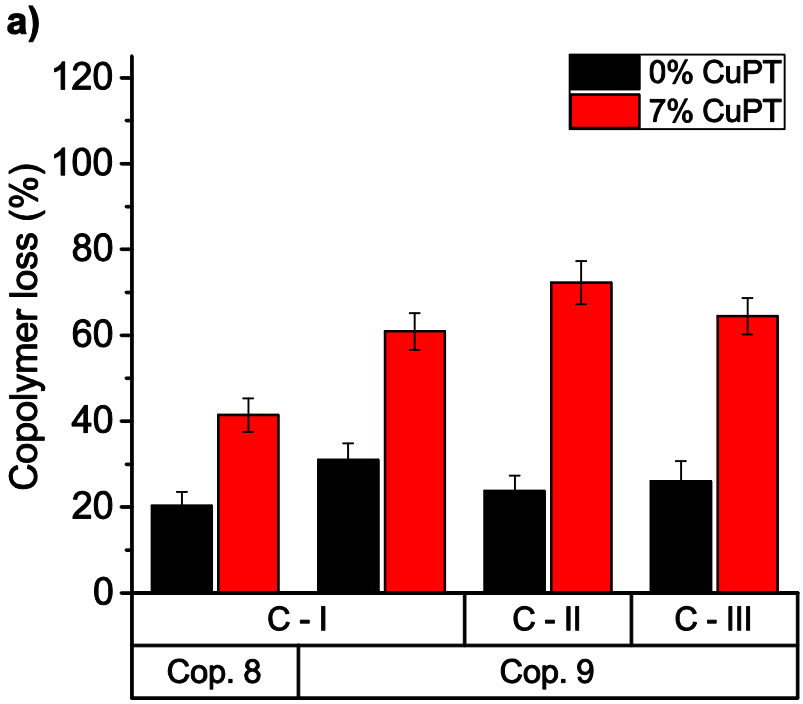

Figure 6.4. Copolymer loss (%) for coatings with different compositions (copolymer, crosslinker and CuPT concentration) containing initially 5 wt% of copolymer and exposed in the laboratory rotor (25°C, 20 knots) for 1 year. Series A in Table 6.2.

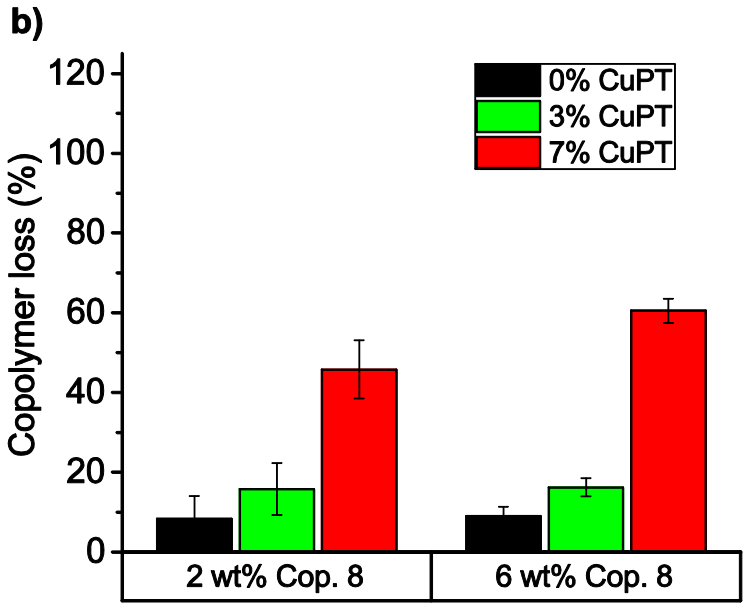

Figure 6.5. Copolymer 8 loss (%) for coatings with different compositions (copolymer and CuPT concentrations) exposed in the laboratory rotor (25°C, 20 knots) for 1 year. Series B in Table 6.2.

Figure 6.5 shows the loss of copolymer from six different coatings (series B in Table 6.2). Similar to what has been shown in Figure 6.4, the initial concentration of CuPT in the coatings appears to have a strong influence on the results, with higher concentrations of CuPT leading to greater losses of copolymer. Nonetheless, coatings with small concentrations of CuPT (3 wt%) seem to behave similarly to biocide-free coatings after 1 year of exposure in the laboratory rotor. The initial amount of copolymer in the coatings does not seem to have a significant effect on the loss of copolymer if the coatings with initially 2 wt% and 6 wt% of copolymer are compared.

6.3.2 Static exposure experiments

The results obtained from short-term (1 year) experiments in the laboratory rotor, presented in Figures 6.4 and 6.5, are compared to coatings exposed to seawater in static conditions as previously detailed.

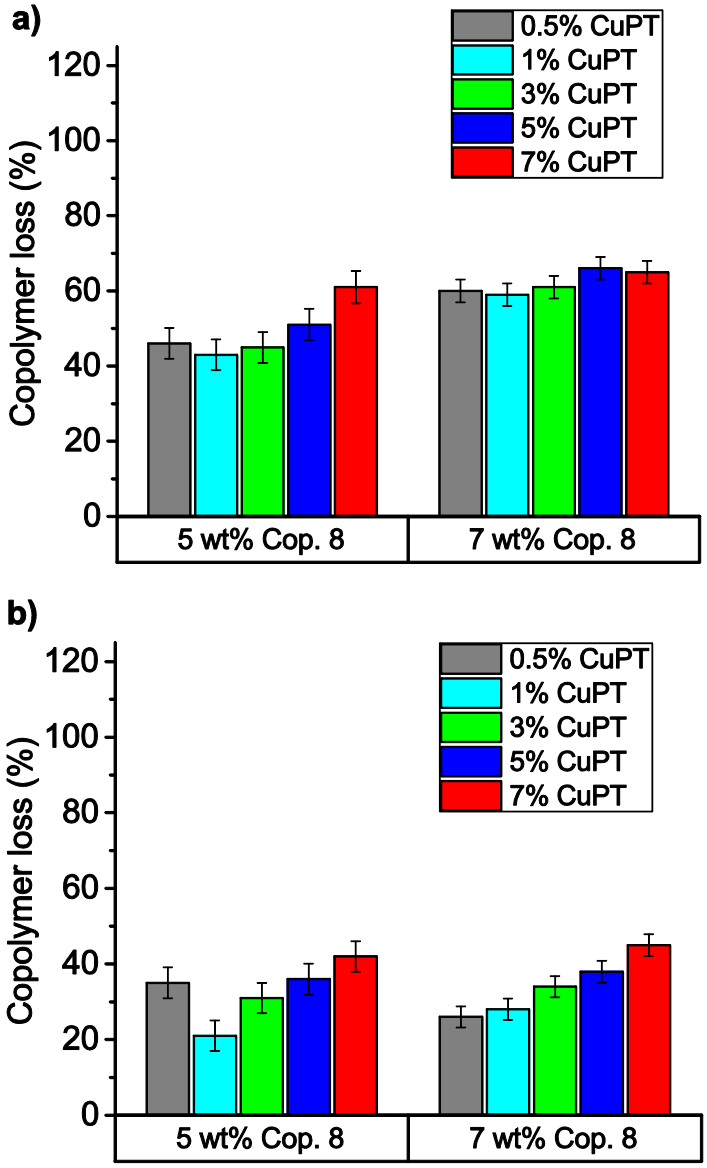

Figure 6.6. Copolymer 8 loss (%) for ten coatings exposed for approximately 2 years in Singapore (a) and Barcelona (b), where different initial copolymer 8 and CuPT concentrations have been used. Series C in Table 6.2.

Figure 6.6 shows the loss of copolymer from ten different coatings (series C in Table 6.2) exposed for about 2 years in Singapore (Figure 6.6a) and Barcelona (Figure 6.6b) in static conditions, where the initial concentration of copolymer and CuPT have been adjusted to different levels. These coatings possess *comparable* compositions to those in Figures 6.4 and 6.5.

It can be clearly seen that the loss of copolymer is distinctly higher in Singapore than in Barcelona when Figures 6.6a and 6.6b are compared. Similar to Figure 6.5, the initial concentration of copolymer in the coating does not seem to influence the copolymer loss, as evidenced by the fact that coatings containing 5 wt% and 7 wt% of copolymer suffer similar copolymer losses after 2 years of exposure. However, a clear difference can be seen between Figure 6.6 and Figures 6.4 and 6.5 regarding the impact of biocide concentration. Now, the initial concentration of CuPT has a little effect (if any) on the loss of copolymer for coatings statically exposed for 2 years in seawater, while it had a very important influence for coatings exposed for 1 year in the laboratory rotor. This disagreement could be due to differences in exposure time (1 vs 2 years) or the distinctness regarding exposure conditions (dynamic vs static).

Finally, coatings with *comparable* compositions to those in Figure 6.6 have been exposed to long-term immersion in Singapore for 3.4 years and Barcelona for 5.2 years (series D in Table 6.2). After exposure, the loss of copolymer was evaluated and the results are plotted in Figure 6.7.

Once more, the loss of copolymer is higher in Singapore compared to Barcelona. Moreover, the initial amount of copolymer in the coatings does not result in significant differences in its loss if coatings with 1 wt%, 3 wt% and 5 wt% in Figure 6.7 are compared (except for a few coatings exposed in Singapore containing low CuPT concentrations, see Figure 6.7a). Nonetheless, the effect of the initial concentration of CuPT on the long-term loss of copolymer shows interesting results, with biocide-free coatings displaying (almost) total loss of copolymer, while biocide-containing coatings retaining 40-50% of the initial copolymer (in BCN after 5.2 years) or 20-40% (in SNG after 3.4 years). This disagrees with the results in Figures 6.4 and 6.5, where after 1 year, biocide-free coatings retained larger amounts of copolymer. It also contrasts with the results in Figure 6.6, where the concentration of CuPT did not appear to influence the loss of copolymer for coatings exposed to seawater for 2 years.

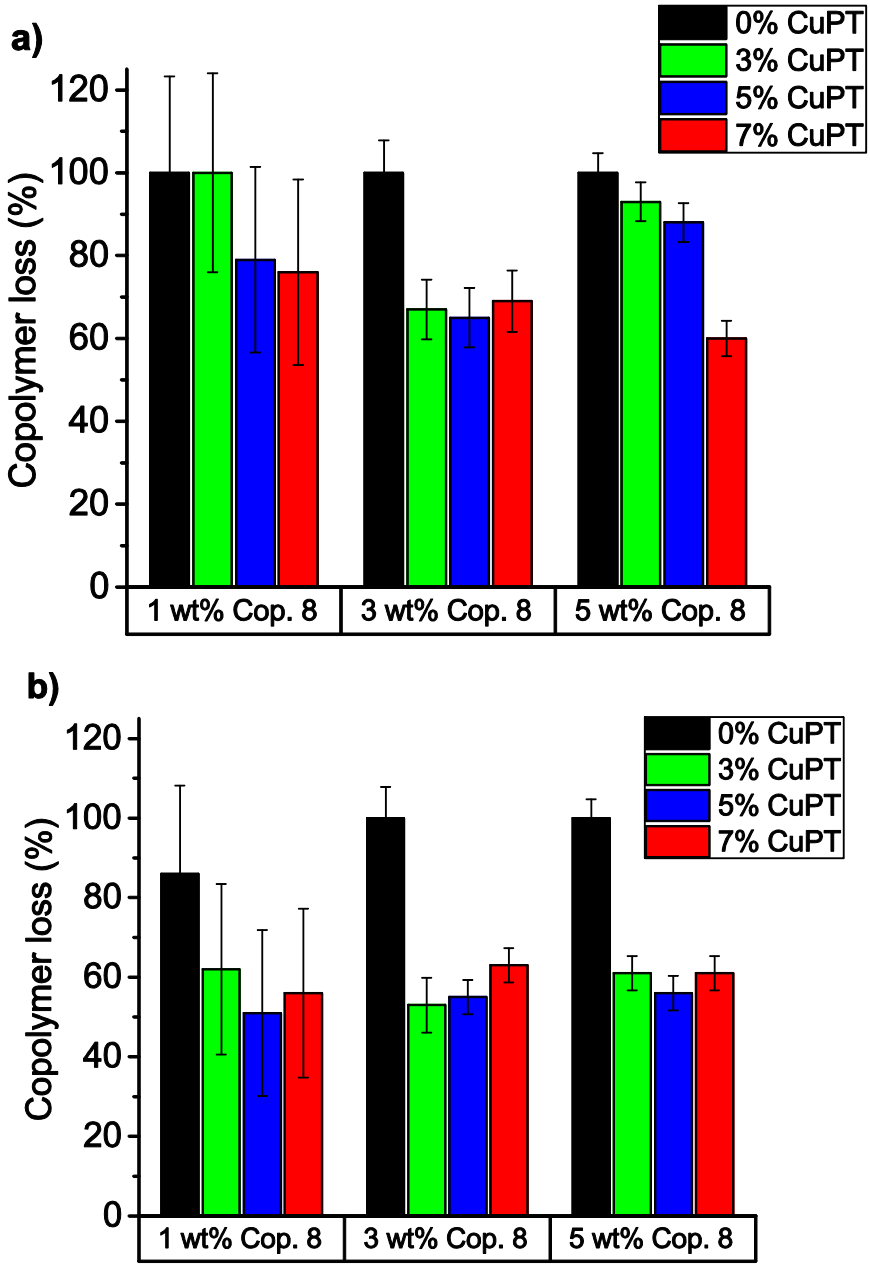

Figure 6.7. Copolymer 8 loss (%) for twelve coatings exposed for 3.4 years in Singapore (a) and 5.2 years Barcelona (b), where different initial concentrations of copolymer 8 and CuPT have been used. Series D in Table 6.2.

6.3.3 Effect of time

Figures 6.4-6.7 have shown the copolymer loss from various coatings exposed in different conditions and some trends have been identified regarding the influence of seawater temperature and initial copolymer concentration. However, the effect of biocide concentration has displayed contradictory results depending on the exposure time and hydrodynamic conditions, with higher CuPT concentrations leading to greater copolymer losses after 1 year of exposure (see Figures 6.4 and 6.5), while showing higher copolymer retention in long-term experiments (see Figure 6.7). To investigate the effect of exposure time on the concentration of copolymer in PDMS coatings, two series of coatings (E and F in

Table 6.2) were exposed to seawater in Singapore and the laboratory rotor, respectively. The copolymer concentration of these coatings has been analysed after different exposure times.

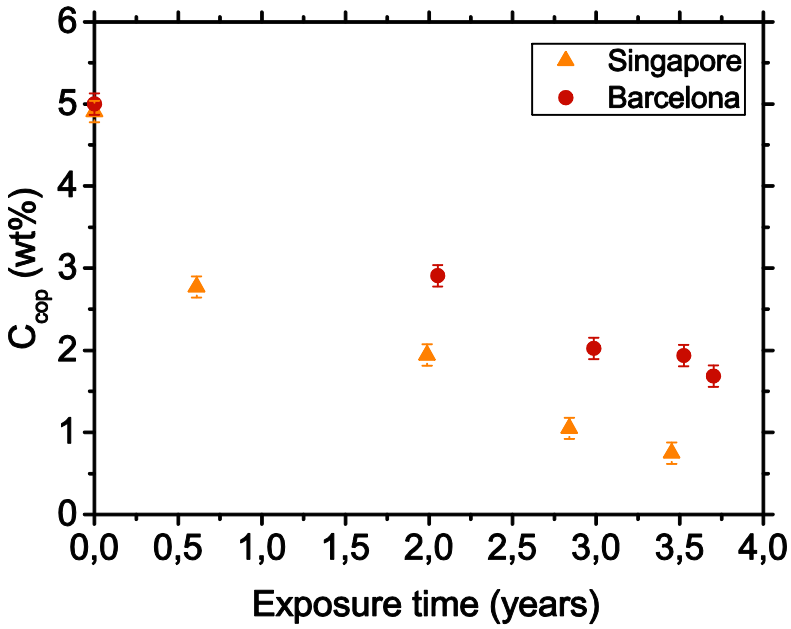

Figure 6.8. Copolymer 8 concentration (wt%) in coatings exposed in Singapore (orange triangles) and Barcelona (red dots) for up to 3.7 years, initially containing 5 wt% of copolymer 8 and 7 wt% of CuPT. Series E in Table 6.2.

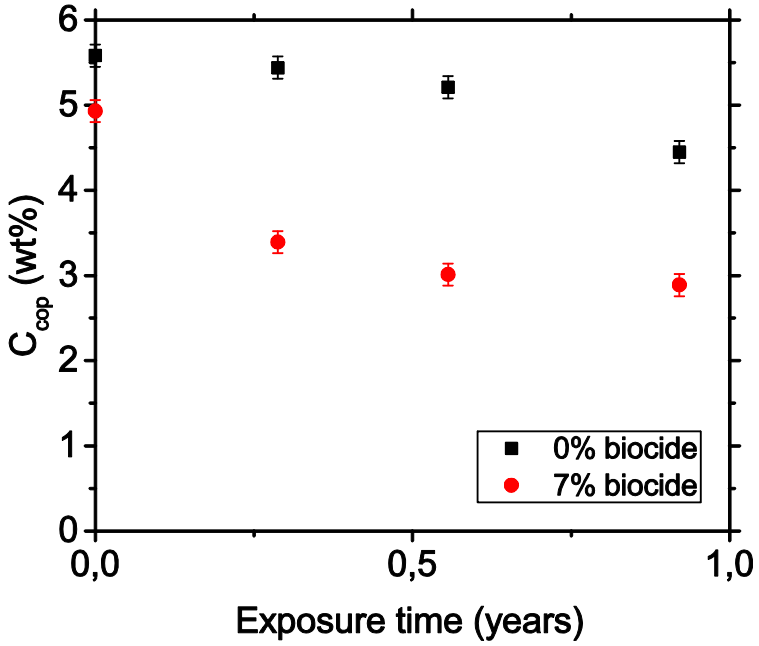

Figure 6.9. Copolymer 8 concentration (wt%) in coatings exposed to the laboratory rotor (25°C, 20 knots) for up to 1 year with different CuPT concentrations. Series F in Table 6.2.

Figure 6.8 shows the concentration of copolymer in coatings exposed in Singapore for up to 3.7 years. These coatings contained initially 5 wt% of copolymer 8 and 7 wt% of CuPT. It appears that the release of copolymer is higher in the beginning and has a tendency to stabilize afterwards for these biocide-

containing coatings. Again, higher copolymer losses are observed in Singapore than in Barcelona, as previously discussed.

Figure 6.9 shows the copolymer concentration over time in coatings exposed to the laboratory rotor for up to 1 year. It can be seen that the loss of copolymer is significantly higher for the biocide-containing coating, in agreement with Figures 6.4 and 6.5. Moreover, different trends can be seen regarding copolymer concentration over time. The copolymer concentration in the biocide-containing coating decreases more rapidly in the beginning, while the loss tends to stabilize, in agreement with Figure 6.8. Conversely, the loss of copolymer in the biocide-free coating appears to be very low in the beginning, though it suffers an important increase after the first half-year. These differences in release/loss trends could explain the contradictory results previously presented. That is, if the tendencies presented in Figure 6.9 are extended to prolonged periods of time, it should be expected that: (1) the loss of copolymer is higher for biocide-containing coatings in short-term exposure, (2) somehow similar to biocide-free coatings in the mid term and (3) significantly lower in the long term. This assumption is consistent with the results presented in Figures 6.4-6.7. However, more experiments are required to confirm this hypothesis.

6.3.4 Final remarks

It is noteworthy that up to 40% of the initial copolymer concentration can be found in some coatings after 3.4 and 5.2 years of exposure in Singapore and Barcelona (see Figure 6.7). This indicates that the release of copolymer can be tuned by changing the composition of PDMS-based fouling-release coatings and can be used as a tool to better design fouling-release coatings with optimized properties. However, the copolymer chemical composition after immersion has not been studied. Hence, the copolymer retained in the coating can have suffered some changes in composition that might have suppressed its biofouling-inhibition properties or its surface-activity. Nonetheless, the copolymer concentration has been estimated based on the copolymer eluting from the SEC system at the same elution time as the pristine copolymer. As discussed in section 5.6, it can be assumed that this copolymer has not suffered degradation. However, it has not been possible to elucidate the cause of the loss of copolymer from the fouling-release coatings analysed. In other words, the decrease in copolymer concentration over time could be due to physical dragging, dissolution or degradation of the copolymer.

It has been additionally shown that the copolymer loss (expressed as percentage, see Equation 6.2) is not dependent on the initial concentration of copolymer. Moreover, for CuPT-containing coatings, the release rate (see Figures 6.8 and 6.9) show a higher loss of copolymer in the beginning, which tends to stabilize. These two facts might be an indication that the copolymer concentration in the coating follows a first-order reaction rate law, governed by an exponential formula such as Equation 6.3.

$$C_{cop}(t) = C_{cop}(t0) \cdot \exp(-k \cdot t) \qquad \textbf{(Equation 6.3)}$$

where k is a constant, t0 corresponds to the unexposed sample and t is the exposure time.

Then, the loss of copolymer shown in Equation 6.2 can be rewritten as Equation 6.4, with the copolymer loss being independent of the initial copolymer concentration.

$$Copolymer\ loss\ (\%) = \frac{C_{cop}(t0) - C_{cop}(t)}{C_{cop}(t0)} \cdot 100 = [1 - \exp(-k \cdot t)] \cdot 100 \quad \textbf{(Equation 6.4)}$$

Note also that the effect of the release of CuPT or the presence of a leached layer have not been studied in this chapter. Moreover, the release of biocides is dependent on the seawater temperature, which could be an important factor when CuPT-containing coatings from Singapore and Barcelona are compared. Furthermore, the differences in copolymer loss between dynamic and static conditions have not been investigated. Differences between dynamic and static conditions are also expected to affect the release of CuPT. Finally, the effect of the copolymer loss on the biofouling-inhibition properties of theses coatings has not been investigated and should be assessed in the future.

In spite of the differences and uncertainties mentioned, it can be clearly seen that valuable results can be acquired from experimental coatings exposed to a range of conditions. By preparing coatings with different compositions and analysing them after exposure, important results can be obtained, which can boost the development process of fouling-release coatings. Therefore, the development of analytical methods to understand and quantify the processes occurring in fouling-release coatings are believed to be a great tool towards the development of robust and long-lasting solutions. The analysis of coatings exposed to real seawater conditions can provide some insights that can largely outweigh the aforementioned uncertainties. In other words, results from field studies can reveal some aspects that are not available in short-term laboratory experiments. However, long waiting times are required to obtain real exposure conditions. Therefore, the development of reliable accelerated tests are still required to promote the research of fouling-release coatings.

6.4 Conclusions

In this field study, the release/loss of PDMS-PEG-based block copolymers from fouling-release coatings has been studied. Different variables such as the M_w of the copolymer, the temperature of seawater or the initial CuPT concentration in the coating have been studied. To that purpose, a method to quantify the concentration of copolymer in PDMS coatings has been developed. Then, approximately 300 experimental coatings exposed to seawater in Singapore and Barcelona have been analysed. The results obtained from these coatings have been compared to coatings exposed in the laboratory rotor in controlled conditions.

The results have shown that the loss of copolymer from fouling-release coatings is strongly dependent on seawater temperature, with coatings exposed to Singapore showing greater losses than their homologues in Barcelona. Conversely, the initial copolymer concentration in the coating has no influence on the loss of copolymer for concentrations between 1 and 7 wt%. This suggests a first order decay behaviour regarding the copolymer concentration in PDMS coatings. In addition, the influence of CuPT concentration has been investigated. The results from seawater and rotary exposure experiments suggest that the release of copolymer from biocide-containing and biocide-free coatings follow different profiles, with the former showing higher copolymer losses in the first immersion stages, while the latter displaying larger losses in long-term experiments. Finally, the molecular weight of the copolymer shows

a limited influence on the release of copolymer from the coating, while the chemistry of the crosslinker does not have any significant effect.

In spite of some uncertainties, the strength of field studies has been proven regarding understanding some key phenomena occurring in fouling-release coatings such as the release of “oils”. New insights can be brought by taking advantage of long-term real exposure when compared to traditional short-term laboratory experiments. Accelerated methods to investigate some of the aforementioned issues could enable a much faster development of robust fouling-release coatings in the future.

6.5 References

[1] M. Lejars, A. Margaillan, C. Bressy, Fouling release coatings: A nontoxic alternative to biocidal antifouling coatings, *Chem. Rev.* **112** (2012) 4347–4390.

[2] A.G. Nurioglu, A.C.C. Esteves, G. de With, Non-toxic, non-biocide-release antifouling coatings based on molecular structure design for marine applications, *J. Mater. Chem. B*. **3** (2015) 6547–6570.

[3] E. Berndt, S. Behnke, A. Dannehl, A. Gajda, J. Wingender, M. Ulbricht, Functional coatings for anti-biofouling applications by surface segregation of block copolymer additives, *Polymer*. **51** (2010) 5910–5920.

[4] T. Miyata, Y. Nakanishi, T. Uragami, Ethanol Permselectivity of Poly(dimethylsiloxane) Membranes Controlled by Simple Surface Modifications Using Polymer Additives, *Macromolecules*. **30** (1997) 5563–5565.

[5] M. Inutsuka, N.L. Yamada, K. Ito, H. Yokoyama, High density polymer brush spontaneously formed by the segregation of amphiphilic diblock copolymers to the polymer/water interface, *ACS Macro Lett.* **2** (2013) 265–268.

[6] A.P. Narrainen, L.R. Hutchings, I. Ansari, R.L. Thompson, N. Clarke, Multi-End-Functionalized Polymers: Additives to Modify Polymer Properties at Surfaces and Interfaces, *Macromolecules*. **40** (2007) 1969–1980.

[7] C.J. Kavanagh, G.W. Swain, B.S. Kovach, J. Stein, C. Darkangelo-Wood, K. Truby, E. Holm, J. Montemarano, A. Meyer, D. Wiebe, The Effects of Silicone Fluid Additives and Silicone Elastomer Matrices on Barnacle Adhesion Strength, *Biofouling*. **19** (2003) 381–390.

[8] J. Seo, L.P. Lee, Effects on wettability by surfactant accumulation/depletion in bulk polydimethylsiloxane (PDMS), *Sensors Actuators, B Chem.* **119** (2006) 192–198.

[9] H.T. Kim, J.K. Kim, O.C. Jeong, Hydrophilicity of surfactant-added poly(dimethylsiloxane) and its applications, *Jpn. J. Appl. Phys.* **50** (2011).

[10] C.H. Loh, R. Wang, Insight into the role of amphiphilic pluronic block copolymer as pore-forming additive in PVDF membrane formation, *J. Memb. Sci.* **446** (2013) 492–503.

[11] H. Susanto, M. Ulbricht, Characteristics, performance and stability of polyethersulfone ultrafiltration membranes prepared by phase separation method using different macromolecular additives, *J. Memb. Sci.* **327** (2009) 125–135.

[12] A. Fatona, Y. Chen, M. Reid, M.A. Brook, J.M. Moran-Mirabal, One-step in-mould modification of PDMS surfaces and its application in the fabrication of self-driven microfluidic channels, *Lab Chip*. **15** (2015) 4322–4330.

[13] H. Madadi, J. Casals-Terré, Long-term behavior of nonionic surfactant-added PDMS for self-driven microchips, *Microsyst. Technol.* **19** (2013) 143–150.

[14] P.C.W. Thorlaksen, Fouling control coating compositions comprising polysiloxane and pendant

hydrophilic oligomer/polymer moieties, WO2013000478 (2013).

[15] S. Tanino, Antifouling coating composition, antifouling coating film, antifouling substrate, and method for improving storage stability of antifouling coating compositions, US2015299515 (2015).

[16] A. Reynier, P. Dole, S. Humbel, A. Feigenbaum, Diffusion coefficients of additives in polymers. I. Correlation with geometric parameters, *J. Appl. Polym. Sci.* **82** (2001) 2422–2433.

[17] S. Kiil, C.E. Weinell, M.S. Pedersen, K. Dam-Johansen, Analysis of self-polishing antifouling paints using rotary experiments and mathematical modeling, *Ind. Eng. Chem. Res.* **40** (2001) 3906–3920.

[18] Anonymous, A Summary of Error Propagation, Physical Sciences, Harvard University (2007).

6.6. Additional results

It has been shown that relatively high concentrations of PDMS-PEG-based copolymers remain in fouling-release coatings after several years of immersion. However, some of these coatings do not provide the same fouling-protection properties as the freshly-applied coatings, in spite of the presence of the copolymer. It has been hypothesized that the lack of fouling-inhibition properties can be attributed to the degradation of the PDMS binder surface instead of the release or degradation of the copolymer. Under this assumption, the increased surface roughness of the coating does not permit coverage of the surface by the surface-active copolymer and favours the settlement and adhesion of biofouling via mechanical interlocking. Hence, it has been investigated whether a freshly-applied low-roughness surface could recover the properties of these coatings.

To that purpose, two experimental coatings with different compositions immersed in Singapore were retrieved after approximately 2 years of exposure. The composition of these coatings consisted of a PDMS binder (containing SiO_2 and Fe_2O_3) modified by addition of a PDMS-PEG-based copolymer, though differed in the initial concentration of CuPT, with one of the coatings being biocide-free and the other ones containing 7 wt% of CuPT. The fouling-inhibition properties of one of these coatings can be seen in Figure 6.10, which started to decline approximately at the time when it was retrieved.

Image								
Exposure time (weeks)	0	16	32	48	64	80	96	112

Figure 6.10. Images of a PDMS-based fouling-release coating containing a PDMS-PEG-based copolymer immersed in seawater in Singapore for approximately 2 years. A picture of the coating was taken every 16 weeks.

The two coatings were cleaned by gentle hand-washing with water and soap and left for drying at room temperature for 24 hours. Then, the bottom half of the coatings were overcoated with an additive-free PDMS coating, following the same strategy explained in section 3.2.2 (see Figure 3.1). These (aged)

half-overcoated panels are referred to as O1 and O2. Simultaneously, the same formulations originally applied in coatings O1 and O2 were freshly applied on PMMA panels, following the procedure explained in section 6.2.3. After curing for 1 week at room temperature, the bottom half of the coating was overcoated with the same additive-free PDMS coating abovementioned. These (new) half-overcoated panels are referred to as N1 and N2. Finally, the additive-free composition used to overcoat panels O1, O2, N1 and N2 was applied on a PMMA substrate. This (reference) coating is named R. A scheme of these five panels is provided in Figure 6.11.

The five panels described above were sent for seawater immersion in Singapore, and images were taken every 8 weeks to evaluate the fouling-inhibition properties of the coatings. The results are shown in Table 6.3.

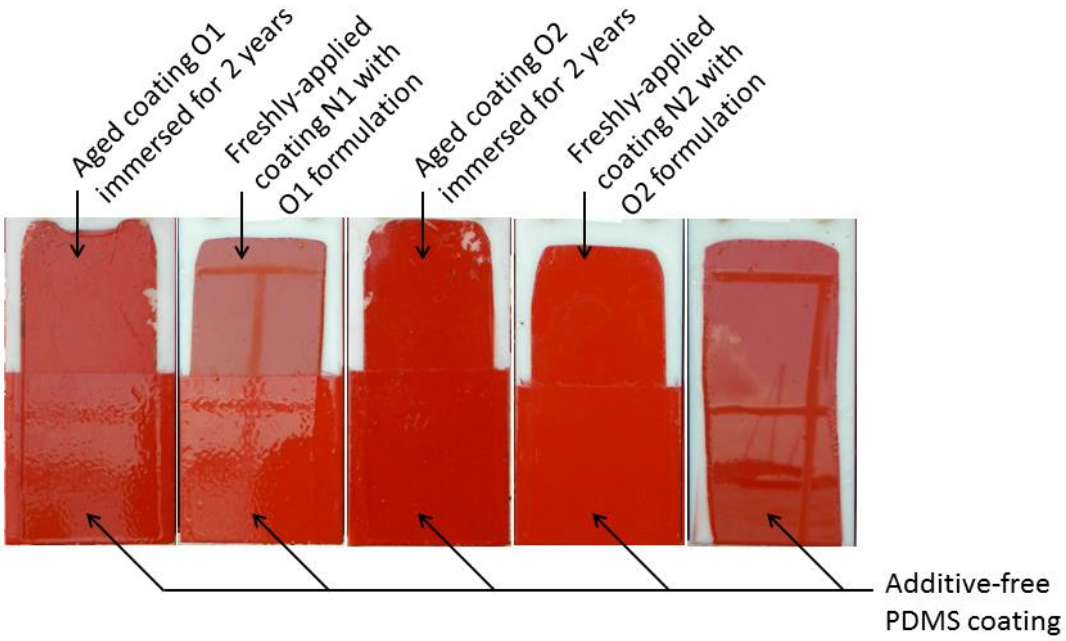

Figure 6.11. Scheme of the five panels exposed to seawater immersion.

The coatings images in Table 6.3 show some interesting results. It can be seen that the application of a layer of fresh PDMS on top of aged fouling-release coatings does not contribute to the recovery of its fouling-inhibition properties. In coating O1, the overcoated area shows the same degree of biofouling as the non-overcoated area, which is significantly higher than for the freshly-applied coating with the same composition, N1. Likewise, coating O2 shows equal amounts of biofouling in both the overcoated and non-overcoated areas, while the degree of biofouling settlement is much lower on the freshly applied N2. Note that the reference panel R does not provide significant fouling-inhibition properties, as expected, given that the surface of this coating is significantly covered by biofouling after short exposure.

These results prove the diffusion capabilities of PDMS-PEG-based copolymers, both in biocide-free and biocide-containing coatings (see N1 and N2 coatings in Table 6.3). These findings are in agreement with the results obtained in Chapter 3 (see Figure 3.10). Furthermore, the application of an overcoat on top of aged fouling-release coatings does not improve the fouling-inhibition properties of the coatings.

This indicates that their decline in fouling protection cannot be attributed to an increase in surface roughness of the binder.

Table 6.3. Images of coatings O1, N1, O2, N2 and R (described above, see Figure 6.11) immersed in seawater in Singapore for approximately 1 year. A picture of the coatings was taken every 8 weeks.

Coating O1						
Coating N1	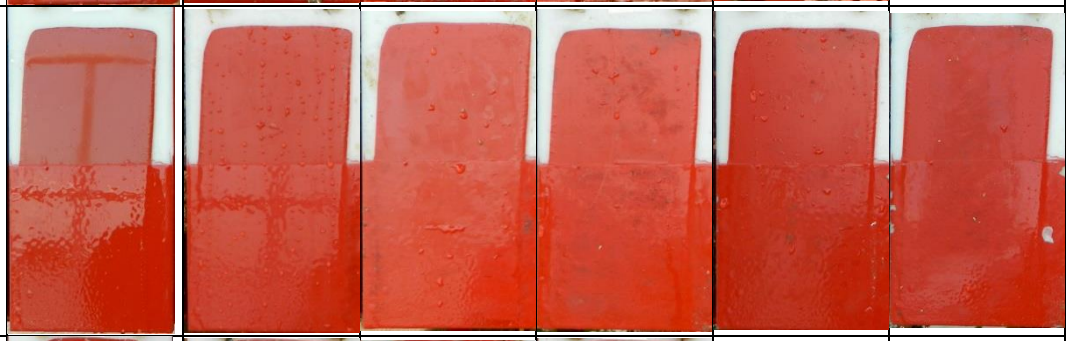					
Coating O2						
Coating N2						
Coating R						
Exposure time	0 weeks	8 weeks	16 weeks	32 weeks	48 weeks	64 weeks

7. Conclusions and future work

7.1 Conclusions

Almost the totality of commercial fouling-release coatings rely on the addition of different (block) copolymers to PDMS-based coatings to confer them with biofouling-inhibition properties. The addition of PEG-based (mostly PDMS-PEG-based) copolymers has been studied in this thesis from different perspectives, focusing on the behaviour and fate of these additives. Various analytical tools have been developed to visualize and quantify the distribution, diffusion, release and degradation of these copolymers in PDMS coatings.

The diffusion capabilities and biofouling-inhibition properties of a range of PEG-based surface-active amphiphiles have been investigated. A novel method based on water contact angle measurements using a PDMS coating film as membrane has been described. The studied amphiphiles consisted of a PEG block (between 7 and 13 ethylene glycol units) combined with a hydrophobic block, selected from (1) an alkyl group, (2) an alkyl-aryl group and (3) a PDMS chain. The diffusion coefficients obtained were relatively high for all the amphiphiles investigated, ranging from $3.2 \cdot 10^{-12}$ to $3.5 \cdot 10^{-11}$ m^2/s .The diffusion coefficient decreases with increasing the M_w following a power dependence ($D = k \cdot M_w^{-0.8}$), though the relationship is less pronounced than for other rubbery polymers. Regarding the polarity of the amphiphiles, the results showed that there is no correlation between the hydrophilic-lipophilic balance (HLB) value and the diffusion coefficient of the amphiphiles studied, for amphiphiles with HLB values between 8 and 14. Images of coatings containing the studied amphiphiles after immersion in seawater showed that the biofouling-inhibition properties of the investigated amphiphiles do not depend on their diffusion coefficient in the PDMS coating. Conversely, biofouling settlement on the coatings strongly depends on the chemistry of the hydrophobic block of the amphiphiles, with PDMS-PEG-based copolymers being the only ones that imparted fouling-inhibition properties. These results suggest that the anchoring capabilities of the copolymer are essential regarding the performance of these FRC.

The distribution and diffusion of PDMS-PEG-based copolymers have been investigated and visualized by help of a synthesized fluorescent-labelled copolymer. The fluorescent molecule used to label the copolymer accounts for only 7% of the total weight of the molecule. It has been thus assumed that the labelling of the copolymer does not result in significant changes in the behaviour of the copolymer in the PDMS film. The labelled copolymer has the same surface-segregation tendency as commercial PDMS-PEG-based copolymers, as confirmed by water contact angle measurements. Confocal laser scanning microscopy has proven to be a powerful tool to visualize the copolymer in the bulk of the coating film. The labelled copolymer molecules assemble in spherical domains in the coating. The size of these domains vary with the depth (z-position), with diameters of approximately 1 µm close to the surface, while achieving values of up to 7 µm in the bulk of the coating. Moreover, the segregation of the labelled copolymer has been successfully studied by following the fluorescence intensity at different depths over time. The results obtained were in agreement with those obtained by contact angle measurements, confirming the high mobility of the copolymer in PDMS films.

Regarding the chemical stability of PDMS-PEG-based copolymers in the bulk of PDMS coatings, FRC immersed in seawater in Singapore for 3 and 30 months have been investigated. The copolymers were extracted and isolated from the exposed coatings by semi preparative SEC and their chemical composition was analysed by IR and NMR means. The chemical composition of copolymers exposed for 3 and 30 months showed only slight differences. Moreover, their elution volumes (which are related to the molecular weight of the copolymers) did not change over time when compared to the pristine copolymer. Hence, it was concluded that the isolated copolymers did not suffer significant degradation under immersion. Some results comprising coatings with different formulations showed that the physical properties and chemical composition of the coatings constituents have a strong influence on the degradation of PDMS-PEG-based copolymers. Some coatings showed that the copolymer was completely degraded after 1 year, both for coatings exposed to seawater and for others kept in the laboratory at room temperature. Analysis of the coatings showed that the degradation products of the copolymer consist mainly of small PEG-homologues with ester groups originating from the oxidative degradation of the PEG block. Such products could not found in immersed coatings, probably due to dissolution to seawater triggered by their hydrophilic character.

Finally, the release/loss of copolymer from FRC coatings has been studied. A method based on solvent extraction by THF and subsequent quantification by SEC was developed. Approximately 300 experimental coatings were analysed. The initial concentration of copolymer in the coating does not result in significant changes in the loss of copolymer under immersion, for coatings containing between 1 and 7 wt% of copolymer. Hence, a first order rate law in the copolymer concentration was established. Moreover, addition of biocide modifies the copolymer loss profile. Biocide-containing coatings exhibit greater loss of copolymer in short-term immersion. Conversely, these coatings retain higher copolymer concentrations at long immersion times. The results also indicated that the loss of copolymer is significantly higher in Singapore than in Barcelona due to the higher seawater temperature found in the former. However, it was proven that some coatings immersed in seawater for up to 5.2 years retain about 40% of the initial copolymer concentration. Therefore, it was investigated whether the physical deterioration of the PDMS binder surface could cause of the decline in biofouling-inhibition properties of FRC. However, it was shown that the application of freshly-applied coatings on top of old FRC could not revert the properties of the coatings.

Therefore, it can be concluded that the physical properties and chemical composition of the investigated copolymers and the rest of constituents in FRC has proven to have strong effects on the long-term performance of FRC, influencing both the diffusion, release and degradation of the copolymers. Moreover, various methods have been developed in the thesis, which are believed to be a valuable tool towards the development of robust and long-lasting FRC with superior fouling-inhibition properties. Extension of the lifetime of fouling-release coatings will lead to significant economical and environmental benefits associated with decreased fuel consumption, diminished biocide release to seawater and lower greenhouse-effect gases emissions to the atmosphere, as well as a reduction in the raw materials used and residues generated.

7.2 Future work

It has been shown that alkyl-PEG-based surfactants are capable of diffusing to the surface of PDMS coatings. However, these compounds failed to impart fouling-inhibition properties to the coatings. This could be attributed to the incapacity of these surface-active amphiphiles to properly cover the surface of the coating. However, it is more plausible that their poor properties arise from the weaker anchoring capabilities of alkyl groups on PDMS, with the fast release of these compounds to seawater. This should be confirmed. Moreover, PEG-based surfactants with long alkyl chains with different structures should be explored as a strategy to increase the anchoring capabilities on the surface. It was also shown that PDMS-PEG-based copolymers with “graft” and triblock-ABA structures could inhibit the settlement of biofouling. However, no research was undertaken to assess the effect of the structure and molecular weight of the PDMS block on the anchoring and long-term biofouling-resistance properties of the coatings. Furthermore, other hydrophobic blocks providing anchoring to the PDMS surface could be investigated. Finally, very high molecular weight PDMS-PEG-based copolymers should be investigated to corroborate that even at high molecular weight the diffusion coefficient does not limit the biofouling-inhibition properties of these additives.

Regarding the release and degradation of PDMS-PEG-based copolymers from PDMS coatings, it has been confirmed that the remaining copolymer concentration in the coating can be measured after exposure. Copolymer molecules extracted from aged coatings and analysed via SEC do not show difference in elution time, and it has thereby been assumed that no degradation has been suffered by these molecules. However, the cause of loss of copolymer occurring in FRC has not been elucidated. The loss of copolymer quantified in this thesis could be due to water dragging/sweeping, dissolution or degradation at the surface of the coating, degradation in the bulk or a combination of these. This is a major question to be answered if long-lasting robust fouling-release coatings are pursued. In addition, it has been shown that the addition of biocide and seawater temperature have a strong influence on the release-profile and final loss of copolymer. The mechanisms behind should be explored to be able to understand the phenomena governing the release of copolymers from fouling-release coatings.

Moreover, some new methods have been developed to visualize and quantify different processes. Labelling a copolymer with a small fluorescent tag has proven to be a valuable tool to visualize these complex systems. This method could be employed to analyse the effect of different variables on the distribution and diffusion of these copolymers in fouling-release coatings. For example, the size and surface area of filler particles, crosslinker chemistry and structure, molecular weight of the copolymer, evaporation rate of the solvent and molecular weight of the PDMS binder could be investigated. The full capabilities of this method have not been exploited due to time constrains but should be addressed.

Finally, it has been shown that it is possible to study, visualize and quantify phenomena occurring in fouling-release coatings using the methods developed. However, these methods are associated with long waiting times which hinder the fast development in this area. Therefore, accelerated methods which can mimic exposure conditions in a reliable way would be a great tool coupled with some of the techniques developed in this project.